UNIVERSITY OF NAPLES FEDERICO II

PH.D. PROGRAM IN

CLINICAL AND EXPERIMENTAL MEDICINE

CURRICULUM IN TRANSLATIONAL MEDICAL SCIENCES

XXXII Cycle

(Years 2017-2020)

Chairman: Prof. Francesco Beguinot

PH.D. THESIS

NEW PREDICTIVE AND PROGNOSTIC BIOMARKERS IN METASTATIC PROSTATE CANCER

TUTOR

Prof. Arturo Genovese
Prof. Johann S. de Bono

PH.D. STUDENT

Dr. Pasquale Rescigno

Table of Contents

DECLARATION 5

ACKNOWLEDGEMENTS 6

ABSTRACT 8

PUBLICATIONS DERIVED FROM THIS THESIS 10

ORIGINAL PAPERS 10

INVITED REVIEWS AND EDITORIALS 12

OTHER RELEVANT PUBLICATIONS 14

1 INTRODUCTION 17

1.1 PROSTATE CANCER: A GLOBAL HEALTH ISSUE 17

1.2 PROSTATE CANCER DIAGNOSIS: CLINICAL FEATURES, MANAGEMENT AND THE ROLE OF PROSTATE-SPECIFIC ANTIGEN IN EARLY DISEASE 18

1.2.1 Use of PSA in Risk Stratification (Prognosis) *20*

1.2.2 Use of PSA During Follow-up After an Initial Diagnosis *20*

1.2.3 Management of Patients with Biochemical Recurrence *21*

1.3 MANAGEMENT OF METASTATIC HORMONE-SENSITIVE AND CASTRATION-RESISTANT PROSTATE CANCER 22

1.4 MOLECULAR LANDSCAPE OF PROSTATE CANCER 25

1.4.1 Biomarkers in Prostate Cancer *28*

2 HYPOTHESIS AND OVERALL OBJECTIVES 36

2.1 CORE HYPOTHESIS 36

2.2 DRIVING HYPOTHESIS FOR EACH CHAPTER 36

2.3 OVERALL OBJECTIVES 38

3 RELEVANCE OF ANDROGEN RECEPTOR (AR) SIGNALLING IN METASTATIC CASTRATION-RESISTANT PROSTATE CANCER (MCRPC): PROGNOSTIC/PREDICTIVE BIOMARKERS OF RESPONSES TO HORMONAL AGENTS 39

3.1 BACKGROUND 39

3.2 SPECIFIC AIMS 43

3.3 RESULTS 43

3.3.1 Early Post-treatment Changes in PSA Following Abiraterone and Enzalutamide Treatment for Advanced Prostate Cancer: An International Collaborative Analysis *43*

3.3.2 Nuclear AR-V7 and AR-NTD Expression Increases as Prostate Cancer Becomes Castration Resistant and Increases Further with Abiraterone Acetate and/or Enzalutamide Resistance *46*

3.3.3 Nuclear AR-V7 Expression Levels but not AR-NTD Levels are Associated with Worse CRPC Prognosis 48
3.3.4 Nuclear AR-V7 Expression and Response to AA 50
3.3.5 CTC AR-V7 positivity is associated with more advanced disease 51
3.3.6 CTC AR-V7 status identifies mCRPC patients with more advanced disease and therefore poorer prognosis 53
3.4 DISCUSSION **55**
4 PTEN LOSS AND ACTIVATION OF ITS PATHWAY: A PROGNOSTIC AND PREDICTIVE BIOMARKER **58**
4.1 BACKGROUND **58**
4.2 SPECIFIC AIMS **60**
4.3 RESULTS **60**
4.3.1 PTEN Protein Loss and Clinical Outcome from mCRPC Treated with Abiraterone Acetate 60
4.3.2 PTEN IHC Loss and Docetaxel Treatment 65
4.3.3 PTEN IHC as a Predictive Biomarker of Response to a Combination of Capivasertib and Enzalutamide 70
4.4 DISCUSSION **73**
5 DNA REPAIR DEFECTS IN LETHAL PROSTATE CANCER **76**
5.1 INTRODUCTION **76**
5.2 SPECIFIC AIMS **78**
5.3 RESULTS **79**
5.3.1 Homologous Recombination Defective mCRPC 79
5.3.2 Mismatch Repair Defective mCRPC 89
5.3.3 Impact of Mismatch DNA Repair Defects on Outcomes of Prostate Cancer 93
5.3.4 Intra-patient dMMR Heterogeneity in Primary Disease 96
5.3.5 PD-L1 Expression and Tumour Infiltrating Lymphocytes (TILs) in dMMR CRPC 98
5.4 DISCUSSION **102**
6 FINAL CONCLUSIONS **107**
7 MATERIALS AND METHODS **109**
7.1 PATIENT POPULATIONS **109**
7.1.1 Chapter 3 (PSA study) 109
7.1.2 Chapter 4 (phase I trial with Enzalutamide and Capivasertib) 109
7.1.3 Chapter 5 (ToparpB phase II trial) 113
7.2 PATIENT SAMPLES **113**
7.2.1 Chapters 3, 4, 5: Sample collection 113
7.3 IMMUNOPHENOTYPING **114**

7.3.1 Immunohistochemistry (IHC) – Technical Aspects *114*
7.3.2 Immunohistochemistry (IHC) – Assay Analyses *120*
7.3.3 Multicolour Immunofluorescence *121*
7.4 AdnaTest mRNA extraction, CTC enumeration, and AdnaTest CTC call 122
7.5 Massive-parallel sequencing (Chapters 4 and 5) 123
7.5.1 DNA Extraction *123*
7.5.2 Targeted Sequencing *124*
7.5.3 Whole Genome Sequencing (Chapter 5) *125*
7.5.4 cfDNA Sequencing (Chapter 5) *125*
7.5.5 Sequencing and Bioinformatics (Chapter 5) *126*
7.6 Statistical Analyses 127
8 BIBLIOGRAPHY 129

Declaration

The work presented herein has been performed by me unless otherwise acknowledged and details the results of projects that I led or actively participated in.

Acknowledgements

The research illustrated in this PhD thesis represents the product of a long journey, both physically and emotionally. For the last three years, I have been regularly travelling between London and Naples. I have been through happy and very sad moments; I am grateful for both because you can learn from laughing and from crying.

These research projects would have been not possible without colleagues, family and friends supporting me throughout every step of my life. My list probably fails at being complete and for this I apologise in advance.

Thank you:

Professor Genovese and Professor de Placido, for your support during my PhD, for giving me the opportunity to split my time between Italy and England, and for advising me through the different steps of my career.

Professor de Bono, for mentoring me through the development of this thesis. Your hard work, dedication, commitment, and love for science are hugely inspirational; I am honoured to have been one of your students. I will treasure all I have learnt from you.

My colleagues (present and past) at the Royal Marsden Hospital: Diletta Bianchini, Roberta Ferraldeschi, Antonella Petremolo, Caterina Aversa, Spyros Sideris, Zafeiris Zafeiriou, Joaquin Mateo, Semini Sumanasuriya, Raquel Perez-Lopez, Nina Tunariu, David Lorente, Michael Kolinsky, Maialen Barrero, and Mariane Fontes. I hugely appreciate your efforts in supporting me on a daily basis. It has been hard work, I know, but I enjoyed every moment I spent with you.

Every member of the Prostate Cancer Targeted Therapy Group, particularly Lucy, Sheena, Jo, Lorena, and Dee; thank you for making my daily life at work much easier.

All the staff of the Cancer Therapeutics/Cancer Biomarkers group and the Institute of Cancer Research (Suzanne Carreira, Adam Sharp, Mateus Crespo, Susana Miranda, Ines Figueiredo, Ruth Riisnaes, Jon Welti, Antje Neeb, Alec Paschalis, Wei Yuan, George Seed, Maryou Lambros, Penny Flohr, Rita Pereira, Ana Ferreira and Gunther Boysen) for providing guidance and support. This thesis would not have been possible without your amazing work and your high levels of scientific knowledge.

Prostate Cancer Foundation, in the person of Howard Soule, for believing in me and my projects; Prostate Cancer UK, Movember, and Cancer Research UK for funding and supporting my research.

To all my family, my dad, brothers, sister, the little Annabella, who love me unconditionally, and to my MUM who did not live long enough to see this day. I hope to make you proud; please keep looking after me wherever you are.

To my friends (the list is huge, I mention just a few), Aidan, Cinzia, Valeria, Assia, Roberta, Gilberto, John and Pat, your affection and support, in London, Naples and wherever we have been have helped me to get through the hardest moments of my life.

To all the patients and their families, to Natalina, Maria Cinzia, George, Carlos, Alastair and many others who smiled and encouraged me during my work, you spent some time of your life forgetting about your pain and thinking about mine. We live to serve you.

Abstract

In this thesis, I discuss the identification of new prognostic and predictive biomarkers in lethal prostate cancers (PCs), derived from studies focused on molecular characterisation as a key element for detection of aberrant pathways in this disease. This approach allows the refinement of patient stratification and delivers more precise and individually tailored clinical care.

Since the discovery of the usefulness of castration in the treatment of PC during the early decades of the last century, therapeutic strategies for treating this disease have improved and now involve the suppression of androgenic signalling, with several hormonal agents currently available, including enzalutamide, abiraterone, apalutamide and darolutamide. This has led researchers to focus their work on mechanisms of resistance to available hormonal manipulations, including androgen receptor (AR) splicing variant expression, AR amplification, and mutations. Here, I explored the importance of interrogating the serum level of prostate-specific antigen (PSA) as early as 4 weeks post-treatment as a biomarker of responses to second generation hormonal agents (SGHAs) and its correlation with overall survival. I also discovered that AR splicing variant 7 (AR-V7) expression, which is negligible in hormone-naïve PC, increases as patients progress into metastatic castration-resistant PC (mCRPC), and that this is correlated with prognosis and can also explain resistance to SGHAs.

Using data gathered from several assays, including sequencing platforms, as well as immunohistochemistry (IHC) and immune-phenotyping assays, I also studied the impact of key tumour suppressor gene aberrations on outcomes of mCRPCs and present this work here as well. I have demonstrated, using IHC, the role of PTEN loss as a biomarker of poor response to abiraterone and investigated its role in docetaxel-treated cancers and in the context of a prospective, randomised, phase I/II trial of enzalutamide with or without the AKT inhibitor, capivasertib.

I have also demonstrated the extreme importance of defects in the mechanism of DNA repair, such as homologous recombination as a sensitizer to PARP inhibition in the context

of synthetic lethality. Finally, I have shown that in mCRPC, mismatch repair defects are associated with worse outcomes and increased likelihood of PD-L1 expression and lymphocyte infiltration, suggesting that these cancers are an ideal subset for immunotherapies.

The work I have presented here, therefore, has shown that the molecular stratification of PC is feasible and can be used to identify new prognostic biomarkers for mCRPCs, as well as identifying predictive biomarkers for both standard and novel therapeutic strategies, offering more precisely targeted and effective care regimens.

Publications derived from this thesis

Original Papers

A Phase I Dose-Escalation Study of Enzalutamide in Combination with the AKT Inhibitor AZD5363 (Capivasertib) in Patients with Metastatic Castration Resistant Prostate Cancer.

Kolinsky MP*, **Rescigno P***, Bianchini D, Zafeiriou Z, Mehra N, Mateo J, Riisnaes R, Crespo M, Figueiredo I, Miranda S, Nava Rodrigues D, Flohr P, Tunariu N, Banerji U, Ruddle R, Sharp A, Welti J, Lambros M, Carreira S, Raynau FI, Swales KE, Plymate S, Luo J, Tovey H, Porta N, Slade R, Leonard L, Hall E, de Bono JS.

(Annals of Oncology, accepted for publication).

Genomics of Lethal Prostate Cancer at Diagnosis and Castration-Resistance.

Mateo J, Seed G, Bertan C, **Rescigno P**, Dolling D, Figueiredo I, Miranda S, Nava Rodrigues D, Gurel B, Clarke M, Atkin M, Chandler R, Messina C, Sumanasuriya S, Bianchini D, Barrero M, Petremolo A, Zafeiriou Z, Fontes MS, Perez-Lopez R, Tunariu N, Fulton BA, Jones R, McGovern UB, Ralph C, Varughese M, Parikh O, Jain S, Elliott T, Sandhu S, Porta N, Hall E, Yuan W, Carreira S, de Bono JS.

J Clin Invest. 2019 Dec 24. pii: 132031. doi: 10.1172/JCI132031.

Olaparib in Patients with Metastatic Castration-Resistant Prostate Cancer with DNA Repair Gene Aberrations (TOPARP-B): a Multicentre, Open-Label, Randomised, Phase 2 Trial.

Mateo J, Porta N, Bianchini D, McGovern U, Elliott T, Jones R, Syndikus I, Ralph C, Jain S, Varughese M, Parikh O, Crabb S, Robinson A, McLaren D, Birtle A, Tanguay J, Miranda S, Figueiredo I, Seed G, Bertan C, Flohr P, Ebbs B, **Rescigno P**, Fowler G, Ferreira A, Riisnaes R, Pereira R, Curcean A, Chandler R, Clarke M, Gurel B, Crespo M, Nava Rodrigues D, Sandhu S, Espinasse A, Chatfield P, Tunariu N, Yuan W, Hall E, Carreira S, de Bono JS.

Lancet Oncol. 2019 Dec 2. pii: S1470-2045(19)30684-9. doi: 10.1016/S1470-2045(19)30684-9.

Clinical Utility of Circulating Tumour Cell Androgen Receptor Splice Variant-7 Status in Metastatic Castration-resistant Prostate Cancer.

Sharp A, Welti JC, Lambros MBK, Dolling D, Rodrigues DN, Pope L, Aversa C, Figueiredo I, Fraser J, Ahmad Z, Lu C, **Rescigno P**, Kolinsky M, Bertan C, Seed G, Riisnaes R, Miranda S, Crespo M, Pereira R, Ferreira A, Fowler G, Ebbs B, Flohr P, Neeb A, Bianchini D, Petremolo A, Sumanasuriya S, Paschalis A, Mateo J, Tunariu N, Yuan W, Carreira S, Plymate SR, Luo J, de Bono JS.

Eur Urol. 2019 Nov;76(5):676-685. doi: 10.1016/j.eururo.2019.04.006.

Early Post-treatment Prostate-specific Antigen at 4 Weeks and Abiraterone and Enzalutamide Treatment for Advanced Prostate Cancer: An International Collaborative Analysis.

Rescigno P, Dolling D, Conteduca V, Rediti M, Bianchini D, Lolli C, Ong M, Li H, Omlin AG, Schmid S, Caffo O, Zivi A, Pezaro CJ, Morley C, Olmos D, Romero-Laorden N, Castro E, Saez MI, Mehra N, Smeenk S, Sideris S, Gil T, Banks P, Sandhu SK, Sternberg CN, De Giorgi U, De Bono JS.

Eur Urol Oncol. 2019 Jul 12. pii: S2588-9311(19)30083-5. doi: 10.1016/j.euo.2019.06.008.

Genomic Analysis of Three Metastatic Prostate Cancer Patients with Exceptional Responses to Carboplatin Indicating Different Types of DNA Repair Deficiency.

Zafeiriou Z, Bianchini D, Chandler R, **Rescigno P**, Yuan W, Carreira S, Barrero M, Petremolo A, Miranda S, Riisnaes R, Rodrigues DN, Gurel B, Sumanasuriya S, Paschalis A, Sharp A, Mateo J, Tunariu N, Chinnaiyan AM, Pritchard CC, Kelly K, de Bono JS.

Eur Urol. 2019 Jan;75(1):184-192. doi: 10.1016/j.eururo.2018.09.048.

Mismatch Repair Defects and Integrative Immunogenomics in Lethal Prostate Cancer

Rodrigues DN*, **Rescigno P***, Liu D*, Yuan W, Carreira S, Lambros MB, Mateo J, Riisnaes R, Mullane S, Margolis C, Miao Dm Miranda S, Dolling D, Clarke M, Bertan C, Crespo M, Boysen

G, Ferreira A, Sharp A, Figueiredo I, Keliher D, Aldubayan S, Burke KP, Sumanasuriya S, Fontes MS, Bianchini D, Zafeiriou Z, Mendes LST, Mouw K, Schweizer MT, Pritchard CC, Salipante S, Taplin ME, Beltran H, Rubin MA, Cieslik M, Robinson D, Heath E, Schultz N, Armenia J, Abida W, Scher H, Lord C, D'Andrea A, Sawyers CL, Chinnaiyan AM, Alimonti A, Nelson PS, Drake CG, Van Allen EM, de Bono JS.
J Clin Invest. 2018 Nov 1;128(11):5185. doi: 10.1172/JCI125184.

Docetaxel Treatment in PTEN- and ERG-aberrant Metastatic Prostate Cancers.
Rescigno P, Lorente D, Dolling D, Ferraldeschi R, Rodrigues DN, Riisnaes R, Miranda S, Bianchini D, Zafeiriou Z, Sideris S, Ferreira A, Figueiredo I, Sumanasuriya S, Mateo J, Perez-Lopez R, Sharp A, Tunariu N, de Bono JS.
Eur Urol Oncol. 2018 May;1(1):71-77. doi: 10.1016/j.euo.2018.02.006.

Circulating Cell-Free DNA to Guide Prostate Cancer Treatment with PARP Inhibition.
Goodall J, Mateo J, Yuan W, Mossop H, Porta N, Miranda S, Perez-Lopez R, Dolling D, Robinson DR, Sandhu S, Fowler G, Ebbs B, Flohr P, Seed G, Rodrigues DN, Boysen G, Bertan C, Atkin M, Clarke M, Crespo M, Figueiredo I, Riisnaes R, Sumanasuriya S, **Rescigno P**, Zafeiriou Z, Sharp A, Tunariu N, Bianchini D, Gillman A, Lord CJ, Hall E, Chinnaiyan AM, Carreira S, de Bono JS; TOPARP-A investigators.
Cancer Discov. 2017 Sep;7(9):1006-1017. doi: 10.1158/2159-8290.CD-17-0261.

Invited Reviews and Editorials

Immunotherapy for Lethal Prostate Cancer.
Rescigno P, de Bono JS.
Nat Rev Urol. 2019 Feb;16(2):69-70. doi: 10.1038/s41585-018-0121-y.

Relevance of Poly (ADP-ribose) Polymerase Inhibitors in Prostate Cancer.
Rescigno P, Chandler R, de Bono J.

Curr Opin Support Palliat Care. 2018 Sep;12(3):339-343. doi: 10.1097/SPC.0000000000000358.

Circulating Biomarkers of Neuroendocrine Prostate Cancer: an Unmet Challenge.

Rescigno P, Rodrigues DN, de Bono JS.

BJU Int. 2017 Jan;119(1):3-4. doi: 10.1111/bju.13550.

Other Relevant Publications

Prostate-specific Membrane Antigen Heterogeneity and DNA Repair Defects in Prostate Cancer.

Paschalis A, Sheehan B, Riisnaes R, Rodrigues DN, Gurel B, Bertan C, Ferreira A, Lambros MBK, Seed G, Yuan W, Dolling D, Welti JC, Neeb A, Sumanasuriya S, **Rescigno P**, Bianchini D, Tunariu N, Carreira S, Sharp A, Oyen W, de Bono JS.

Eur Urol. 2019 Oct;76(4):469-478. doi: 10.1016/j.eururo.2019.06.030.

Genomic Correlates of Clinical Outcome in Advanced Prostate Cancer.

Abida W, Cyrta J, Heller G, Prandi D, Armenia J, Coleman I, Cieslik M, Benelli M, Robinson D, Van Allen EM, Sboner A, Fedrizzi T, Mosquera JM, Robinson BD, De Sarkar N, Kunju LP, Tomlins S, Wu YM, Nava Rodrigues D, Loda M, Gopalan A, Reuter VE, Pritchard CC, Mateo J, Bianchini D, Miranda S, Carreira S, **Rescigno P**, Filipenko J, Vinson J, Montgomery RB, Beltran H, Heath EI, Scher HI, Kantoff PW, Taplin ME, Schultz N, deBono JS, Demichelis F, Nelson PS, Rubin MA, Chinnaiyan AM, Sawyers CL.

Proc Natl Acad Sci U S A. 2019 Jun 4;116(23):11428-11436. doi: 10.1073/pnas.1902651116.

RB1 Heterogeneity in Advanced Metastatic Castration-Resistant Prostate Cancer.

Nava Rodrigues D, Casiraghi N, Romanel A, Crespo M, Miranda S, **Rescigno P**, Figueiredo I, Riisnaes R, Carreira S, Sumanasuriya S, Gasperini P, Sharp A, Mateo J, Makay A, McNair C, Schiewer M, Knudsen K, Boysen G, Demichelis F, de Bono JS.

Clin Cancer Res. 2019 Jan 15;25(2):687-697. doi: 10.1158/1078-0432.CCR-18-2068.

Single-Cell Analyses of Prostate Cancer Liquid Biopsies Acquired by Apheresis.

Lambros MB, Seed G, Sumanasuriya S, Gil V, Crespo M, Fontes M, Chandler R, Mehra N, Fowler G, Ebbs B, Flohr P, Miranda S, Yuan W, Mackay A, Ferreira A, Pereira R, Bertan C, Figueiredo I, Riisnaes R, Rodrigues DN, Sharp A, Goodall J, Boysen G, Carreira S, Bianchini D, **Rescigno P**, Zafeiriou Z, Hunt J, Moloney D, Hamilton L, Neves RP, Swennenhuis J, Andree K, Stoecklein NH, Terstappen LWMM, de Bono JS.

Clin Cancer Res. 2018 Nov 15;24(22):5635-5644. doi: 10.1158/1078-0432.CCR-18-0862.

Molecular and Clinical Implications of CHD1 Loss and SPOP Mutations in Advanced Prostate Cancer

Boysen G*, Rodrigues DN*, Seed G, Dolling D, **Rescigno P**, Riisnaes R, Crespo M, Zafeiriou Z, Sumanasuriya S, Bianchini D, Hunt J, Moloney D, Perez-Lopez R, Tunariu N, Miranda S, Figueiredo I, Ferreira A, Christova R, Gil V, Aziz S, Bertan C, de Oliveira FM, Atkin M, Clarke M, Goodall J, Sharp A, MacDonald T, Rubin MA, Yuan W, Barbieri CE, Carreira S, Mateo J, de Bono JS.

Clin Cancer Res. 2018 Nov 15;24(22):5585-5593. doi: 10.1158/1078-0432.CCR-18-0937.

Clinical Outcome of Prostate Cancer Patients with Germline DNA Repair Mutations: Retrospective Analysis from an International Study.

Mateo J, Cheng HH, Beltran H, Dolling D, Xu W, Pritchard CC, Mossop H, **Rescigno P**, Perez-Lopez R, Sailer V, Kolinsky M, Balasopoulou A, Bertan C, Nanus DM, Tagawa ST, Thorne H, Montgomery B, Carreira S, Sandhu S, Rubin MA, Nelson PS, de Bono JS.

Eur Urol. 2018 May;73(5):687-693. doi: 10.1016/j.eururo.2018.01.010.

CHD1 Loss Sensitizes Prostate Cancer to DNA Damaging Therapy by Promoting Error-Prone Double-Strand Break Repair.

Shenoy TR, Boysen G, Wang MY, Xu QZ, Guo W, Koh FM, Wang C, Zhang LZ, Wang Y, Gil V, Aziz S, Christova R, Rodrigues DN, Crespo M, **Rescigno P**, Tunariu N, Riisnaes R, Zafeiriou Z, Flohr P, Yuan W, Knight E, Swain A, Ramalho-Santos M, Xu DY, de Bono J, Wu H.

Ann Oncol. 2017 Jul 1;28(7):1495-1507. doi: 10.1093/annonc/mdx165.

Analytical Validation and Clinical Qualification of a New Immunohistochemical Assay for Androgen Receptor Splice Variant-7 Protein Expression in Metastatic Castration-resistant Prostate Cancer.

Welti J, Rodrigues DN, Sharp A, Sun S, Lorente D, Riisnaes R, Figueiredo I, Zafeiriou Z, **Rescigno P**, de Bono JS, Plymate SR.

Eur Urol. 2016 Oct;70(4):599-608. doi: 10.1016/j.eururo.2016.03.049.

1 Introduction

1.1 Prostate Cancer: A Global Health Issue

Prostate cancer (PC) is the third most common cancer in men, primarily affecting men aged more than 70 years, with 1.3 million new cases worldwide during 2017 [1, 2]. Different data series have presented discordant information about the frequency of this cancer; however, there is a clear trend showing increased incidence in high income countries [3], with the consequence that >70% of all new diagnoses and >50% of all PC-specific deaths occur in less than 20% of the world's population [4].

Ethnicity also seems to play a role in PC epidemiology. Men of African origin are at increased risk of developing PC and generally exhibit worse outcomes than men of Caucasian or Asian descent [3, 4]. While access to health care systems in some countries can explain some of the dramatic differences seen in incidence and mortality related to PC [4, 5], some of these clinical differences among ethnic groups can also be explained by distinct molecular differences among these populations [6].

Lifestyle and environmental risk factors can also influence the development of PC and its clinical course [7-9]. Low levels of physical activity and diets rich in animal fat can modulate ethnic differences to such a degree that Asians born in the USA have an increased risk of PC that is directly correlated with the time spent living in the USA [10]. Similarly, Asian countries known for low PC incidence and mortality have seen an upward trend in both

parameters, partially due to an increasingly Westernised lifestyle [4, 11]. It is intuitive that the level of cholesterol and its metabolism may play a crucial role in a disease that is primarily hormonal driven.

In summary, PC is a common and multifactorial disease that is one of the leading causes of death globally.

1.2 Prostate Cancer Diagnosis: Clinical Features, Management and the Role of Prostate-Specific Antigen in Early Disease

The anatomical position of the prostate results in urinary manifestations being the most common signs of prostate cancer [12]. More specifically, urinary retention, increased frequency of urination, urination hesitancy, nocturia, and haematuria are all associated with a small but statistically significant increase in the likelihood of a diagnosis of PC [12]. Other symptoms can include haematospermia and, particularly in more advanced disease, weight loss and bone pain [12-14].

Nevertheless, prostate adenocarcinomas are among the most clinically silent neoplasms, as suggested by studies of autopsies in the general population [15]. The discrepancy between the incidence of PCs and the number of cancer-related specific deaths can be explained by the indolent nature of some of these cancers [16, 17]. Herein lies a controversial aspect of the management of local prostate cancer: when stratified by risk for localised disease (such

as by Gleason score, TNM stage, or prostate-specific antigen [PSA] at diagnosis), treatments for patients in low-risk group, such as radical prostatectomy or radiotherapy, can be described as unnecessary [18].

In a similar way, the incorporation of serum PSA testing as a screening tool for PC, introduced by the medical community in the USA during the 1990s, has shown that this method is able to detect both untreatable and non-fatal tumours, as well as leaving an unknown number of tumours undetected [19]. The 'detection of cancer that would not otherwise clinically manifest or not result in cancer-related death', is, in other words, the definition of *cancer over-diagnosis* and applies to the use of mass PSA screening [20, 21]. As confirmation of this experience, in the European Randomized Study of Screening for Prostate Cancer (ERSPC) trial, which randomised 1134 men into screening or non-screening groups, a PSA cut-off concentration of 3 µg/L was used to suggest patients who should undergo a biopsy. Approximately 75% of men who underwent biopsy were found not to have cancer. Furthermore, approximately 70% of the cancers that were detected were found to be of a low grade (i.e. were likely to be indolent) [22-24].

Taken together, these experiences should inform physicians that focusing on mass screening to identify prostate cancer in its preclinical and locally confined state is not sufficient to radically cure this disease. **The scientific community should instead concentrate its efforts on defining biomarkers of '*biological aggressiveness*', in order to offer radical treatment only to those patients with localised cancers that are more likely to spread and metastasise if not promptly diagnosed and treated.**

1.2.1 Use of PSA in Risk Stratification (Prognosis)

In addition to its use in screening, PSA levels in combination with specific clinical and pathological factors are widely used to assess the prognosis of patients with newly diagnosed prostate cancer [25-27], with an approximately linear relationship existing between PSA levels at initial diagnosis and clinical outcome [27-29]. This association is particularly relevant in patients with low or intermediate grade disease (i.e. a Gleason score [GS] ≤7), while in some patients with high grade disease (GS, 8–10; PSA level ≤2.5 μg/L) it may actually predict a particularly poor outcome [28]. Notably, PSA prognostic accuracy is limited if used alone [30]. Categories of risk based on PSA levels have recently been defined in the joint guidelines produced by the American Urological Association, the American Society for Radiation Oncology, and the Society of Urologic Oncology and state that men with PSA concentrations of <10 μg/L should be classified as very low or low risk. Men with PSA concentrations of 10 to <20 μg/L should be regarded as being at intermediate risk of recurrence, while those with values ≥20 μg/L should be considered as being at high risk of recurrence, with the caveat that these values are combined with specific clinical and pathological features [31].

1.2.2 Use of PSA During Follow-up After an Initial Diagnosis

Management options for patients with newly diagnosed localised prostate cancer include radical prostatectomy, radiotherapy with or without androgen deprivation therapy (ADT), brachytherapy, and active surveillance (the last is only used for patients deemed to be at low risk of recurrence). Following successful radical prostatectomy for men with localised disease, PSA concentrations should decrease to undetectable levels (<0.1 μg/L) within 2

months [32]. Biochemical recurrence (BCR) is then defined by two consecutive increasing PSA concentrations of >0.2 μg/L [33]. Alternatively, following radiotherapy, brachytherapy or ADT, PSA levels may decrease without ever reaching undetectable levels. Therefore, in these cases, BCR is defined as an increase in PSA concentration of 2 μg/L or more above the nadir (i.e. the lowest PSA level achieved) [34].

1.2.3 Management of Patients with Biochemical Recurrence

Although the presence of BCR indicates an increased risk of clinical recurrence, many such patients continue to remain free of symptoms [35]. Following radical prostatectomy, BCR has been associated with poor outcomes mostly in patients with a short PSA-doubling time (DT) and high GS. Although there is no standardised definition of its timing, a PSA-DT of <12 months is generally correlated with an increased risk of recurrence [36]. Since many men with evidence of BCR never develop clinical evidence of recurrence, it is unclear if or when ADT should be started (i.e. whether to administer ADT at the time of biochemical relapse or await clinical evidence of metastatic disease) [29, 37-39]. Despite increasing PSA levels, some of these men will indeed show no evidence of metastasis when conventional imaging techniques are used. Such disease is referred as castrate-resistant prostate cancer (CRPC), and is defined as a 25% increase from the nadir (or at least 2 μg/L where undetectable values represent the nadir), in two consecutive PSA readings, at least 1 week apart, with testosterone levels <1.7 nmol/L (<50 ng/mL). Three prospective, randomised trials have recently shown that the administration of novel androgen receptor (AR) antagonists, such as enzalutamide, apalutamide or darolutamide, improved metastasis-free survival in men who had non-metastatic CRPC with PSA doubling times of ≤10 months [40-42].

1.3 Management of Metastatic Hormone-Sensitive and Castration-Resistant Prostate Cancer

Androgen deprivation therapy (ADT) remains a mainstay in the treatment of metastatic or relapsed PC, since the discovery 70 years ago by Huggins and others [43-45] that castration results in regression of PC. ADT can be achieved either pharmacologically, with Luteinizing-releasing hormone (LHRH) analogues, or surgically, via orchiectomy. Alternatively, some patients wishing to maintain sexual potency may elect for treatment with antiandrogens, although outcomes are inferior to ADT in the metastatic setting [46]. The management of metastatic CRPC (mCRPC) has undergone profound changes in the last two decades (**Figure 1**). The spindle toxin **Docetaxel** was the first compound to show a survival benefit in this setting. Docetaxel is a semi-synthetic analogue of paclitaxel (Taxol), an extract from the bark of the rare Pacific yew tree, *Taxus brevifolia* [47-49]. Its cytotoxic action is exerted by promoting and stabilising microtubule assembly, while preventing physiological microtubule depolymerisation/disassembly, leading to a significant decrease in free tubulin. Therefore, microtubules accumulate inside cells, preventing cell division and nuclear translocation of the androgen receptor and causing initiation of apoptosis [50].

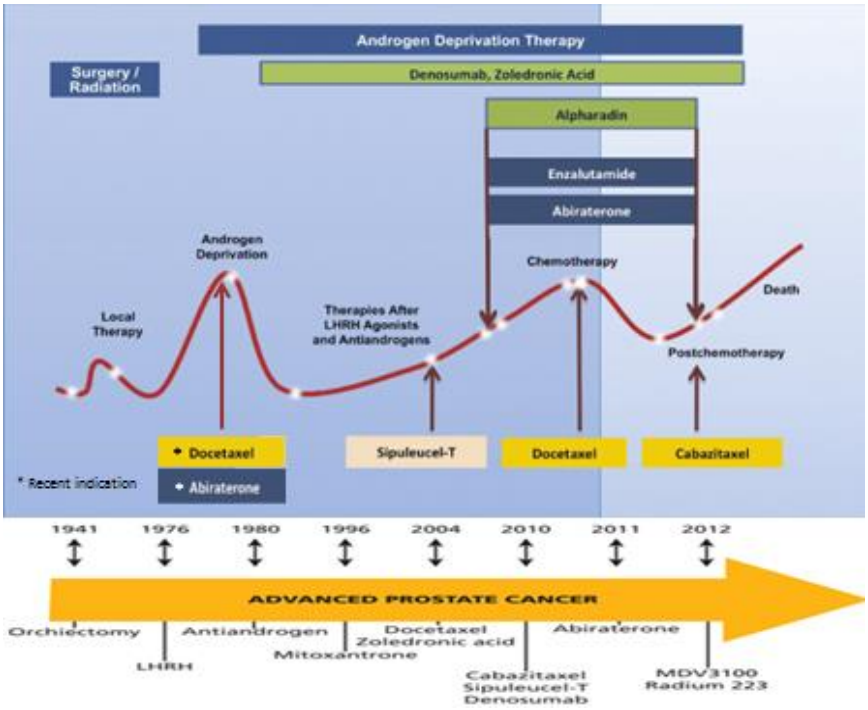

Figure 1 Changes in the management of prostate cancer, from the 1940s to the present.

Abiraterone Acetate (AA), which inhibits androgen synthesis (and thus androgen serum levels) by irreversibly binding to the enzyme CYP17A1, has been shown to increase overall survival (OS) in both pre- and post-taxane settings [51, 52]. Similarly, **Enzalutamide**, which binds directly to ARs and acts as an irreversible antagonist to these receptors, was also shown to increase OS in both taxane-naïve and taxane-resistant settings [53, 54]. These trials have conclusively proven that most tumours remain sensitive to androgen targeting agents, despite progressing on LHRH [55]; this led to the development of new compounds that disrupt this AR signalling, such as **Apalutamide**, a novel AR antagonist, which has recently been shown to increase the time to metastases in non-metastatic settings [56]. The second taxane to be approved in the mCRPC setting was **Cabazitaxel**, which improved OS in patients whose disease had progressed during or after docetaxel-based therapy [57].

Other strategies beyond cytotoxic and androgen-signalling directed interventions have also been successfully tested. The alpha-emitting radiopharmaceutical compound, **Radium-223** dichloride, which has an affinity for areas with high bone-turnover rates [58], was approved for the treatment of mCRPC with bone metastases only. In a phase III randomised placebo-controlled clinical trial, Radium-223 prolonged OS in patients with mCRPC, with a 30% reduction in the risk of death compared with the risk in the placebo group [59]. **Sipuleucel-T** is an immunotherapeutic procedure comprising the *ex vivo* activation of autologous mononuclear cells with prostatic antigens and leucocyte growth factors followed by their re-introduction into a patient's bloodstream [60]. In a phase III clinical trial, Sipuleucel-T increased the OS of patients with asymptomatic and minimally symptomatic mCRPC compared with the OS of patients in the control group [60]; however, this drug has not been deemed reimbursable in Europe.

If the management of mCRPC has changed somewhat in recent years, the treatment for metastatic hormone-sensitive PC (mHSPC) has been drastically transformed. The role of ADT in combination with other treatments or with local therapies has been investigated in many phase III trials, leading to a paradigm shift in the approach to treatment. The benefit of adding docetaxel (75 mg/m^2, for six courses) to ADT for the treatment of mHSPC was established during three phase III trials: GETUG-AFU 15 [61], CHAARTED [62] and STAMPEDE [63]. While the first of these trials demonstrated a benefit for the combination of docetaxel plus ADT in terms of PSA progression-free survival (22.9 vs. 12.9 months) and radiographic progression-free survival (23.5 vs. 15.4 months), the other two trials reported a statistically significant longer OS for patients treated within the combination arm (57.6 vs. 44 months for the CHAARTED trial and 81 vs. 71 months for the STAMPEDE trial); this advantage was

shown to be greater in patients with higher burdens of disease [61, 63]. The addition of abiraterone to ADT was demonstrated to improve OS in two phase III trials, LATITUDE and STAMPEDE [64, 65]. In both studies, abiraterone was given at a dose of 1000 mg plus 5 mg prednisone daily, until disease progression or unacceptable toxicity occurred. In a similar way, the benefit of adding enzalutamide (160 mg daily) to ADT has been established by two phase III studies, ARCHES and ENZAMET [66, 67]. However, while the primary end-point for ARCHES was improved radiographic progression-free survival (rPFS), the primary end-point for ENZAMET was OS. The advantage of using a combination treatment, in terms of OS, was also confirmed for Apalutamide in the phase III TITAN trial [68].

1.4 Molecular Landscape of Prostate Cancer

Primary and advanced PCs are characterised by multiple recurrent genomic aberrations, of which some are clonal and mutually exclusive events [69], with the most common (identified in up to 60% of tumours) being fusions involving oncogenes of the E26 transformation-specific (ETS) family [69-71]. Among these oncogenes, ERG alone accounts for 30% to 40% of cases, but other ETS family members include ETV1, ETV4 and FLI1 [69, 70, 72]. These gene fusions induce overexpression of ETS as a result of placing transcriptional regulation under the influence of androgen responsive or prostate-specific elements [70, 73]. Notably, mouse models have shown that ETS fusions alone are insufficient to generate carcinomatous cells [74, 75].

The mechanism that generates genomic rearrangements in PC is known as *chromoplexy* [76]. In chromoplexy, multiple DNA strands, commonly from distinct chromosomes recruited to transcriptional hubs, are severed and then inappropriately resolved, resulting in structural rearrangements with frequent loss of genetic material [77]. Other mechanisms implicated in chromosomal instability, such as breakage-fusion-bridge (BFB) cycles with asymmetrical chromosomal segregation, have been proposed as mechanisms that could explain the aneuploidy observed in many PCs [78].

In addition to ERG rearrangements, multiple studies have identified recurrent somatic mutations and copy number alterations in both primary and advanced PC. These include point mutations in *SPOP, FOXA1* and *TP53* and copy number alterations involving MYC, RB1, *PTEN* and *CHD1*. Tumor protein p53 (TP53) plays a role in cell cycle, apoptosis, and genomic stability, through various mechanisms. It can activate DNA repair proteins when DNA has sustained damage, and it can arrest growth by pausing the cell cycle at the G1/S regulation point upon recognition of DNA damage. If the damage to DNA proves to be irreparable, TP53 can initiate the process of programmed cell death, or apoptosis [79]. Along with the alterations in *PTEN*, changes affecting *TP53* are the most common aberrations in PC [80]. The speckle-type POZ protein (*SPOP*) gene encodes a component of the E3-ubiquitin ligase complex which, functionally, acts as a tumour suppressor by targeting pro-oncogenic factors for degradation [81, 82]. Forkhead box A1 (*FOXA1*) is a winged-helix pioneering transcription factor of the forkhead superfamily that binds to compact chromatin and relaxes it, facilitating the binding of hormonal transcription factors, including the androgen receptor [83]. Both oncogenic and tumour suppressive functions have been reported for this gene. Chromodomain helicase DNA-binding protein 1 (CHD1) is an ATPase-dependent helicase

that mediates a variety of biological processes, including the maintenance of open chromatin, DNA damage repair, and transcription [84]. The retinoblastoma protein (RB1) is a tumour suppressor protein and is one of the main regulators of the cell cycle, preventing it progressing from the G1 (first gap) to the S (synthesis) phase [85].

Alterations in ERG and PTEN usually co-occur, in line with their synergistic role in promoting oncogenesis, while CHD1 alterations tend to co-occur with *SPOP* mutations [85]. On the other hand, *TP53* and *RB1* mutations occur at high frequency in neuroendocrine PCs [86, 87], conferring an aggressive behaviour [88, 89]. However, RB1 alterations have a tendency toward mutual exclusivity with alterations in AR. Notably, although primary and advanced PCs show similarities in terms of the disrupted pathways involved in their biology and evolution, advanced PCs show significantly higher mutational and copy number aberrations due to their higher genomic instability [90-92]. It remains unclear whether these differences are the result of different evolutionary processes in response to therapy exposure, or whether they reflect different disease sub-types with differing outcomes.

Overall, at least seven major pathways are disrupted in mCRPC: i) androgen signalling and splicing variants, ii) PI3K-Akt, iii) cell cycle, iv) chromatin remodelling, v) DNA repair, vi) Wnt-signalling, and vii) RAS-RAF-MEK-ERK (**Figure 2**) [92]. Throughout this project, I have investigated new biomarkers associated with some of these pathways, with the aim of identifying specific subtypes of mCRPC and improving patient care through a more precise and personalised approach.

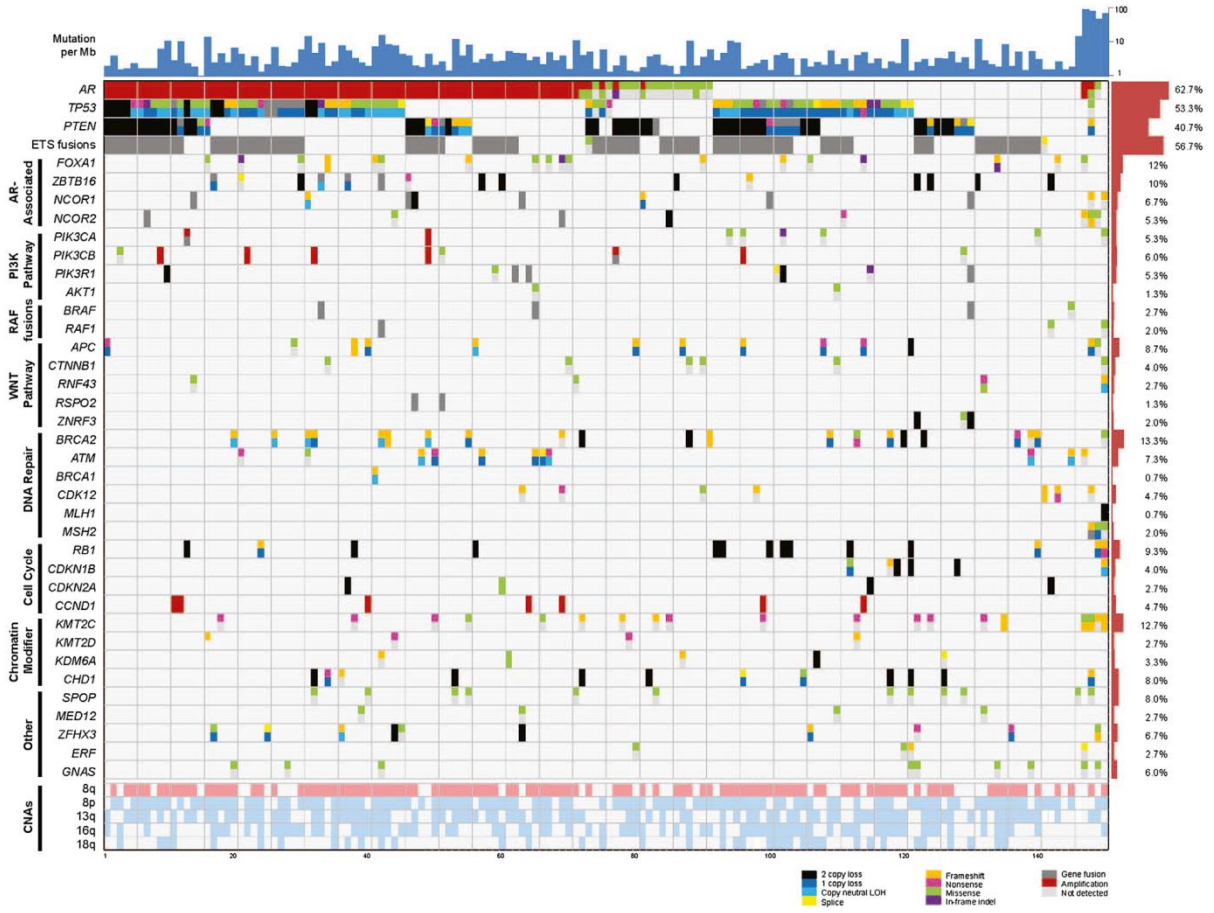

Figure 2 Integrative landscape analysis of somatic and germline aberrations in metastatic CRPC obtained through DNA and RNA sequencing of clinically obtained biopsies, taken from [90].

1.4.1 Biomarkers in Prostate Cancer

A biomarker is '*a characteristic that is objectively measured and evaluated as an indicator of normal biologic processes, pathogenic processes, or pharmacologic responses to a therapeutic intervention*' [93]. The successful use of biomarkers requires thorough analytical validation and determination of assay reproducibility and variability. Biomarkers can be of vital importance to early clinical trials, ensuring that the key scientific/clinical questions are addressed and answered with confidence [94]. Biomarkers may be categorised as either pre-treatment or post-treatment measures. Pre-treatment biomarkers can be prognostic or aid in the selection of study participants; post-treatment biomarkers function as

pharmacodynamic or intermediate ('surrogate') end-points and can act as substitutes for a clinical end-point.

Prognostic biomarkers

A *prognostic biomarker* is a clinical or biological characteristic that provides information on likely patient health outcomes (e.g. disease recurrence, overall survival), irrespective of their treatment.

Pharmacodynamic (PD) biomarkers

PD biomarkers are useful for proof of mechanism studies, to confirm target and pathway modulation (i.e. confirmation of target blockade) and, in phase I trials, to help identify the biologically active dose range [95]. They are usually conducted in easily acquired tissue, such as hair follicles, whole blood or plasma, or less accessible tumour biopsies. However, PD biomarkers can be affected by inter-patient variation, which can influence both treatment-related responses and toxicities [95, 96]. PD biomarkers might involve immunohistochemistry (IHC) or immunofluorescence, or they may involve more quantitative assays, such as enzyme-linked immunosorbent assays (ELISA).

Predictive/intermediate end-point biomarkers

Predictive biomarkers indicate the likely benefit to a patient from a treatment (or their lack of response), compared with their condition at baseline [97]; they can also be useful in proof of concept studies, to interrogate the hypothesis in question. Predictive biomarkers can be used for selecting patients for treatment with biologically active drug doses, and may

involve DNA sequencing, fluorescent *in situ* hybridization, gene expression or genomic analysis, or IHC [98].

Intermediate end-point biomarkers are usually used to identify the anti-tumour activity imparted by drug effects and to acquire proof of concept. They can include radiological measurement of tumours (by computerised tomography scans), measures of tumour cell proliferation (e.g. Ki67 immunostaining), apoptosis (e.g. cleaved caspase 3 immunostaining), evaluation of antiangiogenic effects (e.g. by dynamic contrast enhanced magnetic resonance imaging), evaluation of circulating blood biomarkers such as tumour markers (PSA), or circulating tumour cell (CTC) counts.

Below, I will describe some of the prognostic and predictive biomarkers associated with the pathways that are most commonly disrupted in prostate cancer.

1.4.1.1 Androgen Signalling

The AR is a nuclear steroid hormone receptor that contains a central DNA-binding domain (DBD), a ligand-binding domain (LBD), a hinge region and a large N‑terminal domain (NTD) [99]. A genomic aberration involving a component of the androgen signalling pathway is present in >70% of mCRPCs and, in >60% of these tumours, AR is directly affected [90]. Focal amplification of Xq11-Xq12 (the locus of *AR*), which induces overexpression of the receptor, is the most common genomic aberration of the androgen signalling axis and is present in 30% to 50% of CRPCs [90, 100]. Point mutations of *AR* involve changes to the LBD which alters the receptor specificity and allows promiscuous activation by anti-androgens (which

activate, for example, AR-T878A and AR-W741C mutants), glucocorticoids (which activate AR-L702H), and adrenal androgens and progesterones (which activate AR-V715M) [55]. Clinical data indicate that these aberrations confer resistance to abiraterone [101, 102], and **can therefore be used to predict a patient's lack of response to AR-targeting agents.**

Persistent AR signalling can also be maintained by alternative splicing of AR mRNA [103]. The abnormal variants allow a constitutively active status of ARs without requiring a cognate ligand [104]. The detection of splice variants of AR, particularly AR-V7, has been shown to confer resistance to abiraterone and enzalutamide in PC models [105, 106], and this also correlates with a lack of response to these anticancer treatments in patients [107]. By using an AR-V7 targeting antibody in an immunofluorescence study of CTCs, Scher and colleagues showed that patients with AR-V7 positive CTCs exhibited better OS when treated with taxanes compared with OS in patients following treatment with AR signalling agents [108], providing evidence that **splice variants could be a useful predictive biomarker and assist physicians to tailor treatment to patients.**

PSA is a pivotal downstream target gene of the AR. As a blood-based cancer biomarker, PSA offers the unique opportunity to be used during all of the main phases of prostate cancer detection and patient management (i.e. in screening, risk stratification for recurrence, surveillance following diagnosis, and monitoring therapy). Its role during the early stages of the disease was described in the previous section. In advanced disease, its role is more controversial. One of the problems when using PSA to monitor responses to ADT, for example, is related to the fact that PSA production is controlled by androgens; this therapy can therefore lower PSA levels without necessarily impacting tumour bulk. Although PSA is

used in assessing responses to standard treatments for mCRPC, **changes in the levels of this biomarker have been associated with patients survival** [108, 109].

In ***Chapter 3,*** I describe the association between clinical outcomes and early PSA changes in mCRPC patients treated with abiraterone and enzalutamide, as well as the prognostic role of AR-V7 status detected in tissues and circulating tumour cells.

1.4.1.2 PI3K-AKT Pathway

Genomic aberrations in the PI3K-AKT axis are common in primary PC and are enriched in mCRPCs [90, 92]. Hyperactivity of this pathway promotes cell growth, cell cycle progression, and cell proliferation [110]. This frequently occurs a result of *PTEN* inactivation, which acts as a negative regulator of the pathway, but may also occur due to genomic aberrations in *PIK3CA*, *PIK3CB*, *PIK3R1*, *PIK3R3* and *AKT1* [90, 111]. Notably, a negative feedback loop between AR signalling and the PI3K-AKT pathway has been demonstrated *in vitro* [112, 113], such that the inhibition of either one results in the activation of the other. This phenomenon suggests that the inhibition of both pathways might represent a strategic treatment option to improve outcomes in mCRPC.

Genomic inactivation of *PTEN*, mainly through the loss of its locus on 10q23.31, is by far the most common molecular aberration involving the PI3K-AKT axis, and occurs in approximately 40% of CRPCs [90, 92, 114-116]. However, mutations and complex genomic rearrangements, including inversions, can also occur [76, 117, 118]. IHC assays have consistently shown that the loss of PTEN expression is associated with poor prognostic

factors, such as an overall higher GS [119], as well as the upgrading, in prostatectomy specimens, of low-grade tumours based on the GS of needle biopsies [120]. Overall, these data indicate that the loss of PTEN expression delineates an aggressive subset of tumours.

In Chapter 4, I show that PTEN loss as indicated by IHC is associated with shorter overall survival and shorter response times to abiraterone, whereas no difference in terms of response to docetaxel chemotherapy is seen between PTEN-loss and PTEN normal groups.

Finally, the availability of compounds which are able to inhibit PI3K kinases and other downstream targets, such as AKTs, raise the possibility that **aberrations in the PI3K-AKT pathway might be a useful predictive biomarker to these drugs.**

1.4.1.3 DNA-Repair Defects

Pathogenic germline variants in DNA repair genes are found in approximately 12% of men who progress to advanced PC [121], with somatic aberrations found in nearly a quarter of CRPCs [90, 114]. Genes involved in homologous recombination (HR), including *BRCA2, BRCA1, PALB2* and *ATM*, are the ones most commonly affected in CRPC [90, 114], which has important clinical implications. Patients with deleterious germline *BRCA2* mutations have an overall increased risk of PC [122, 123]; however, the prognostic value of these aberrations and their usefulness in predicting responses to standard treatments for mCRPC remain controversial [124, 125]. Targeting cancers with HR defects through a synthetic lethal model has proven successful in carcinomas of the breasts and ovaries [126, 127], and more

recently the anti-tumour activity of olaparib, a poly-(adenosine diphosphate [ADP]-ribose) polymerase (PARP) inhibitor has also been demonstrated in mCRPC patients with both somatic and germline aberrations in HR genes [128]. This study led to the US Food and Drug Administration (FDA) granting a 'Breakthrough Designation' in January 2016 to support the accelerated approval of olaparib as a monotherapy for mCRPC patients with mutated *BRCA1, BRCA2* or A*TM* genes.

Other forms of DNA repair, including mismatch repair (MMR), have also been implicated in mCRPC, with individuals with Lynch syndrome who are carriers of deleterious aberrations of MMR genes also associated with increased prostate cancer risk [129, 130]. The prevalence of MMR aberrations ranges between 3% and 12%, depending on the assay and population selected [90, 129, 131]. MMR deficiency (dMMR) is associated with microsatellite instability (MSI) and a high mutational load. Since a high mutational load is correlated with increased numbers of tumour-specific neoantigens, this could represent a new biomarker of responses to novel immunotherapy strategies that activate cytotoxic T cell (CTL) responses [132, 133].

In **chapter 5,** I present data derived from a phase II trial that investigated the efficacy of olaparib in a population of mCRPC patients who were selected based on HR defects, and I demonstrate how **circulating free DNA (cfDNA) analyses can provide predictive, prognostic, response, and resistance data in patients treated with olaparib**. Furthermore, by using conventional assays already approved for the detection of dMMR colorectal carcinomas, i.e. IHC of MMR proteins and the Promega v1.2 PCR-based MSI assay, I studied the prevalence of these aberrations in a cohort of >100 mCRPC samples. Using targeted sequencing data, I determined the mutational load and MSI based on the satellites present

in the panel and show that, although some dMMR mCRPCs show higher mutational rates and MSI, some clearly lack these features. Finally, using multispectral imaging, computer image analyses, and PD-L1 IHC staining, I show that, although PD-L1 positivity is more common in dMMR tumours, some MMR-proficient mCRPCs can be highly inflamed and also express this immune-checkpoint marker.

2 Hypothesis and Overall Objectives

2.1 Core Hypothesis

Molecular characterization of prostate cancers leads to improved prognostication and patient stratification.

2.2 Driving Hypothesis for Each Chapter

- **Chapter 3: Relevance of androgen receptor (AR) signalling in metastatic castration-resistant prostate cancer (mCRPC).**

I hypothesised that i) ***Prostate-specific antigen (PSA) remains a useful biomarker in the castration-resistant setting in patients receiving hormonal treatment (such as abiraterone and enzalutamide), since it is a pivotal downstream target gene of the AR.*** Therefore, ii) ***Interrogating serum PSA level at as early as 4 weeks from treatment initiation correlates with responses to second generation hormonal agents (SGHA) and overall survival***. iii) ***AR splicing variant 7 (AR-V7) expression, which is negligible in hormone-naïve PC, increases as patients progress into mCRPC, correlates with prognosis and can explain resistance to SGHA.***

- **Chapter 4: PTEN loss and activation of its pathway: A prognostic and predictive biomarker.**

I hypothesised that i) ***Carcinomas of the prostate which exhibit loss of PTEN expression are clinically aggressive and will often relapse with PTEN-negative disease,*** ii) ***patients with PTEN loss do not benefit from treatment with SGHA but respond as well as PTEN-***

proficient patients to docetaxel, *and iii)* ***patients with impaired PTEN/PI3K/AKT pathway can benefit from combined AR and AKT blockade.***

- **<u>Chapter 5: DNA-repair defects as new targets for treatment of mCRPC.</u>**

I hypothesised that i) ***Patients with defects in the DNA repair system known as homologous recombination (HR) will benefit from treatment with PARP inhibitors and*** ii) **circulating free DNA (cfDNA) analyses can provide predictive, prognostic, response, and resistance data in patients treated with the PARPi olaparib.** iii) ***Cancers with defective mismatch repair machinery (dMMR) will characteristically exhibit a high mutational load and microsatellite instability in lethal prostate cancer, with increased lymphocytic infiltration and PD-L1 expression compared with those of non-dMMR tumours,*** iv) ***dMMR tumours have a distinct clinical behaviour compared with that of non-dMMR tumours***, and therefore v) ***patients affected by dMMR PC constitute the ideal subset to treat with immunotherapies***.

2.3 Overall Objectives

I) To ***determine the prognostic and predictive power of the biomarkers*** studied in this project.

II) To ***identify new treatment targets in metastatic castration-resistant prostate cancer (mCRPC)***.

III) To ***explore the clinical relevance of DNA-repair defects in mCRPC.***

3 Relevance of Androgen Receptor (AR) Signalling in Metastatic Castration-Resistant Prostate Cancer (mCRPC): Prognostic/Predictive Biomarkers of Responses to Hormonal Agents

3.1 Background

Androgen signalling is crucial for the development, differentiation and stability of the prostatic epithelium, but plays also a determinant role in the pathogenesis of PC. Therefore, androgen deprivation treatment (ADT) has long been the mainstay of therapy for advanced PC. For decades it was thought that tumours progressing in patients on ADT were hormone refractory and therefore independent of androgen signalling. This paradigm shifted during the early 2000s with the development of second generation hormonal treatments, such as abiraterone acetate (AA), leading to a change in nomenclature (i.e. introduction of the term castration-resistant) and, more importantly, in the pharmacological strategies employed to treat this disease.

Androgen signalling is mediated by the androgen receptor (AR), a 110-kDa hormonal nuclear receptor and encoded by an 8-exon gene that maps to Xq11-Xq12 (Figure 1). Exon 1 encodes the amino-terminal (NTD) domain of the receptor and contains transactivation units 1 and 5 (TAU1 and TAU5), which are essential for AR transcriptional activation [134]. The NTD domain is variable in length due to CAG*n* and CGN*n* repeat units which, in extreme cases, are associated with Kennedy's disease [135]. Exons 2 and 3 encode the zinc fingers

that constitute the highly conserved DNA-binding domain (DBD). Exons 4–8 encode a flexible hinge region, the ligand-binding domain (LBD) and the transcriptional activation function 2 (AF2) co-regulator binding interface.

One of the pivotal downstream target genes of AR, prostate-specific antigen (PSA), is a member of the human kallikrein (KLK) family of serine proteases [136], which are synthesised as preproenzymes [137] then proteolytically processed by removal of the signal peptide prior to secretion as inactive proenzymes. PSA levels often increase in the serum of PC patients, and PSA has been used, although not without controversy, as an easily accessible and clinically relevant biomarker for early diagnosis as well as signalling the emergence of recurrent, castration-resistant disease [138, 139]. PC working group 3 (PCWG3) criteria recommend reporting PSA response as a continuous variable in the form of waterfall plots, although declines in PSA levels of both 30% and 50% are also commonly reported, usually at the nadir and at 12 wk from the start of anticancer treatment, and both are associated with improved survival [140]. A 30% decline in PSA has been consistently shown to have a stronger association with survival than a 50% decline [141-143]. Similarly, PSA progression according to PCWG3 criteria is associated with shorter survival times [66, 144]. Despite these findings, no studies have validated PSA decline as a surrogate of overall survival (OS), although a recently published pooled analysis of the COU-301 and COU-302 trials indicated that PSA kinetics, including PSA doubling time, satisfied the Prentice criteria for OS surrogacy [145]. Defining the best time to assess response is also challenging. According to the PCWG3 criteria, PSA progression should not be determined during the first 12 weeks because of late responses and flare reactions [140, 146, 147]. Therefore, there are

insufficient data regarding the clinical relevance of early changes in PSA levels in patients with mCRPC treated with abiraterone acetate (AA) [148].

In this chapter, I report on an international study involving thirteen cancer centres that evaluated the association between early PSA changes (after 4 weeks of treatment) and outcomes from mCRPC after treatment with AA and enzalutamide. We envisioned that early changes in PSA levels could help facilitate earlier decisions to switch treatment.

Different genomic aberrations involving the AR gene have been described as a possible mechanism of resistance to AR targeting agents in the CRPC setting, particularly copy number gains but also point mutations clustering at the ligand-binding domain. Often induced by the selective pressure exerted by ADT, these alterations can help cancer cells to proliferate in an androgen-starved environment [90]. There is a large subset of CRPCs, however, for which a genomic mechanism of androgen signalling reactivation cannot be identified. Recently, alternative splicing of AR has emerged as a putative mechanism of AR signalling reactivation in CRPC.

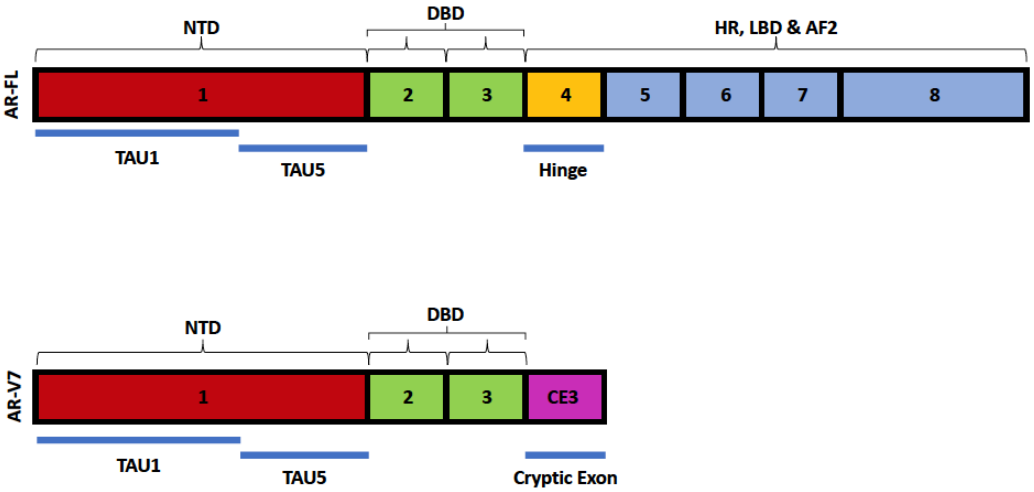

Figure 1 Schematic representation of the androgen receptor (AR) structure. AR-FL (full length) consists of an amino-terminal domain (NTD) of variable length encoded by exon 1, a DNA-binding domain (DBD) encoded by exons 2 and 3, and a hinge region (HR), a ligand-binding domain (LBD) and a co-regulator-binding interface domain (AF2). Almost 20 AR splice variants have been reported, of which AR-V7 is among the most abundantly expressed.

The use of splicing enables eukaryotic cells to remove non-coding (intronic) segments from newly synthesised RNA strands [149]. More than 90% of human pre-mRNA species are thought to be amenable to alternative splicing [150], increasing the repertoire of mature mRNA transcripts that participate in the development of complex tissues and giving cells the flexibility to cope with stress and injury [151, 152]. However, alternative splicing may also play a key role in the pathophysiology of human malignancies [153]. In this context, AR splice variants, and particularly AR-V7, have been considered as potential negative predictive biomarkers for anti-androgenic therapy [107].

To date, almost 20 different AR splice variants have been reported [154, 155]; most of them lack the ligand-binding domain, and some have been shown to be able to drive androgen signalling in the absence of AR ligands [156]. The splice variant AR-V7 is the most common of the AR splice variants [157]. It is characterised by the insertion of a cryptic exon, 3Eb, and it is formed by the transcription and splicing of a segment of intron 3 into the mature mRNA transcript (Figure 1). The unique sequence of this cryptic exon could, hypothetically, generate a highly specific peptide which could be targeted and quantified by immunophenotyping assays.

In this chapter, I present data suggesting that expression of AR-V7 in tumour and CTCs are prognostic of poor survival and can therefore be used as a putative predictive biomarker of no response to enzalutamide or AA.

3.2 Specific Aims

- To study the correlation between early changes in serum levels of PSA, responses to second generation hormonal agents (SGHA), and overall survival.
- To determine the prognostic and predictive power of AR splice variant 7 (AR-V7) expression in tumour and CTCs.

3.3 Results

3.3.1 Early Post-treatment Changes in PSA Following Abiraterone and Enzalutamide Treatment for Advanced Prostate Cancer: An International Collaborative Analysis

I identified 1358 patients treated with either AA or enzalutamide as a first-line hormonal agent for mCRPC in the pre- or post-chemotherapy setting in a cooperative effort involving thirteen cancer centres worldwide. A total of 1133 patients had a PSA result available after 4 wk, with survival data, while 948 patients had PSA results available at both 4- and 12-wk time-points; of these, 938 patients had survival data. Overall, 583 of 1133 (52%) patients

had a 30% PSA decline at 4 wk. Of the 948 patients with PSA results available at both 4 and 12 wk, 432 of 494 (87%) patients achieved a PSA decline at 4 and 12 wk. PSA at 4 and 12 wk were strongly correlated (r = 0.91; 95% confidence interval [CI]: 0.90–0.92; p < 0.001). Conversely, 11 of 152 (7%) patients progressing by PSA at 4 wk, which represented 1.1% of the overall population, met the criteria for a 30% PSA decline at 12 wk (Table 1).

Table 1 Relationship between week-4 and week-12 PSA changes in patients on first-line regimen of abiraterone acetate or enzalutamide.

PSA change at week 4	PSA change at week 12		
	No change	Progression	Decline
No change	113 (37%)	100 (33%)	89 (29%)
Progression	19 (13%)	122 (80%)	11 (7%)
Decline	48 (10%)	14 (3%)	432 (87%)

PSA = prostate-specific antigen.

Table 2 Landmark (week 4) multivariable Cox model for association with overall survival.

	n	%	HR	95% CI	*p* value
PSA change after 4 wk					
No change	344	30	1.00	–	<0.001
Progression	206	18	1.38	0.99–1.94	–
Decline	583	52	0.67	0.51–0.88	–
Chemotherapy status					
Prechemotherapy	531	47	1.00	–	<0.001
Postchemotherapy	602	53	1.67	1.26–2.22	–
PSA change × chemotherapy status					
No change and postchemotherapy	188	31	1.00	–	0.75
Progression and postchemotherapy	111	18	0.87	0.57–1.34	–
Decline and postchemotherapy	303	50	0.89	0.63–1.25	–
Treatment					
Abiraterone	911	80	1.00	–	0.13
Enzalutamide	222	20	0.84	0.67–1.05	–
Gleason Index at diagnosis					
<8	519	53	1.00	–	0.86
≥8	464	47	1.02	0.85–1.22	–
M status at diagnosis					
M0	469	43	1.00	–	0.79
M1	612	57	1.02	0.86–1.22	–
N status at diagnosis					
N0	428	61	1.00	–	0.44
N1	278	39	1.08	0.88–1.32	–
T status at diagnosis					
T <3	253	35	1.00	–	0.89
T ≥3	465	65	0.98	0.80–1.21	–
Opiates at start of treatment					
No	745	68	1.00	–	<0.001
Yes	350	32	1.46	1.22–1.73	–
Lab values at start of treatment	**Med**	**IQR**	**HR**	**95% CI**	***p* value**
Hb (log_{10} g/dl)	1.08	1.02–1.11	0.95	0.62–1.46	0.8
ALP (log_{10} U/l)	2.07	1.88–2.37	2.28	1.86–2.81	<0.001
LDH (log_{10} U/l)	2.32	2.23–2.50	1.62	1.14–2.28	0.007
NLR (log_{10})	0.48	0.30–0.62	1.57	1.12–2.20	0.008

A 30% PSA decline at 4 wk was associated with longer OS (median: 23 mo; 95% CI: 21–25) compared with OS in patients with no change (median: 17 mo; 95% CI: 15–18) or progression (median: 13 mo; 95% CI: 10–15; Figure 2). The results from multivariable Cox models, adjusted for known prognostic factors for mCRPC, such as alkaline phosphatase (ALP), LDH, and neutrophils to lymphocytes ratio (NLR) are shown in **Table 2**.

Patients with a 30% PSA decline at 4 wk had a reduced incidence of mortality compared with mortality in patients with no change in PSA (adjusted hazard ratio [aHR]: 0.67; 95% CI: 0.51–0.88, $p < 0.001$); there was no statistically significant evidence of a difference in terms of reduced mortality for patients with a 25% increase in PSA compared with that in patients with no change (aHR: 1.38; 95% CI: 0.99–1.94). The results at the 12-wk time point were similar, with a 30% decline in PSA associated with longer OS (median: 22 mo; 95% CI: 19–24; HR: 0.71, 95% CI: 0.50–1.02, $p < 0.001$) compared with OS in patients with no change in PSA (median: 16 mo; 95% CI: 12–18) or progression (median: 11 mo; 95% CI: 8–13; Figure2).

When the AA and enzalutamide groups were considered separately, there was no evidence that the association between OS and declines in PSA differed by first-line treatment. There was no formal evidence of a difference in survival for patients with no change at 12 wk compared with survival in those with a 30% decline (HR: 0.71; 95% CI: 0.50–1.02) or a 25% increase (HR: 1.44; 95% CI: 0.97–2.14).

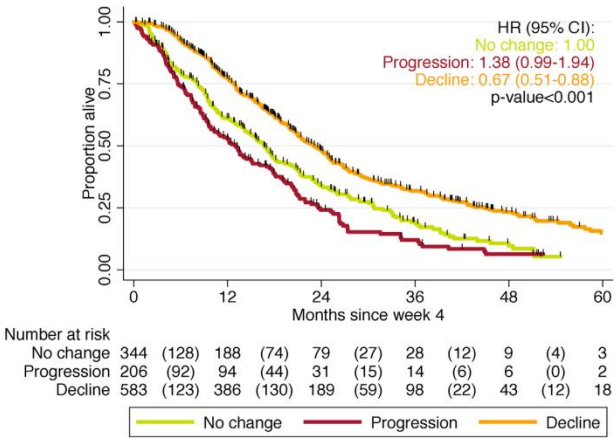

Figure2 Kaplan–Meier curves of overall survival by change in PSA at 4 wk. CI = confidence interval; HR = hazard ratio; PSA = prostate-specific antigen.

3.3.2 Nuclear AR-V7 and AR-NTD Expression Increases as Prostate Cancer Becomes Castration Resistant and Increases Further with Abiraterone Acetate and/or Enzalutamide Resistance

To investigate changes in the nuclear expression of AR-V7 and AR-NTD, we studied matched hormone-sensitive prostate cancer (HSPC) and CRPC tissue from 33 patients. Four extra unpaired CRPC samples were also available. To compare the H-scores of each disease state in our patient cohort, samples were divided into HSPC, pre-abiraterone acetate (AA)/enzalutamide (EZ) CRPC, and post-AA/EZ CRPC; H-score data for AR-V7 and AR-NTD expression were calculated from IHC.

The levels of nuclear AR-V7 expression significantly increased (Mann–Whitney test; $p < 0.0001$) as patients progressed from HSPC (median HS 50, IQR 17.5–90) to CRPC (HS 135, IQR 80–157.5) (Figure 8A). Although an increase in nuclear AR-V7 H-scores in CRPCs (26/35; 74.28%) was the norm, a small subset of cases did show expression levels that were either similar to or higher in HSPCs (Figure 8A). A similar trend was observed with AR-NTD nuclear

expression, with HSPCs showing significantly lower H-scores (HS 80, IQR 60–110) ($p < 0.0001$) than CRPCs (HS 180, IQR 95–215) (Figure 3). To determine the effect of AA or EZ treatment on nuclear AR-V7 and AR-NTD expression, patients with CRPC biopsies (n = 37; 33 patients from the matched cohort and four patients with CRPC biopsies only) who received treatment with AA or EZ were divided into two groups: patients who had biopsies prior to AA or EZ treatment (n = 14) and patients who had biopsies following AA or EZ treatment (n = 21). These were compared with the HSPC biopsies (33 patients from the matched cohort).

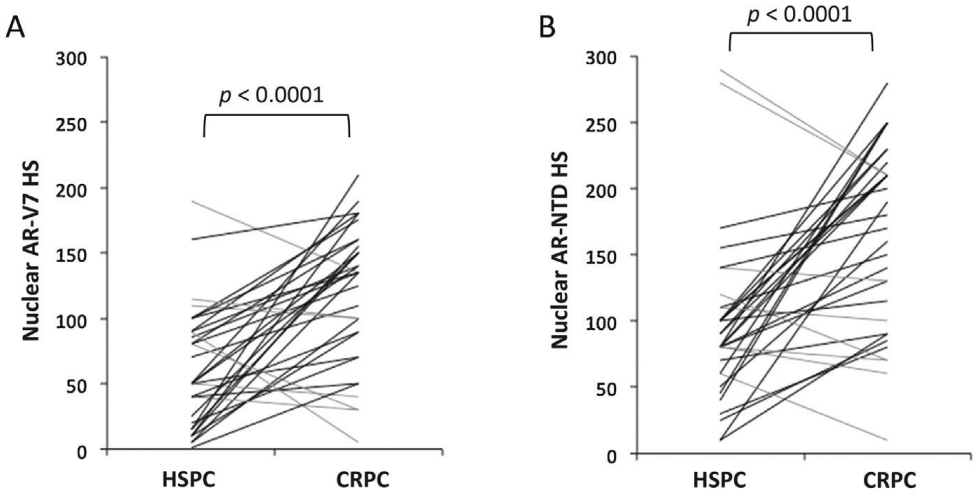

Figure 3 (A) The majority of cases showed an increase in AR-V7 nuclear H-scores using the EP343 IHC assay. Some cases showed a decrease in V7 expression. (B) AR-NTD IHC also showed a significant increase in CRPCs compared with that in HSPCs.

Mean nuclear AR-V7 expression showed a progressive increase from HSPC (HS 50, IQR 17.5–90) to pre-AA/EZ mCRPC (HS 80, IQR 30-136.3), reaching the highest levels in post-AA/EZ mCRPC (HS 105; 105-167.5) (Figure 4). Importantly, although the differences in AR-V7 H-scores were statistically significant when post-AA/EZ CRPC samples were compared with either HSPC or pre-AA/EZ CRPC samples (Mann–Whitney; $p < 0.0001$ and $p = 0.007$, respectively), differences between HSPC and pre-AA/EZ CRPC samples were not significant (Mann–Whitney; $p = 0.139$) (Figure 4). Overall, **these data showed that nuclear AR-V7 expression increases as prostate cancer becomes castration-resistant and increases**

further with AA and/or EZ resistance. Nuclear AR-NTD H-scores were significantly higher in CRPCs compared with those in HSPCs, but lower when pre- and post-AA/EZ samples were compared.

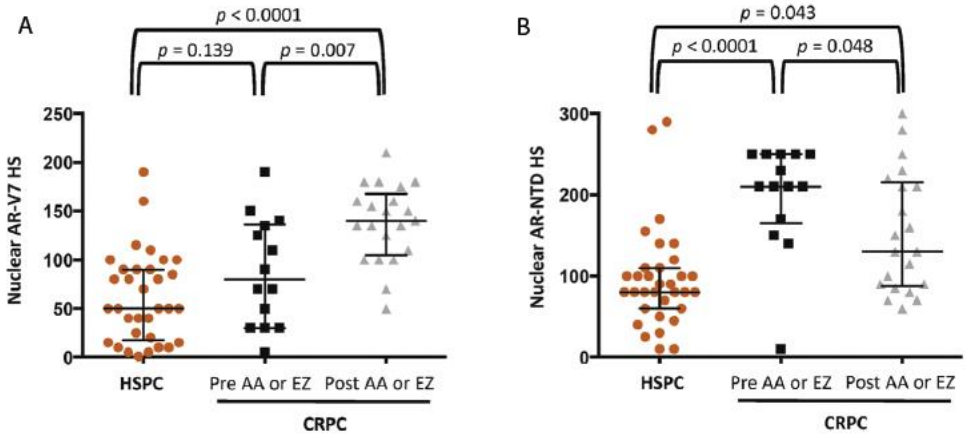

Figure 4 (A) Mean nuclear H-scores using EP343 IHC increased as tumours transitioned into the castration-resistant state, further increasing after resistance to AA/EZ developed. (B) AR-NTD nuclear H-scores increased from HSPC to CRPC, but was lower when pre- and post-AA/EZ cases were compared.

3.3.3 Nuclear AR-V7 Expression Levels but not AR-NTD Levels are Associated with Worse CRPC Prognosis

Thirty-seven patients had CRPC biopsies and were evaluable for OS from the time of CRPC biopsy. To determine the prognostic significance of AR-V7 IHC levels determined using the EP343 assay, OS from the time of CRPC biopsy was evaluated and the association of OS with nuclear AR-V7 and AR-NTD H-scores was investigated. The ratio of nuclear AR-V7/AR-NTD H-scores in CRPC biopsies was also queried as a prognostic biomarker. Baseline characteristics for the 37 patients included in these analyses are shown in **Table 3**.

Table 3 Patient demographics and clinical data

Parameter	Results
Median age, yr (IQR)	67.5 (64.2-75.3)
ECOG PS, n (%)	
0	4 (10.8)
1	32 (86.5)
2	1 (2.7)
Visceral metastasis at dx (n)	12
Lung	4
Liver	7
Adrenal	1
Treatment at/before dx (%)	
Docetaxel	28 (75.7)
Cabazitaxel	9 (24.3)
Abiraterone	20 (54.1)
Enzalutamide	3 (8.1)

The median OS from the time of CRPC biopsy was 10.7 mo (95% CI 8.9–12.5). Overall, the nuclear EP343 AR-V7 H-score as a continuous variable had a small but statistically significant effect on OS (HR 1.012, 95% CI 1.004–1.020; p = 0.003). For the survival analysis, I compared the upper quartiles of the AR-V7 and AR-NTD nuclear H-scores with the remaining lower three quartiles, aiming to determine whether the extremes of high expression adversely impact prognosis. The mean OS from biopsy was 12.52 months (IQR 9.713–15.33). A statistically significant difference was observed (log-rank test; p = 0.0002) between the two groups, with the mean OS from biopsy of patients in the upper quartile of CRPC nuclear AR-V7 H-scores being 6.37 months (95% CI 3.456–9.169), which was less than half that of the

remaining population, i.e. 14.52 months (95% CI 11.19–17.84) (Figure 5 A). In contrast, differences in OS from biopsy between the upper quartile of nuclear AR-NTD H-scores and the remaining population were not statistically significant (p = 0.9783; HR 0.8363, 95% CI 0.3933–1.778) (Figure 5 B).

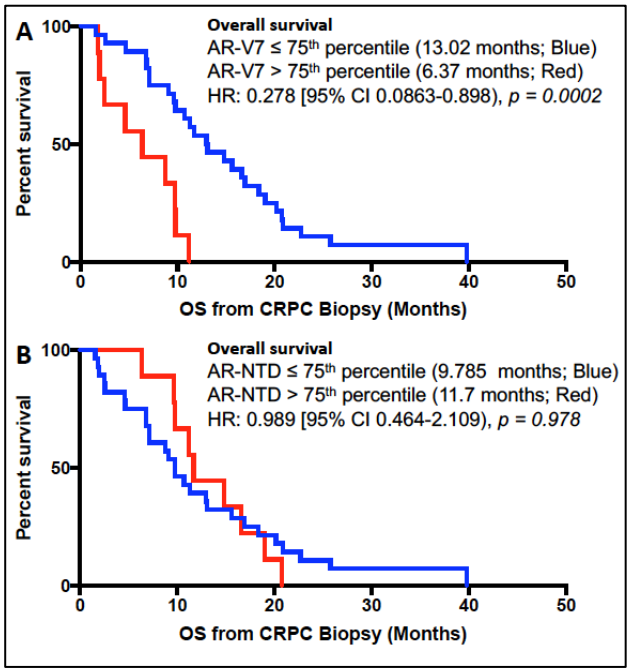

Figure5 (A) Kaplan–Meier (KM) curves of the AR-V7 IHC top quartile vs. the remaining population. EP343 IHC staining was prognostic. (B) KM curves of the AR-NTD IHC top quartile vs. the remaining population were not prognostic.

3.3.4 Nuclear AR-V7 Expression and Response to AA

Twelve patients had CRPC biopsies prior to treatment with AA and evaluable PSA response data. The median time for a CRPC biopsy before AA treatment initiation was 2.0 mo (IQR 0–9). There was a significant association between the magnitude of PSA decline at 12 wk and the AR-V7 HS (p = 0.043). Two (17%) patients experienced PSA responses (50% change from the baseline) after 12 wk of treatment (Figure 6). Patients who responded to AA had lower

median nuclear AR-V7 (n = 2; HS 30, IQR 30–30) than patients who did not respond (n = 10; HS 80, IQR 45–128.8), although the difference was not significant (p = 0.197).

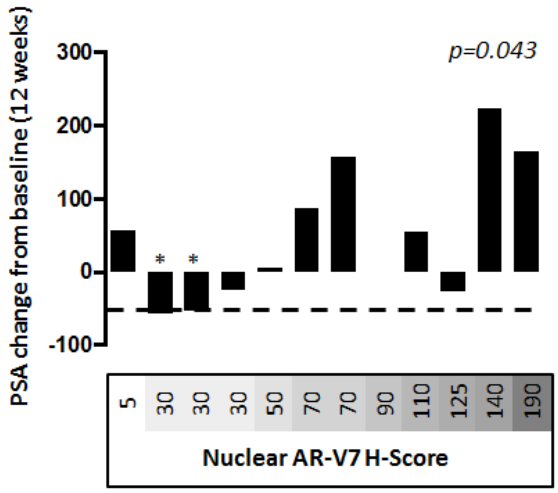

Figure 6 Percentage PSA response at 12 weeks compared to baseline is shown for patients treated with abiraterone ranked in order of their nuclear AR-V7 H-score. Dotted line represents >50% decrease in PSA and patients meeting this are shown (*). p-value for the association between the magnitude of PSA decline at 12 weeks and nuclear AR-V7 expression using univariate linear regression model is shown.

3.3.5 CTC AR-V7 positivity is associated with more advanced disease

Having analysed the prognostic role of ARV7 status by IHC in tissue, we then evaluated the relevance CTC AR-V7 status based on Adna-Test in mCRPC, compared CTC AR-V7 status with clinical characteristics and determined its impact on clinical outcomes.

The AdnaTest was performed on 277 peripheral blood (PB) draws from 181 patients with mCRPC. Overall, 95/277 samples (34%) were CTC-, 86/277samples (31%) were CTC+/AR-V7-, and 96/277 samples(35%) were CTC+/AR-V7+ (**Figure 7**). There was evidence of differences in CellSearch CTC count (p<0.001), Eastern Cooperative Oncology Group Performance Status (ECOG PS; p= 0.03), the number of taxane therapies received (p<0.001), haemoglobin (p= 0.009), alkaline phosphatase (p= 0.0006), lactate dehydrogenase (p= 0.001), and PSA (p=

0.0002) by CTC/AR-V7 status (Table 4). Taken together, these data suggest that CTC+/AR-V7+ samples were taken from patients with a higher disease burden at the time of PB draw.

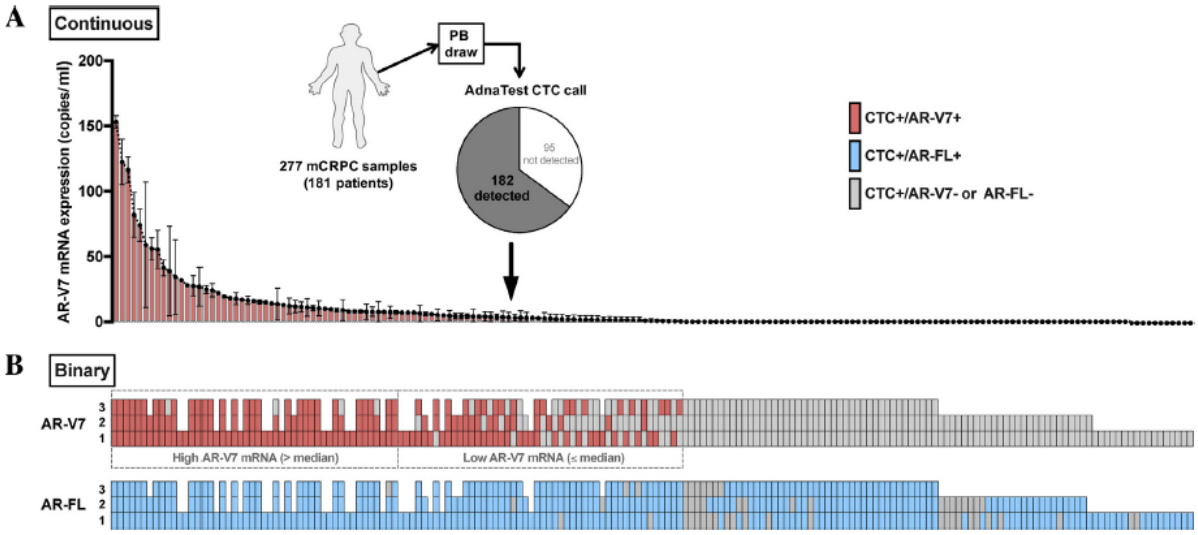

Figure 7 (A) Continuous (mean SD) AR-V7 mRNA expression (copies/ml; red bars) from technical replicates is shown. (B) Binary CTC AR-V7 (red boxes positive; grey boxes negative) and AR-FL (blue boxes positive; grey boxes negative) results shown for each technical replicate (numbered 1–3). AR-V7 = androgen receptor splice variant-7; CTC = circulating tumour cell; mCRPC = metastatic castration-resistant prostate cancer; SD = standard deviation.

Table 4 Patient baseline characteristics at time of peripheral blood draw (whole PB cohort)

Characteristic	CTC– (N = 95)		CTC+/AR-V7– (N = 86)		CTC+/AR-V7+ (N = 96)		p value[a]
	N	%	N	%	N	%	
CellSearch CTC count							
<5	38	40.0	27	31.4	6	6.3	<0.001
≥5	28	29.5	38	44.2	65	67.6	–
Missing analysis	29	30.5	21	23.1	25	26.0	–
ECOG PS at draw							
0	12	12.6	13	15.1	6	6.3	0.03
1	66	69.5	57	66.3	60	62.5	–
≥2	7	7.4	11	12.8	23	24.0	–
NR	10	10.5	5	5.8	7	7.3	–
Metastatic sites							
Lymph node only	12	12.6	8	9.3	9	9.4	0.8
Visceral	17	17.9	21	24.4	23	24.0	0.5
Bone	71	74.7	74	86.1	81	84.4	0.1
AR-targeting therapies							
0	4	4.2	7	8.1	0	0.0	0.08
1	51	53.7	50	58.1	54	56.3	–
2	30	31.6	25	29.1	36	37.5	–
NR	10	10.5	4	4.7	6	6.3	–
Taxane therapies							
0	23	24.2	20	23.3	12	12.5	<0.001
1	43	45.3	33	38.4	27	28.1	–
2	19	20.0	29	33.7	51	53.1	–
NR	10	10.5	4	4.7	6	6.3	–

Characteristic	CTC– (N = 95)		CTC+/AR-V7– (N = 86)		CTC+/AR-V7+ (N = 96)		p value[b]
	Median	IQR	Median	IQR	Median	IQR	
Age (yr)	71.0	66.8–75.6	69.6	64.9–72.3	70.4	65.3–74.6	0.07
Hb (g/dl)	11.7	10.4–12.8	11.4	10.3–12.8	10.7	9.7–12.3	0.009
ALT (U/l)	16.0	12.5–23.0	14.0	10.0–19.0	15.0	11.0–19.0	0.03
ALP (U/l)	83.0	66.0–163.0	111.5	76.3–200.5	180.0	93.8–346.0	0.0006
Albumin (g/l)	35.0	32.5–38.0	35.0	31.8–39.0	34.0	31.0–37.0	0.1
LDH (U/l)	179.5	146.3–241.3	184.5	151.3–266.0	230.0	175.5–433.5	0.001
PSA (µg/l)	110.0	29.0–300.5	147.0	51.0–345.0	244.5	109.3–746.8	0.0002

ALP = alkaline phosphatase; ALT = alkaline transferase; AR = androgen receptor; AR-V7 = androgen receptor splice variant-7; CTC = circulating tumour cell; ECOG PS = European Cooperative Oncology Group performance status; Hb = haemoglobin; IQR = interquartile range; LDH = lactate dehydrogenase; N = number; NR = no result; PB = peripheral blood; PSA = prostate-specific antigen.
a x2 test.
b Kruskal-Wallis equality-of-populations rank test.

3.3.6 CTC AR-V7 status identifies mCRPC patients with more advanced disease and therefore poorer prognosis

Having demonstrated CTC AR-V7 positivity to be associated with more advanced disease, we next determined whether this impacted survival analyses in an unselected cohort of 162 mCRPC patients (prognostication cohort). Overall, 56/162 (35%) samples were CTC-, 53/162 (33%) CTC+/AR-V7-, and 53/162 (33%) CTC+/AR-V7+.

The median (95% CI) survival was 12.5 (9.8–14.6) months and the median (IQR) follow-up among patients who did not die was 19 (11–31) months. In univariable analysis, CTC AR-V7 status ($p < 0.001$), Cell-Search CTC count ≥5 ($p < 0.001$), higher ECOG PS ($p < 0.001$), receiving more taxane therapies ($p < 0.001$), lower haemoglobin ($p < 0.001$), higher alkaline phosphatase ($p < 0.001$), lower albumin ($p < 0.001$), higher lactate dehydrogenase ($p < 0.001$), and higher PSA ($p < 0.001$) were associated with worse overall survival (OS; Fig. 8 A and **Table 5**). In light of CTC+/AR-V7+ being associated with more advanced disease, we performed a multivariable analysis to adjust for imbalances in baseline characteristics. There remained a significant association with CTC AR-V7 status ($p = 0.02$), CellSearch CTC count ≥5 ($p < 0.001$), ECOG PS ($p = 0.01$), and ALP ($p = 0.05$; **Table 5**). The bootstrapped (number of replications = 1000) C-index for the multivariable model was 0.789, and the C-index values were 0.777, 0.773, 0.771, and 0.781 for multivariable models with CTC AR-V7 status, CellSearch CTC count, ECOG PS, and ALP, respectively. The bootstrapped C-index for the multivariable model without CTC AR-V7 status and CellSearch CTC count was 0.752.

However, differences in OS by CTC AR-V7 status appeared to be due to worse survival in CTC+/AR-V7+ patients compared with CTC- patients (hazard ratio [HR] 2.13; 95% CI 1.23–3.71; $p = 0.02$). There was no evidence of significantly inferior OS in CTC+/AR-V7+ patients compared with CTC+/AR-V7- patients (HR 1.26; 95% CI 0.73–2.17; $p = 0.4$; Fig. 8 B). These data suggest that CTC AR-V7positivity identifies mCRPC patients with more advanced disease and subsequent worse prognosis.

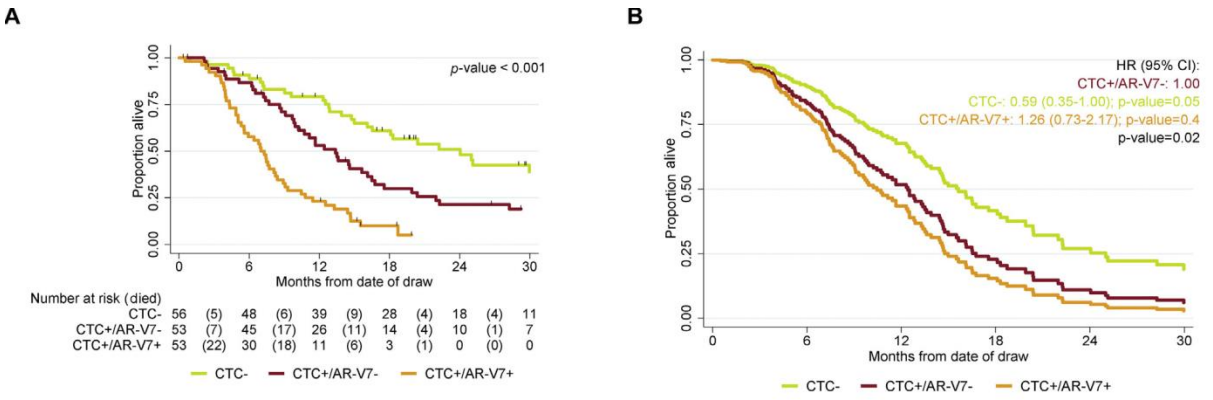

Figure 8 (A) Kaplan-Meier curve shows overall survival (OS) from peripheral blood draw for mCRPC patients divided by CTC, CTC+/AR-V7, and CTC+/AR-V7+ status. The p value was calculated using the log-rank test. (B) Estimated survivor function for CTC, CTC+/AR-V7, and CTC+/AR-V7+ groups with other covariates at their mean from the multivariable Cox model.

Table 5 Univariable and multivariable Cox models of overall survival from date of draw (prognostic cohort)

Characteristic	Univariable			Multivariable		
	HR	95% CI	*p* value	HR	95% CI	*p* value
AR-V7						
CTC+/AR-V7−	1.00	–	<0.001	1.00	–	0.02
CTC+/ARV7+	2.62	1.68–4.07	–	1.26	0.73–2.17	–
CTC−	0.59	0.37–0.93	–	0.59	0.35–1.00	–
CellSearch CTC count						
<5	1.00	–	<0.001	1.00	–	<0.001
≥5	5.45	3.23–9.18	–	3.23	1.65–6.31	–
Missing CTC	1.32	0.77–2.28	–	1.19	0.62–2.29	–
ECOG PS at draw						
0	1.00	–	<0.001	1.00	–	0.01
1	2.12	1.16–3.88	–	2.07	0.97–4.42	–
≥2	4.69	2.31–9.54	–	3.42	1.38–8.47	–
NR	121.8	11.82–1254.16	–	26.6	2.03–349.5	–
Metastatic sites						
Lymph node only	0.64	0.34–1.23	0.18	0.17	0.02–1.76	0.14
Visceral	1.39	0.93–2.07	0.11	0.89	0.56–1.44	0.6
Bone	1.54	0.83–2.87	0.17	0.17	0.02–1.69	0.13
AR-targeting therapies	1.37	0.99–1.89	0.06	1.07	0.73–1.56	0.8
Taxane therapies	1.52	1.21–1.91	<0.001	1.02	0.76–1.39	0.9
Age (per 10 yr)	0.88	0.70–1.11	0.28	0.79	0.59–1.06	0.12
Hb (per dg/l)	0.70	0.63–0.79	<0.001	0.96	0.35–2.61	0.9
ALT ($\log_{10}$ U/l)	0.58	0.25–1.34	0.20	0.75	0.40–1.41	0.4
ALP ($\log_{10}$ U/l)	2.73	1.77–4.21	<0.001	0.94	0.89–1.00	0.05
Albumin (g/l)	0.91	0.87–0.95	<0.001	2.58	0.89–7.44	0.08
LDH ($\log_{10}$ U/l)	3.10	1.75–5.48	<0.001	1.33	0.96–1.84	0.08
PSA ($\log_{10}$ µg/l)	1.80	1.36–2.37	<0.001	0.79	0.59–1.06	0.12

3.4 Discussion

Prostate cancer, unlike other solid tumours, such as breast, lung and colorectal cancer, has a clinically useful protein biomarker that can be used both for diagnostic purposes and follow-up after treatment. Prostate-specific antigen (PSA) has shown reasonable sensitivity for the

detection of incipient cancer and can also be used to predict responses to treatment [158]. One of the drawbacks with PSA, however, is its low specificity, such that benign hyperplasic conditions can also be associated with an increase in PSA [159]. In the localised setting, a PSA increase of >0.5 ng/mL after prostatectomy or 2 ng/mL above the nadir after radical radiotherapy has been shown to be a sensitive biomarker for identifying men who are at a high risk of relapse or death [35, 160].

Conversely, in the metastatic setting, consensus criteria based on PSA and radiological biomarkers are inconsistently used. A recent study into clinical management decisions made by physicians in relation to mCRPC showed that, despite being considered an important biomarker, 41.4% of the population interviewed stated that they disregarded changes in PSA before 12 weeks of treatment had elapsed, while the majority of physicians (90.5%) only switched treatment based on clinical progression [161]. A decline in PSA of 30% after 12 weeks of the start of treatment has been associated with OS in mCRPC [142, 143]. In the work presented in this chapter, I collected survival data for 1133 patients with mCRPC who were treated with either AA or enzalutamide (second generation hormonal treatment, SGHT) in thirteen cancer centres worldwide. I have confirmed the clinical relevance and prognostic value of early declines in PSA in patients treated with SGHT before or after chemotherapy. In this study, I confirmed that, unlike chemotherapy, an early PSA flare (defined as an increase of >25% in the first 4 weeks followed by a decline of >30% from the baseline by week 12) is very uncommon following treatment with AA and enzalutamide, involving only 1% of the overall population treated with SGHT.

In this chapter, I also investigated the prognostic role of AR-V7 and explored its possible use as a predictive biomarker of a patient's response to SGHT. Splice variants of the androgen receptor are under intense scrutiny since their initial identification in the early 2000s; they have been mainly reported as a feature of advanced disease, with increasing levels observed with the progression of disease [108]. In the work I have presented here, I confirmed that the expression of AR-V7 increases with the development of the castration-resistant status. I observed a significant increase in nuclear AR-V7 protein levels in the progression from HSPC to CRPC in this patient cohort. Interestingly, a small subset of patients showed the reverse trend, with a decrease in nuclear AR-V7. This may possibly be explained by the fact that, while some tumours express AR-V7 in response to androgen ablation, others may acquire resistance to AA or EZ through increased androgen biosynthesis, resulting in lower AR-V7 expression [162]. An alternative explanation for this decrease could be that there is an increase in other AR variants that are constitutively active [163].

Moreover, consistent with previous studies utilising CTC AR-V7 assays [108], we demonstrate that 33% of mCRPC patients are CTC+/AR-V7+ and that CTC AR-V7 positivity is associated with more advanced disease.

In conclusion, these studies highlight that **AR-V7+ status in tissue and CTC is a biomarker of poorer prognosis that increases with emerging drug resistance**.

4 PTEN Loss and Activation of its Pathway: A Prognostic and Predictive Biomarker

4.1 Background

The phosphatidylinositol-3-kinase (PI3K)/AKT/mammalian target of rapamycin (mTOR) is one of the most commonly activated signalling pathways in cancer, leading to cell proliferation, survival and differentiation [164]. PI3Ks are members of a large family of lipid kinases that exert their function by phosphorylating plasma membrane phosphatidylinositol molecules. There are three different PI3K classes: I, II and III. In mammals, class I PI3Ks are present in all cell types. Class I PI3Ks are further divided into A and B subtypes; class IA is by far the best understood and most commonly implicated in cancer [165]. Class IA PI3Ks are dimers comprising a regulatory (p85α, p85β, p55α, p55γ, p50α) and a catalytic (p110α, p110β, p110δ) subunit. p110α and p110β PI3Ks are ubiquitously expressed in mammalian tissues/organs and play fundamental roles during cell growth and development. Therefore, their homozygous knockout is embryonic-lethal [166]. In contrast, p110γ and p110δ PI3Ks are highly enriched in white blood cells, so their knockdown impairs immune responses [167]. PI3K can mainly be activated by one of three different mechanisms: i) activated receptor tyrosine kinases, ii) G protein-coupled receptors and iii) interaction with activated RAS/RAF/ERK oncogenic signalling [164, 168].

Activated PI3Ks generate phosphatidylinositol-3,4,5-bisphosphate (PIP3), a second messenger that provides a docking site for several enzymes containing a pleckstrin homology domain. The binding to PIP3 in the cell membrane and subsequent activation of

the phosphoinotide-dependent kinases PDK1 and PDK2 induces the phosphorylation and activation of the serine-threonine kinase, AKT. The activation of AKT kinases regulates a plethora of key cellular processes, including the construction of the actin cytoskeleton, angiogenesis, apoptosis, autophagy, blood cell development, cell cycle progression, cell survival, DNA repair, epigenetic regulation, gene expression regulation, genomic stability, GTP biosynthesis, ion transport, metabolism, metastasis, protein synthesis, and ribosomal RNA synthesis [168].

The phosphatase and tensin homologue (*PTEN*) gene on chromosome 10 (locus 10q23) is a key negative regulator of PI3K/AKT/mTOR activity, through its PIP3 lipid phosphatase activity, which dephosphorylates PIP3 into PIP2. Other tumour suppressive functions have been described: by interacting with cytosolic proteins, PTEN is able to inhibit cell migration and cell cycle progression [169, 170], while in the nucleus, PTEN contributes to chromosome integrity, DNA repair, and genomic stability [171, 172]. Multiple mechanisms can account for the loss of PTEN protein expression, including genomic deletion, mutations and promoter methylation [173]. Finally, the loss of PTEN may be responsible for immunosuppression, resulting in tumour tolerance [174, 175].

PTEN has attracted a great deal of interest as a biomarker in PC. Immunohistochemistry (IHC) analysis for PTEN status is a reliable method that has been established for routinely processed formalin-fixed and paraffin-embedded (FFPE) clinical and pathological specimens [176]. Importantly, the assessment of PTEN protein expression by IHC offers the advantage of detecting the loss of PTEN by mechanisms other than genomic deletion [117, 177].

In this chapter I will describe the prognostic value of PTEN loss in mCRPC patients and explore its predictive role for responses to abiraterone and docetaxel. Finally, I explore the impact of PTEN loss and PI3K/AKT activating mutations on responses to a combination of enzalutamide and the AKT inhibitor, capivasertib.

4.2 Specific Aims

- To test PTEN as a prognostic and predictive biomarker of response to abiraterone in lethal PC.
- To test PTEN as a prognostic and predictive biomarker of response to docetaxel in lethal PC.
- To test PTEN loss and mutations in PI3K/AKT as putative biomarkers of response to combination treatment using AKT inhibitors and enzalutamide.

4.3 Results

4.3.1 PTEN Protein Loss and Clinical Outcome from mCRPC Treated with Abiraterone Acetate

Overall, 200 tissue samples from 144 patients, who received abiraterone acetate (AA) in a post-docetaxel setting, were stained with PTEN IHC for this study. Tissue characteristics are displayed in **Table 1**.

Table 1 Samples and PTEN IHC status breakdown

	n = 200	PTEN-positive	PTEN-negative	p-value*
		No (%)	No (%)	
Primary tumours (HSPC)	140	86 (61%)	54 (38%)	0.13
Core biopsies	119	79	40	
TURP*	16	6	10	
Radical prostatectomy	5	1	4	
Distant metastases (CRPC)	60	30 (50%)	30 (50%)	
Liver biopsy	10	3	7	
Bone marrow trephine	34	17	17	
Soft tissue	16	10	6	

TURP = trans-urethral resection of the prostate; *Pearson chi-square test

A single sample was available from 95 patients; 42 patients had two samples collected at different time points, and seven patients had three tissue samples available for analysis. Pearson chi-square testing showed no significant association between PTEN IHC loss and disease state, i.e. HSPC or CRPC (p = 0.1); intra-sample heterogeneity for PTEN IHC staining was observed in nine HSPC samples (6.4%; 6/140). Overall, **PTEN IHC loss was observed in 40% of patients** (57/144).

To investigate the concordance of PTEN status between HSPC and CRPC samples from the same patient, 42 patients with matched HSPC and CRPC sample pairs were evaluated. Overall, the concordance rate was 85.7% (36/42) (e.g. Fig 1A1 and 1A2), however, 13% (3/23) of the PTEN IHC positive HSPC samples relapsed at a later stage with a PTEN IHC negative CRPC tumour (e.g. **Figure 1B1** and **1B2**). Conversely, 10.5% (2/19) of patients showing PTEN IHC negative disease in their HSPC sample had a PTEN IHC positive CRPC. Intra-sample heterogeneity was observed in five HSPCs, of which three later developed

PTEN IHC negative disease, one became a PTEN IHC positive (**Figure 1C1**, **1C2**) cancer, while one tumour retained PTEN IHC heterogeneity at the CRPC stage.

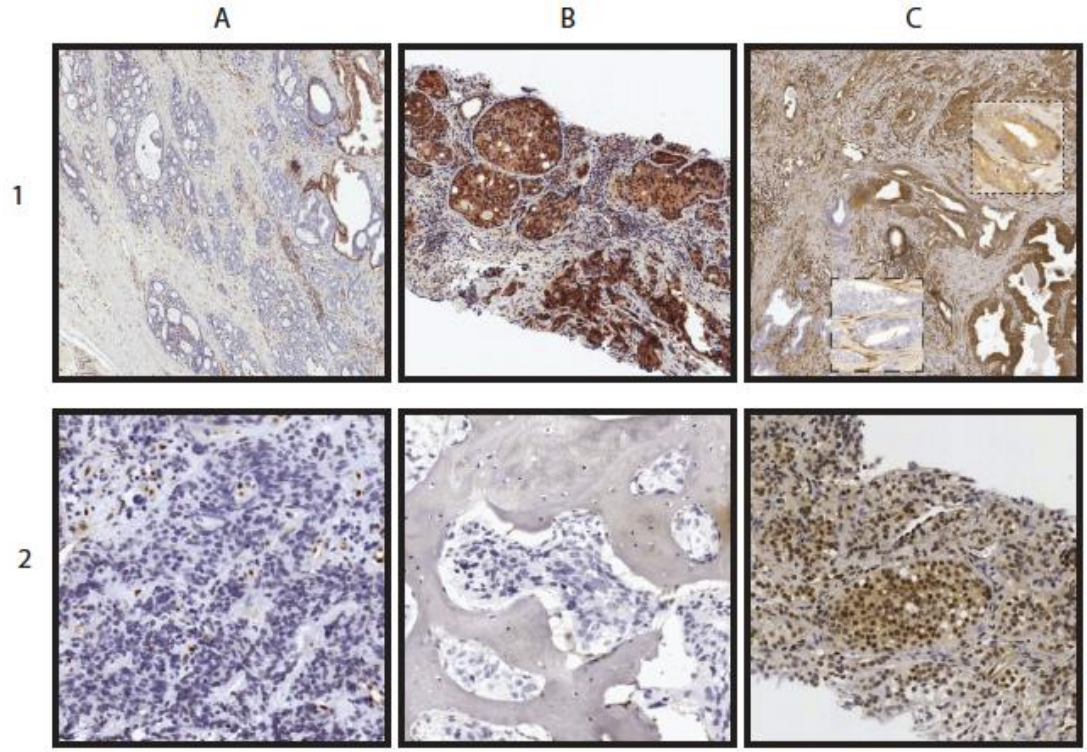

Figure 1 Matched cases. (A1, A2) PTEN IHC negative primary and PTEN IHC negative mCRPC. (B1, B2) PTEN IHC positive disease in primary and PTEN IHC negative mCRPC. (C1, C2) PTEN IHC heterogeneous primary and PTEN IHC positive mCRPC.

Baseline characteristics and known prognostic factors for mCRPC at the time of the start of AA are shown in **Table 2**.

Table 2 Summary of clinical and pathological data.

		Overall	PTEN IHC Neg	PTEN IHC Pos	p-value
		n = 144	n = 57	n = 87	
Age, years	**Median**	68.4	66.1	69.4	>0.9a
	Range	40.5-87.1	40.4-79.9	43.4-87.1	
Gleason score	**≤6**	15 (10%)	7 (12%)	8 (10%)	0.06b
	7	33 (23%)	19 (33%)	14 (16%)	
	≥8	71 (49%)	23 (41%)	48 (55%)	
	NA	25 (17%)	8 (14%)	17 (19%)	
Specimen	**Bone**	128 (88%)	52 (91%)	76 (87%)	0.7c
	Nodal	75 (51%)	28 (48%)	47 (54%)	0.7c
	Visceral	25 (17%)	14 (24%)	11 (12%)	**0.03c**
ECOG PS	**0**	35 (24%)	13 (23%)	22 (25%)	0.4b
	1	86 (60%)	35 (61%)	51 (59%)	
	2	7 (5%)	4 (7%)	3 (3%)	
	NA	16 (11%)	5 (9%)	11 (13%	
PSA µg/L	**Median**	213	155	237	0.5a
	Range	1.5-10325	2.1-10325	1.5-6385	
Haemoglobin, g/dL	**Median**	11.6	11.8	11.5	0.9a
	Range	8.6-15.0	8.6-15	8.7-14.8	
	NA	17	4	13	
Alkaline phosphatase, IU/L	**Median**	131	155	124	0.2a
	Range	46-1110	47-1110	46-1028	
	NA	13	4	9	
Lactate dehydrogenase, IU/L	**Median**	188	216	181	>0.9a
	Range	72-1546	72-1349	119-1546	
	NA	22	7	15	
Albumin, g/L	**Median**	35	35	36	0.4a
	Range	20-47	24-44	20-47	
	NA	14	10	4	
Previous systemic therapies	**Doce**	144 (100)	57 (100)	87 (100)	(-)
	Cabazi	11 (8)	4 (7)	7 (8)	0.8c

	Other	19 (21)	8 (14)	11 (12)	0.8c
Systemic treatments post-AA	**Cabazi**	43 (30)	17 (30)	26 (30)	>0.9c
	Other	42 (29)	24 (42)	31 (36)	0.3c

a = Mann–Whitney; b = Chi-square test for trend; c = Pearson Chi-square test

The most common sites of metastatic disease were bone (88.89%; 128/144), lymph nodes (52%; 75/144), and visceral (17.36%; 25/144). The majority of patients (84%; 121/144) had an Eastern Cooperative Oncology Group (ECOG) performance status of 0 or 1. The median follow-up was 16 months (range: 1–90 months).

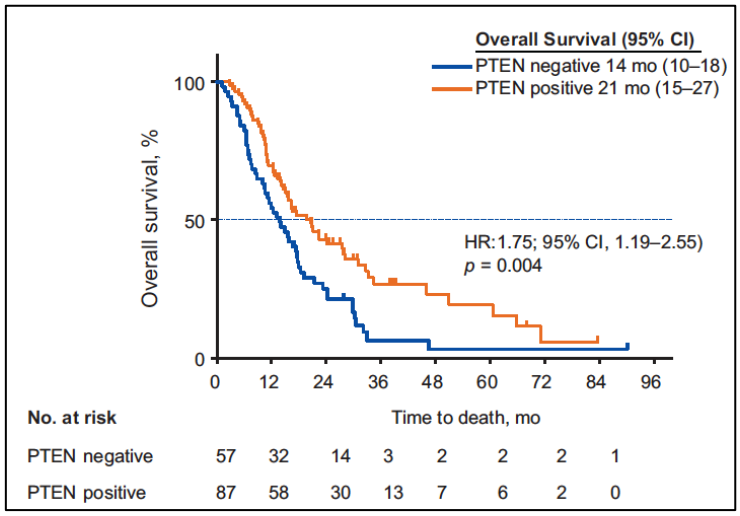

Figure 2 Kaplan–Meier curves from commencement of AA treatment. Patients with PTEN IHC negative tumours had worse outcomes.

Overall, the PTEN+ and PTEN- groups were balanced in terms of their clinical and pathological variables. However, the PTEN- group exhibited a higher incidence of visceral metastases (24% vs. 12%; p = 0.03) (**Table 2**). Crucially, PTEN IHC negative disease was associated with a shorter median overall survival (OS) from start of AA in univariate analyses (14 vs. 21 months; hazard ratio [HR]: 1.75; 95% CI, 1.19–2.55; p = 0.004; **Figure 2**).

In multivariate Cox regression analyses, PTEN- disease, high levels of lactate dehydrogenase, and the presence of visceral metastases were identified as independent prognostic factors (**Table 3**). Finally, the median duration of AA treatment for patients in the PTEN- group was statistically significantly shorter than that for the PTEN+ group (24 vs. 28 weeks; HR: 1.6; 95% CI, 1.12–2.28; p = 0.009).

Table 3 Multivariate Cox regression for overall survival.

Parameter	HR	95% CI		
		Lower	Upper	P-value
PTEN status (negative vs positive)	1.563	1.02	2.396	0.04
Low Albumin (yes v no)	0.956	0.433	2.114	0.912
High ALP (yes v no)	1.386	0.833	2.306	0.209
Low Haemoglobin (yes v no)	1.807	0.94	3.473	0.076
High LDH (yes v no)	1.589	1.004	2.515	**0.048**
Visceral metastases (yes v no)	1.972	1.095	3.552	**0.024**
logPSA**	1.092	0.797	1.495	0.584
Age*	1.021	0.983	1.061	0.286
ECOG PS 2 (yes v no)	0.968	0.332	2.825	0.953
Previous cabazitaxel (yes v no)	1.96	0.724	5.303	0.185

4.3.2 PTEN IHC Loss and Docetaxel Treatment

We identified 215 patients who received treatment with docetaxel and had tissue available for PTEN analysis. A single tissue sample was available for 160 patients, while 55 patients had matched samples collected at the time of diagnosis and in the castration-resistant phase. A total of 270 samples were scored for PTEN by IHC. Intra-patient concordance was present in 87% of the matched samples (48 of 55), with a change in PTEN status observed in just seven of 55 patients (13%). Overall, PTEN loss was demonstrated in 83 out of the 215 patients (39%). Key baseline patient characteristics are listed in **Table 4**.

Table 4 Patient characteristics at baseline when starting docetaxel treatment.

	Overall	PTEN-positive	PTEN loss	*p* value
Patients (*n*)	215	132	83	
Median age, yr (IQR)	70 (66–75)	68 (63–73)	66 (61–72)	0.23
Gleason score at diagnosis, *n* (%)				0.66
≤6	17 (7.9)	10 (7.6)	7 (8.4)	
7	51 (23.7)	28 (21.2)	23 (27.7)	
8–10	113 (52.6)	71 (53.8)	42 (50.6)	
Missing	34 (15.8)	23 (17.4)	11 (13.3)	
Sites of metastases at start of DTX, *n* (%)				0.78
Bone only	84 (39.1)	48 (36.4)	36 (43.4)	
Nodal	63 (29.3)	40 (30.3)	23 (27.7)	
Visceral	33 (15.4)	21 (15.9)	12 (14.5)	
Missing	35 (16.3)	23 (17.4)	12 (14.5)	
ECOG performance status, *n* (%)				0.46
0	78 (36.3)	30 (36.1)	48 (36.4)	
1	78 (36.3)	33 (39.8)	45 (34.1)	
2	5 (2.3)	3 (3.6)	2 (1.5)	
Missing	54 (25.1)	17 (20.5)	37 (28.0)	
Prostate-specific antigen				0.15
Median, ng/ml (IQR)	116 (47–404)	139 (58–569)	109 (32–369)	
Missing, *n* (%)	59 (27.4)	39 (29.6)	20 (24.1)	
Hemoglobin				0.81
Median, g/dl (IQR)	12 (11–13)	12 (11–13)	12 (11–13)	
Missing, *n* (%)	80 (37.2)	53 (40.2)	27 (32.5)	
Alkaline phosphatase				0.02
Median, IU/l (IQR)	127 (76–259)	116 (72–203)	211 (81–435)	
Missing, *n* (%)	79 (36.7)	52 (39.4)	27 (32.5)	
Lactate dehydrogenase				0.35
Median, IU/l (IQR)	192 (149–239)	188 (146–239)	197 (156–245)	
Missing, *n* (%)	84 (39.1)	56 (42.4)	28 (33.7)	
Albumin				0.19
Median, g/l (IQR)	36 (32–38)	36 (33–39)	35 (32–38)	
Missing, *n* (%)	80 (37.2)	53 (40.2)	27 (32.5)	
Neutrophils				0.99
Median (IQR)	4.6 (3.5–6.8)	4.6 (3.6–6.9)	4.5 (3.3–6.9)	
Missing, *n* (%)	81 (37.7)	54 (40.9)	27 (32.5)	
Lymphocytes				0.72
Median (IQR)	1.2 (0.8–1.6)	1.2 (0.8–1.6)	1.1 (0.8–1.7)	
Missing, *n* (%)	81 (37.7)	54 (40.9)	27 (32.5)	
Neutrophil/lymphocyte ratio				0.65
Median (IQR)	4.0 (2.5–8.8)	4.0 (2.4–9.0)	4.0 (2.4–8.6)	
Missing, *n* (%)	81 (37.7)	54 (40.9)	27 (32.5)	
Previous abiraterone, *n* (%)				0.69
Yes	51 (23.7)	31 (23.5)	20 (24.1)	
No	159 (74.0)	97 (73.5)	62 (74.7)	
Missing	5 (2.3)	4 (3.0)	1 (1.2)	

IQR = interquartile range; DTX = docetaxel; ECOG = Eastern Cooperative Oncology Group.

Patients received a median of eight cycles of docetaxel, with median treatment duration of 5.1 mo. There were no significant differences in haemoglobin, albumin, lactate dehydrogenase, neutrophil/lymphocyte ratio, or performance status between PTEN-negative and PTEN-positive patients before docetaxel initiation; only alkaline phosphatase levels were higher in PTEN-negative patients (p = 0.02). Overall, 33 patients (15.4%) had visceral metastases at docetaxel initiation, with no significant difference between the groups (14.5% vs. 15.9%; p = 0.77).

Table 5 PSA and RECIST responses to docetaxel.

	Univariable		Multivariable	
	HR (95% CI)	*p* value	HR (95% CI)	*p* value
PTEN status (loss)	1.66 (1.23–2.34)	0.001	1.73 (1.21–2.46)	0.003
Previous abiraterone	1.52 (1.06–2.17)	0.02	1.40 (0.90–2.18)	0.13
Hemoglobin (g/dl)	1.00 (0.97–1.03)	0.94	–	–
Albumin (g/l)	0.92 (0.87–0.97)	0.002	0.94 (0.88–1.00)	0.05
ALP (log_{10} IU/l)	2.02 (1.14–3.58)	0.02	1.11 (0.59–2.11)	0.73
LDH (log_{10} IU/l)	5.33 (1.39–20.49)	0.02	4.78 (1.33–17.22)	0.02
NLR (log_{10})	1.09 (0.78–1.52)	0.62	–	–
ECOG PS ≥1	1.74 (1.23–2.46)	0.001	1.45 (0.94–2.24)	0.09
Gleason score ≥8	1.43 (1.02–2.00)	0.04	1.37 (0.93–2.02)	0.11
Visceral disease	1.65 (1.10–2.46)	0.01	1.57 (0.97–2.53)	0.07

HR = hazard ratio; CI = confidence interval; ECOG PS = Eastern Cooperative Oncology Group performance status; PSA = prostate-specific antigen; ALP = alkaline phosphatase; LDH = lactate dehydrogenase; NLR = neutrophil/lymphocyte ratio.

The median OS from the start of docetaxel treatment for the entire cohort was 29.3 mo (95% CI, 26.6–35.1); 180 patients (83.7%) had died by the time of data cut-off. The median PFS was 8.9 mo (95% CI 8.1–10.3). Patients with PTEN loss had worse OS than patients with

normal PTEN expression (25.4 vs. 34.7 mo; univariate hazard ratio [HR] 1.66, 95% CI 1.23–2.24; p = 0.001; **Figure 3**) in both univariable and multivariable (MVA) Cox regression analyses (**Table 5**). PTEN loss, higher lactate dehydrogenase levels and lower albumin remained strongly associated with worse OS in MVA ($p < 0.05$).

There was no difference in PFS observed between patients whose tumours had PTEN loss and those with PTEN+ disease (median 8.0 vs. 9.1 mo; HR 1.20, 95% CI 0.86–1.68; p = 0.28; **Figure 3**), with a similar median number of docetaxel cycles (7.5 vs. 8.0; p = 0.29) and median time on docetaxel (5.0 mo [95% CI 4.2– 5.5] vs. 5.2 mo [95% CI 4.7–6.0]; p = 0.23).

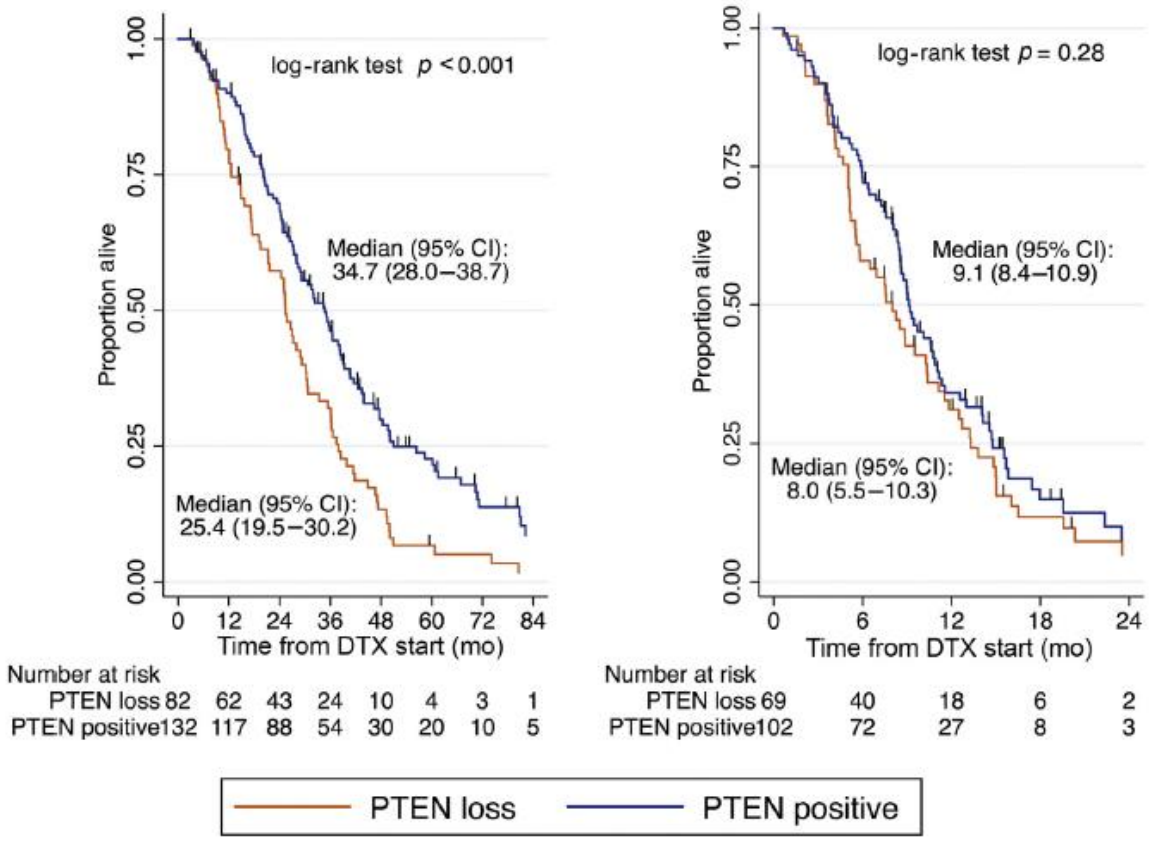

Figure 3 Kaplan-Meier curves for (left) median overall survival (OS) and (right) median progression-free survival (PFS) from the start of docetaxel chemotherapy for patients with PTEN loss and those with PTEN-positive tumours. CI = confidence interval; DTX = docetaxel.

Overall, 86 patients (40.1%) received further treatment with cabazitaxel; of these, 56 (65.1%) had tumours with PTEN loss. Data on PSA response were available for 143 patients. The overall median PSA decline was 53.3% (95% CI 61.7% to 42.9%); 74 of the 143 patients (51.8%) experienced a PSA response. Patients receiving docetaxel as first-line therapy for mCRPC were more likely to experience a PSA response than those receiving second-line docetaxel (58.4% vs. 38.5%; p = 0.03). There was no difference in PSA response rate between patients with and without PTEN loss (53.5% vs. 50.6%; p = 0.795; **Figure 4**). Furthermore, 128 patients (59.5%) had scans available for assessment of radiological response.

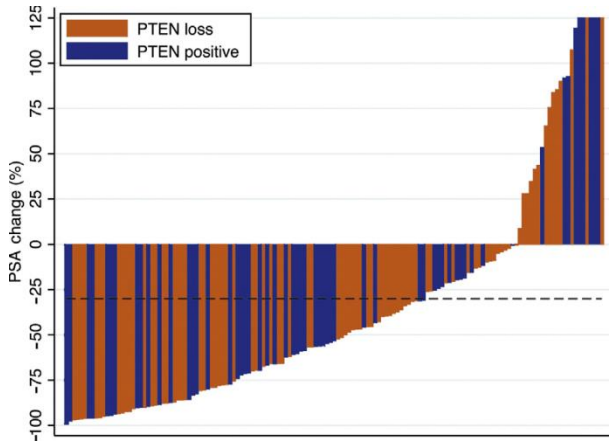

Figure 4 A waterfall plot of prostate-specific antigen (PSA) change for patients with PTEN loss and those who were PTEN-positive. The bar indicates a 30% decline in PSA from baseline.

Of these 128, 55 patients (43.0%) had bone-only disease and 73 (57.0%) had measurable disease by RECIST. Among the latter 73 evaluable patients, 23 (31.5%) had a partial response during docetaxel treatment or at treatment completion. Response rates were not different between PTEN- and PTEN+ mCRPC (28.6% vs. 33.3%; p = 0.67; **Table 6**).

Table 6 PSA and RECIST responses to treatment.

	Patients, *n* (%)			*p* value
	Total	PTEN-positive	PTEN loss	
PSA response [a]	74 (51.8)	43 (50.6)	31 (53.5)	0.74
No PSA response	69 (48.3)	42 (49.4)	27 (46.6)	
RECIST response (PR)	23 (31.5)	15 (33.3)	8 (28.6)	0.67
No RECIST response (SD or PD)	50 (68.5)	30 (66.7)	20 (71.4)	

PSA = prostate-specific antigen; RECIST = Response Evaluation Criteria in Solid Tumors; PR = partial response; SD = stable disease; PD = progressive disease.
[a] A PSA response was defined as a 30% PSA decline from baseline.

4.3.3 PTEN IHC as a Predictive Biomarker of Response to a Combination of Capivasertib and Enzalutamide

Between December 2014 and May 2016, sixteen patients were recruited to a phase I trial for evaluating the safety of the combination of enzalutamide and the AKT inhibitor capivasertib in patients who failed docetaxel, abiraterone and/or enzalutamide. Overall, 15 patients received study treatment; of these, two patients were not assessable for dose-escalation decisions: one withdrew consent prior to completing the dose limiting toxicity (DLT) window without experiencing a DLT and the other had dose delays during the DLT window for non-drug related adverse events (AE). At the time of data cut-off (10 March 2017), all patients had discontinued treatment, twelve due to progressive disease, one due to AE, and two who withdrew consent without experiencing disease progression. Their baseline characteristics are presented in **Table 7**.

Table 7 Baseline characteristics of patients recruited to the phase 1 safety evaluation of the combination of enzalutamide and the AKT inhibitor capivasertib.

Age	Median (IQR)	70.4 (68.0-72.6)
Ethnicity	Caucasian	15 (93.8%)
	African-Caribbean	1 (6.3%)
Gleason score at diagnosis	<8	4 (25%)
	≥8	9 (56.3%)
	NA	3 (18.8%)
Metastatic disease at diagnosis	Yes	8 (50%)
	No	7 (43.8%)
	NA	1 (6.3%)
Prior systemic therapy	Abiraterone	14 (87.5%)
	Cabazitaxel	8 (50%)
	Docetaxel	16 (100%)
	Enzalutamide	8 (50%)
Prior local treatment	Surgery*	3 (18.8%)
	Radiotherapy	6 (37.5%)
	Surgery* and radiotherapy	2 (12.5%)
*Surgery includes radical prostatectomy and transurethral resection of prostate (TURP)		

Ten patients completed 12 weeks of treatment in the study and were considered evaluable for responses; treatment of three patients was discontinued prior to week 12 due to progressive disease. Of the ten evaluable patients, all were evaluable by PSA, seven by RECIST v1.1, and seven by CTC enumeration. Three patients met at least one response criteria, with only one showing conflicting response criteria (conversion of CTC count to <5/7.5 mL whole blood, but increasing PSA; **Table 8**, **Figure 5**). One of these patients, who previously had progressive disease on both abiraterone and enzalutamide, met all three response criteria and remained on treatment for 25 weeks. Additionally, one patient who

withdrew consent prior to completing the first cycle of combination therapy had a 41.4% PSA reduction at 4 weeks.

Table 8 Response assessment.

		n	%	Response rate (95%
RECIST	Response	1	14.3	14.3%
N=7	No response	6	85.7	(0.4 – 57.9)
PSA	Response	2	20.0	20.0%
N=10	No response	8	80.0	(2.5 – 55.6)
CTC	Response	3*	42.9	42.9
N=7	No response	4	57.1	(9.9 – 81.6)
Overall	Response	3	30.0	30.0%
N=10	No response	7	70.0	(6.7 – 65.2)

*Includes two non-confirmed CTC count conversions.

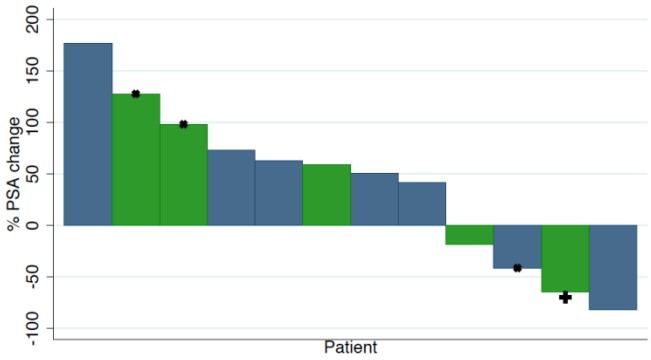

Figure 5 Percentage change in PSA at 12 weeks relative to baseline PSA. Each bar represents an individual patient. Green indicates the patient previously received treatment with both abiraterone and enzalutamide; blue indicates prior treatment with only abiraterone and not enzalutamide. Patients indicated with an ✕ discontinued treatment before four cycles but safety follow-up results are available. The patient indicated with an ✚) also met response criteria for RECIST and CTC conversion.

PTEN loss was found in 6 of 16 patients, while targeted NGS identified pathogenic mutations in PI3K/AKT/mTOR pathway genes in 2 of 16 In the three responders, two had PTEN loss by

IHC, while the third had normal PTEN and harboured an activating AKT E17K mutation. Another patient who had a ≥30% PSA response at 4 weeks, but withdrew from the trial prior to completing the 35-day DLT window, was found to be PTEN-normal and to have a PIK3CA I391M single nucleotide aberration of uncertain significance.

4.4 Discussion

Loss of PTEN is a common molecular aberration in PC and is believed to be critically important in regulating AR signalling output [113, 178, 179]. While PI3K/AKT/mTOR activation can suppress AR transcriptional output and stability [180], PI3K/AKT/mTOR signalling is activated following androgen deprivation, especially in patients with PTEN loss [181]. In the first two sections of this chapter, I confirmed the prognostic role of PTEN loss in mCRPC. However, while I also showed that PTEN status by IHC may serve as a predictive biomarker for response to AA, I found no evidence that docetaxel antitumour activity is impaired in PTEN-loss mCRPC, with no difference in the number of cycles administered, the duration of docetaxel treatment, or the PSA or RECIST response between PTEN- and PTEN+ tumours. This might be different in earlier stages of the disease, where PTEN loss has been associated with shorter PFS among 57 patients treated on a trial of adjuvant docetaxel after radical prostatectomy [182].

In the third section of this chapter, I explored the antitumour activity of the combination of enzalutamide with the Akt inhibitor capivasertib in a heavily pretreated mCRPC population. Molecular analyses demonstrated that all patients meeting the response criteria had

pathogenic events within the PI3K/AKT/mTOR pathway, either PTEN loss by IHC or an activating somatic mutation in PI3K/AKT, suggesting them as putative biomarkers of response to this class of drugs. Another putative predictive biomarker of AKT inhibition may be extracellular signal-regulated kinase (ERK) [183, 184]. AKT negatively regulates ERK activation through the phosphorylation of N-terminus inhibitory sites of Raf [185-187]; therefore, inhibition of AKT releases cross-inhibition of Raf and increases phosphorylation of ERK. We found that among patients with evaluable pre- and post-treatment biopsies, IHC pERK scores substantially increased in responders.

Interestingly, a recent randomised phase II trial of abiraterone with or without the AKT inhibitor ipatasertib provided additional support for co-targeting the AR and AKT [188]. Radiographic progression-free survival (rPFS), the primary endpoint of the trial, was significantly longer in patients with PTEN-loss disease in both arms, i.e. 200 and 400 mg of ipatasertib plus AA. However, patients with PTEN-loss tumours in the AA-plus-placebo arm had significantly shorter rPFS when compared with that of the PTEN+ group. The high prevalence of PTEN loss by IHC in clinically aggressive prostate cancer, at 43% of the trial population, was not, however, enough to extract a statistically significant predictive signal in the overall intent-to-treat population. These results have encouraged the further evaluation of ipatasertib in a large, randomised phase III trial in molecularly unstratified patients, with PTEN and other PI3K/AKT biomarker studies prospectively planned. Co-primary endpoints for this trial in pre-chemotherapy patients naïve to both abiraterone and enzalutamide include rPFS in the overall intention-to-treat population and rPFS in the PTEN-loss population.

Taken together, these data suggest that **PTEN loss is a biomarker of a lack of response to AA and that docetaxel might be a preferable option for this patient population**.

Finally, although PTEN is by far the most commonly deleterious aberration of the PI3k/AKT/mTOR pathway, aberrations involving PI3K components (including PIK3CA, PIK3CB, activating mutations and alterations impacting the regulatory function of PIK3R1), or AKT itself (AKT1 activating mutations) have also been reported in lethal prostate cancer and can be used to predict responses to new agents that inhibit AKT, such as ipatasertib and capivasertib. Therefore, in the near future, as the availability of massive parallel sequencing platforms increases and the cost per megabase of sequence decreases, DNA-based assays will be incorporated into patient management algorithms as orthogonal assays to IHC, in order to deliver a more tailored therapeutic strategy to the patient, increasing clinical benefits and reducing exposure to ineffective and toxic treatment.

5 DNA Repair Defects in Lethal Prostate Cancer

5.1 Introduction

Genomic instability is a common denominator of many different cancers. This instability is mainly due to the high rate of cell division that is responsible for the fast accumulation of genomic aberrations [189]. Therefore, defects in the DNA damage response (DDR) play a key role in the promotion of cancer growth through the insurgence of mutations and escape from apoptosis [190]. Most of the insults to cells that affect the DNA can cause single-strand breaks (SSBs), although double-strand breaks (DSBs) are more lethal to cells. Thus, most DDR-directed therapies target the repair mechanisms associated with DSBs, increasing replication stress; or inhibit cell cycle checkpoints that facilitate DNA repair. More specifically, defects in (or inhibition of) the high-fidelity DDR system, such as homologous recombination (HR), increase genomic instability, since cells will try to rely on compensatory mechanisms of repair that are often error-prone in order to survive [191, 192]. This describes the main mechanism of action of the class of drugs that target the poly(ADP-ribose) polymerase (PARP) proteins that play crucial roles in various aspects of the DDR. They mainly detect SSBs, recruit DNA repair machinery and stabilize replication forks during repair processes [193]. The pharmacological activity of this class of drugs, however, goes beyond the simplistic inhibition of the catalytic activity of PARP; unrepaired SSBs and an accumulation of stalled replication forks trap PARP in a complex with the DNA strand, inducing DSBs and ultimately cell death [193]. The effectiveness of PARP inhibition was initially shown in ovarian cancers with germline *BRCA1* or *BRCA2* (BRCA1/2) mutations, and is based on the concept of synthetic lethality [194]. The combination of a functional genetic

defect in an HR-related gene with the pharmacological inhibition of a compensatory DDR pathway component leads to insuperable genomic instability and cell death [193, 194]. To date, five PARP inhibitors (PARPi) — olaparib, rucaparib, niraparib, talazoparib and veliparib — have been used, in several clinical trials. Although their ability to inhibit PARP is similar, they vary markedly in terms of their PARP-trapping abilities.

Olaparib was the first PARPi to be tested in mCRPC, in the single-arm phase II TOPARP-A trial. The overall response rate was significantly higher in patients with DDR gene aberrations (including BRCA1/2, PALB2, CDK12 and ATM mutations) than in the unselected population (88% versus 33%) [128]. More recently, considerable interest has surrounded other mechanisms of repair as a therapeutic target in mCRPC, especially since studies have indicated that cancers associated with defective mismatch repair (dMMR) may benefit from immune checkpoint-inhibiting therapies [132].

The MMR system is a post-replicative, high-fidelity, single-strand repair mechanism that recognises and reverses DNA base mismatches and insertion/deletion (indel) loops; compromised MMR results in microsatellite instability and a hypermutator phenotype that has been associated with chemotherapy resistance but immunotherapy sensitivity [195]. Immunotherapy sensitive cancers, such as melanomas, tend to harbour high mutational loads [196, 197], which have been positively correlated with neoantigen burden [198]. Conversely, mCRPCs have, on average, lower detectable mutation loads of approximately four mutations per megabase [90]. A variable prevalence (3%–12%) of dMMR machinery has been reported in different studies of PC; this variation could be related to the technical limitations of the assays available to detect these genomic aberrations [129, 199]. Only

preliminary clinical data are available for the efficacy of immunotherapies in treating mCRPC. Multiple approaches have been developed to define this subset of mCRPC, including mutational signatures associated with dMMR [197] and the evaluation of microsatellite instability (MSI) using next-generation sequencing (MSI-NGS) [200].

In this chapter, I will describe the relevance of HR defects as predictors of response to PARPi, as emerged in a recent phase II trial. I will also provide an integrated characterization of the clinical, pathological, genomic and immunological features of a cohort of patients with dMMR mCRPC.

5.2 Specific Aims

- To evaluate the antitumour activity of olaparib in mCRPC patients.
- To study HR defects as a predictive biomarker of response to PARP inhibition.
- To study the predictive and prognostic role of circulating free DNA (cfDNA) analyses in mCRPC patients treated with olaparib.
- To perform immunohistochemistry (IHC) for MMR proteins and commercially available PCR-based assays on consecutive cases of mCRPCs to determine the frequency of such alterations detected using these assays in lethal prostate cancer.
- To determine microsatellite instability and mutational load using NGS targeted data and compare this with results obtained from IHC and PCR-based assays.

- To determine the clinical impact of defective MMR as defined by the aforementioned assays.
- To perform multicolour immunofluorescence to characterise lymphocytic infiltration in mCRPCs.
- To perform PD-L1 IHC in tumours with defective MMR and in MMR proficient tumours to determine if there is enrichment for PD-L1 positive cases among dMMR tumours.

5.3 Results

5.3.1 Homologous Recombination Defective mCRPC

5.3.1.1 HR Defects as Predictive Biomarkers of Response to Olaparib

Between April 1, 2015 and Aug 30, 2018, 711 patients consented to NGS pre-screening for an open-label, investigator-initiated, randomised phase II trial where patients with DDR gene aberrations were randomly assigned (1:1) to receive 400 mg or 300 mg olaparib twice-daily, given continuously in 4-week cycles until disease progression or unacceptable toxicity.

For 681 patients with at least one tissue sample available, 779 tumour samples were analysed (637 [82%] primary tumour samples and 142 [18%] CRPC biopsies). For 89 (13%) patients, biomarker determination was not possible because the sample or the sequencing data did not fulfil quality control parameters. Of the 592 patients with evaluable tissue samples, 161 (27%) had DDR gene aberrations on the basis of NGS. The proportion of aberrations detected are depicted in **Figure 1** for the intention-to treat population (98 patients).

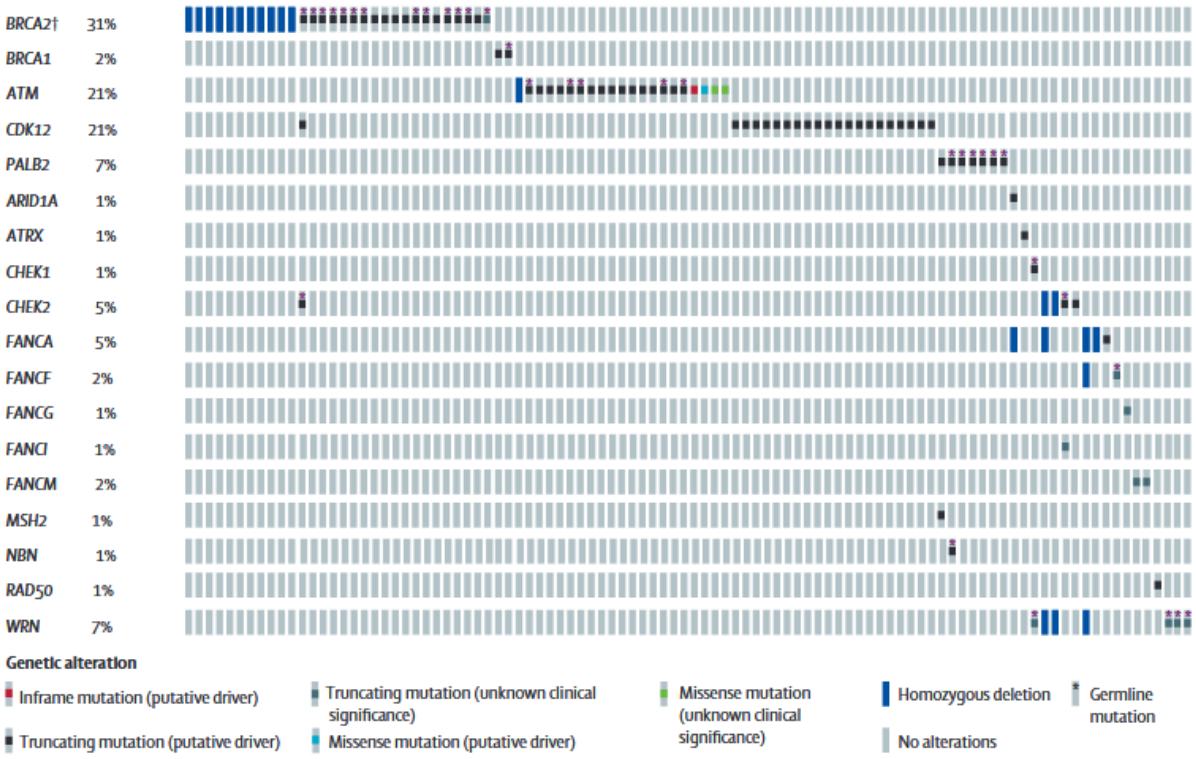

Figure 1 DDR gene alterations in the intention-to-treat population (n=98).

The primary endpoint of this trial was 'confirmed response'. This was defined as a composite of all patients presenting with any of the following outcomes: radiological objective response (as assessed by Response Evaluation Criteria in Solid Tumors 1.1), a decrease in prostate-specific antigen (PSA) of 50% or more (PSA50) from baseline, or conversion of circulating tumour cell (CTC) count (from ≥5 cells per 7·5 mL blood at baseline to <5 cells per 7·5 mL blood). A confirmed response in a consecutive assessment after at least 4 weeks was required for each component.

The median follow-up time was 24·8 months (interquartile range (IQR) 16·7–35·9). The baseline characteristics of all patients assigned to a dose cohort are shown in **Table 1**. All

patients had previously received docetaxel, and 88 (90%) had also been treated with one or both of abiraterone acetate and enzalutamide prior to entering the study.

Table 1 Baseline characteristics of patients in the intention-to-treat population.

	300 mg dose group (n=49)	400 mg dose group (n=49)
Age at trial entry (years)	67·3 (61·2–72·1)	67·6 (63·2–72·7)
Years from initial diagnosis	3·5 (2·4–6·4)	5·2 (3·6–7·3)
Years from diagnosis of CRPC	2·4 (1·2–3·7)	3·0 (1·8–4·0)
Metastatic disease at diagnosis		
Yes	24 (49%)	25 (51%)
No	24 (49%)	21 (43%)
Not available	1 (2%)	3 (6%)
Gleason score at diagnosis		
≤7	4 (8%)	15 (31%)
≥8	42 (86%)	29 (59%)
Not available	3 (6%)	5 (10%
Previous treatment for PC		
Prostatectomy	7 (14%)	6 (12%)
Radical radiotherapy	22 (45%)	21 (43%)
Radium-22	36 (12%)	8 (16%)
Docetaxel	49 (100%)	49 (100%)
Cabazitaxel	15 (31%)	22 (45%)
Abiraterone	24 (49%)	22 (45%)
Enzalutamide	27 (55%)	29 (59%)
Evidence of progression		
PSA only	15 (31%)	12 (24%)
Radiographic progression	34 (69%)	37 (76%)
Site of metastatic disease *		
Lung	4 (8%)	4 (8%)
Lymph nodes	34 (69%)	32 (65%)
Liver	11 (22%)	12 (24%)
Bone	41 (84%)	41 (84%)
PSA at trial entry, ng/mL	151·5 (49·0–446·0)	158·0 (45·5–472·0)

CTC count per 7·5 mL blood		
<5	17 (35%)	17 (35%)
≥5	31 (63%)	32 (65%)
Not available	1 (2%)	0
RECIST 1·1 soft tissue disease		
Bone lesions only	5 (10%)	5 (10%)
Non-measurable disease (with or without bone lesions)	5 (10%)	8 (16%)
Measurable disease (with or without bone lesions)	39 (80%)	36 (73%)
DNA damage response gene aberration subgroup‡		
BRCA1/2	15 (31%)	17 (35%)
ATM	10 (20%)	11 (22%)
CDK12	15 (31%)	6 (12%)
PALB2	3 (6%)	4 (8%)
Other	10 (20%)	11 (22%)

*More than one site could be reported. ‡Non-mutually exclusive subgroups.

Overall, 92 patients (46 in each dose cohort) were evaluable for the primary endpoint. There were 70 (76%) evaluable patients for the RECIST 1.1 response, 89 (97%) for the PSA response, and 55 (60%) for CTC conversion. A confirmed composite response was observed in 25 (54·3%; 95% CI 39·0–69·1) of 46 patients in the 400 mg cohort and 18 (39·1%; 25·1–54·6) of 46 patients in the 300 mg cohort (p = 0·14; **Table 2**). A radiological response according to RECIST 1.1 was observed in eight (24·2%; 95% CI 11·1–42·3) of 33 evaluable patients in the 400 mg cohort and six (16·2%; 6·2–32·0) of 37 in the 300 mg cohort; a PSA50 response was observed in 17 (37·0%; 23·2–52·5) of 46 and 13 (30·2%; 17·2–46·1) of 43, respectively; and CTC count conversion was observed in 15 (53·6%; 33·9–72·5) of 28 and 13 (48·1%; 28·7–68·1) of 27, respectively (**Figure 2**). Based on the first 44 evaluable patients included in each cohort, 25 (57%) confirmed responses were recorded in the 400 mg cohort and 18 (41%) in the 300 mg cohort; thus, the predefined criteria for success was met for the

400 mg regimen but not for the 300 mg regimen. When only the 55 evaluable patients with a CTC count of ≥5 cells per 7·5 mL blood at baseline were included in the analysis, a confirmed composite response was observed in 17 (60·7%; 95% CI 40·6–78·5) of 28 evaluable patients in the 400 mg cohort and 13 (48·1%; 28·7–68·1) of 27 in the 300 mg cohort.

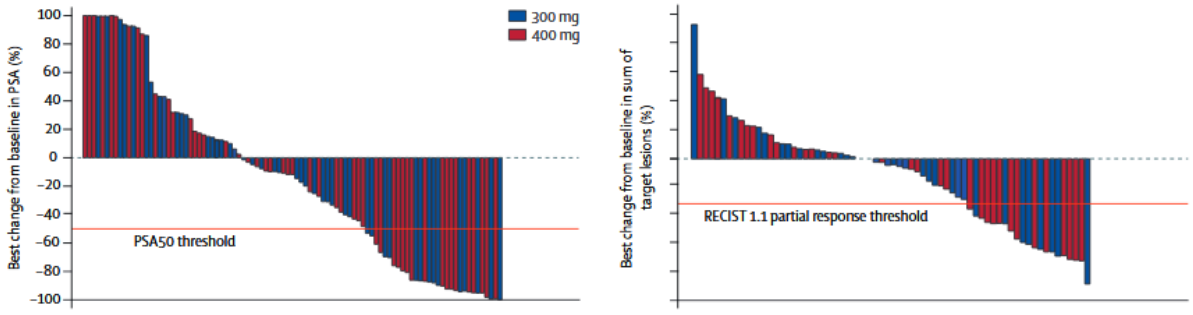

Figure 2 Antitumour activity by allocated dose cohort (intention-to-treat population). (Left) Best percentage change from baseline in PSA during treatment. (Right) Best percentage change from baseline in the sum of target lesions (Response Evaluation Criteria in Solid Tumors 1·1) during treatment.

The median radiographic progression-free survival was 5·5 months (95% CI 4·4–8·3) in the 400 mg cohort and 5·6 months (3·7–7·7) in the 300 mg cohort. A total of 39 (80%) patients on 400 mg and 38 (78%) patients on 300 mg died, with a median overall survival of 14·3 months (9·7–18·9) in the 400 mg cohort and 10·1 months (9·0–17·7) in the 300 mg cohort.

The BRCA1/2 subgroup (32 patients; 13 had germline mutations in BRCA2, six had somatic mutations in BRCA2, 11 had homozygous deletions in BRCA2, and two had mutations in BRCA1) had the highest number of responses both for the composite endpoint of confirmed response and across all its component outcomes, as well as the longest median radiographic progression-free survival of all DDR gene aberration subgroups. There were 21 patients with suspected deleterious ATM aberrations who were treated (one with a homozygous deletion

and 20 with germline or somatic mutations affecting the kinase domain) and 19 were evaluable for responses.

No confirmed PSA50 or RECIST responses were observed in the 20 evaluable patients in the CDK12 subgroup, although five patients achieved CTC conversion (including one who had a concomitant BRCA1/2 alteration). Conversely, four of seven patients with PALB2 mutations responded to treatment. There were 20 patients evaluated in the subgroup who had other gene alterations associated with DDR or PARP inhibitor sensitivity. PSA50 responses were seen in two patients: one with a somatic nonsense mutation in FANCA and one with a CHEK2 mutation. Antitumour activity by DDR aberration is shown in **Figure 3**.

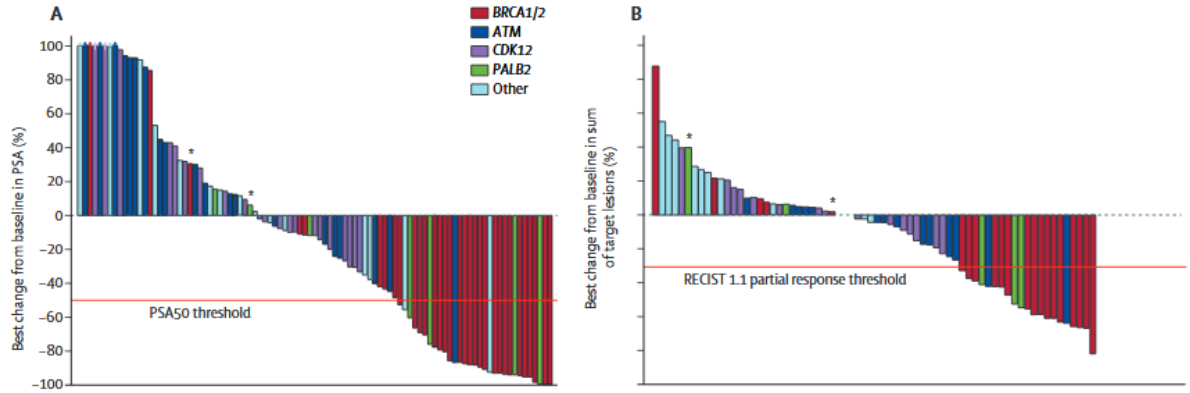

Figure 3 Antitumour activity by gene aberration subgroup (intention-to-treat population, pooled 300 mg and 400 mg cohorts). (A) Maximum percentage change from baseline in PSA during treatment. (B) Maximum percentage change from baseline in the sum of target lesions (Response Evaluation Criteria in Solid Tumors 1·1) during treatment.

5.3.1.2 cfDNA to Guide Prostate Cancer Treatment with PARP Inhibition

Patient characteristics

For this study, data were gathered from the TOPARP-A trial where 50 patients (unselected for DDR) were treated with olaparib at a dose of 400 mg; 49 were evaluable for response (as described in the previous section), with 16 patients responding to treatment. Overall, 16 of these 49 patients had prostate cancers associated with a deleterious aberration in homologous recombination DNA-repair genes; of these, 14 were classified as responders. Serial samples for cfDNA studies were available for 46 of 49 patients (94%). Overall, the median cfDNA baseline concentration across the trial population was 31.6 ng/mL (IQR, 19.4–57.1). Next-generation targeted sequencing of cfDNA was successful for 43 of 46 patients (93%).

Prognostic relevance of changes in cfDNA concentration following PARP inhibition

Changes in cfDNA concentration were evaluated in patients who responded (n = 16) or did not respond (n = 30) to olaparib. After 4 weeks of therapy, there was a median −51.4% change in responders (IQR, −72.6% to −29.5%) and a median −33.4% change in non-responders (IQR, −52.3% to +5.5%; p = 0.07). After 8 weeks of therapy, responders continued to experience sustained declines (median −49.6% change; IQR, −76.5% to −20.4%), differing significantly from non-responders (median +2.1% increase; IQR, −43.6% to +57.8%; p = 0.006). The concentration of cfDNA decreased as early as within 4 weeks of starting therapy; this was robustly correlated with radiologic progression-free survival (rPFS) (hazard ratio (HR), 1.70; CI, 1.13–2.55; p = 0.01 for cfDNA log-fold change; HR, 0.41; 95% CI, 0.21–0.80; p = 0.009 for absence/presence of ≥50% decrease from the baseline cfDNA

concentration). Decreases in cfDNA concentration after 8 weeks of olaparib correlated with both prolonged rPFS and OS (Figure 4). These associations were confirmed by the multivariable analyses, including established prognostic factors, such as LDH and CTC count conversion (Table 2).

Table 2 Multivariable Cox regression analyses of the association cfDNA plasma concentrations (ng/mL) with patient outcome, including established prognostic factors.

	rPFS HR (95% CI) p	OS HR (95% CI) p
4 weeks		
LDH	1.00 (1.00–1.00) 0.058	1.00 (1.00–1.00) 0.012
ECOG status 2 (vs. 0–1)	1.48 (0.50–4.38) 0.48	1.74 (0.60–5.06) 0.31
Radiological progression at trial entry (vs. PSA progression only)	1.01 (0.42–2.43) 0.98	0.20 (0.07–0.52) 0.001
Measurable disease at trial entry	0.32 (0.13–0.79) 0.014	0.50 (0.20–1.29) 0.154
Baseline CTC	1.00 (0.99–1.00) 0.20	1.00 (1.00–1.00) 0.34
Baseline cfDNA	1.00 (1.00–1.01) 0.54	1.00 (1.00–1.01) 0.23
CTC conversion	0.19 (0.07–0.05) 0.001	0.41 (0.17–1.01) 0.051
≥50% cfDNA [c] decline		
8 weeks		
LDH	1.00 (1.00–1.01) 0.036	1.00 (1.00–1.01) <0.001
ECOG status 2 (vs. 0–1)	2.45 (0.73–8.24) 0.15	2.55 (0.81–7.98) 0.11
Radiological progression at trial entry (vs. PSA progression only)	1.37 (0.47–4.00) 0.57	0.24 (0.08–0.72) 0.011
Measurable disease at trial entry	0.49 (0.18–1.31) 0.15	0.53 (0.19–1.50) 0.24
Baseline CTC	1.00 (1.00–1.00) 0.83	1.00 (0.99–1.00) 0.24
Baseline cfDNA	1.00 (0.99–1.00) 0.32	1.00 (0.99–1.01) 0.89
CTC conversion	0.10 (0.03–0.28) <0.001	0.35 (0.15–0.85) 0.020
≥50% cfDNA [c] decline	0.09 (0.03–0.30) <0.001	0.19 (0.06–0.56) 0.003

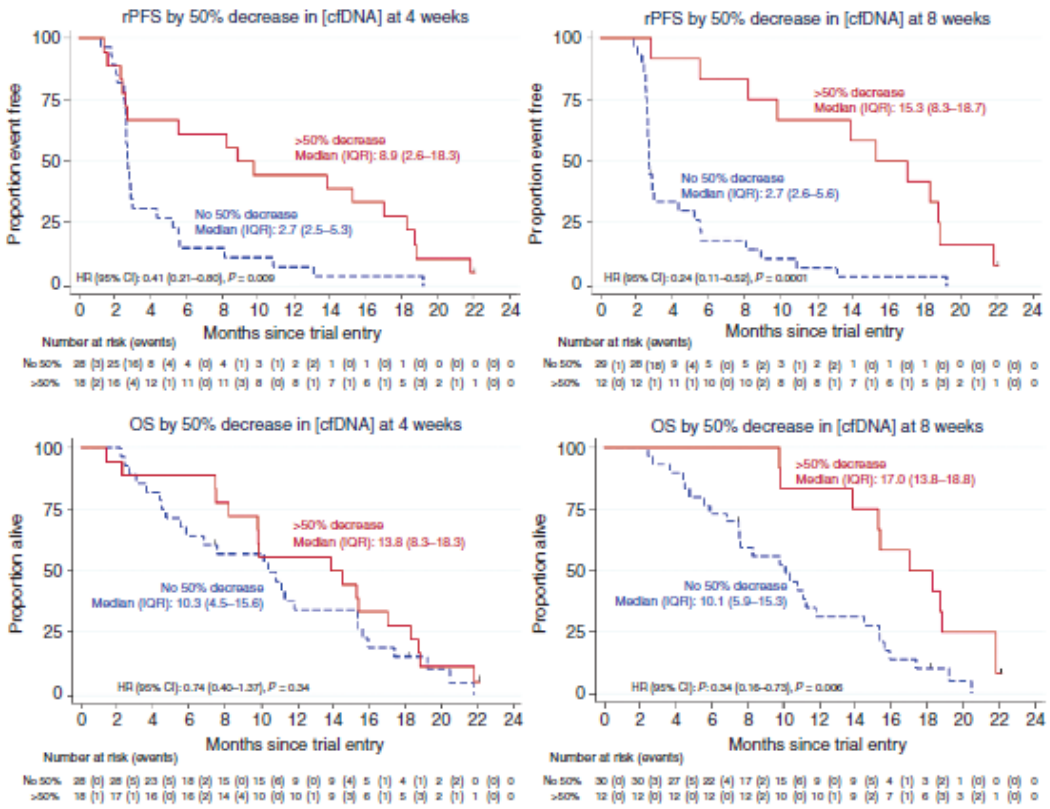

Figure 4 Kaplan–Meier plots showing differences in rPFS and OS based on the presence or absence of a ≥50% decrease in total cfDNA concentration after 4 and 8 weeks of therapy with olaparib.

Changes in allele frequency of somatic mutations

A total of 254 plasma samples were analysed using next-generation targeted sequencing to assess the allele frequency of somatic mutations during PARP inhibitor therapy as an indirect estimate of tumour burden. Olaparib treatment led to sustained decreases in cfDNA mutation allele frequencies in responding patients; however, sustained (≥8 weeks) decreases in cfDNA somatic mutation allele frequencies were not observed in non-responders.

Mechanisms of PARP inhibitor resistance detected in cfDNA

Ten of 16 patients who exhibited an initial tumour response to olaparib had cfDNA samples acquired at the time of resistance and disease progression. In addition to targeted

sequencing, whole-exome sequencing (WES) was performed using paired plasma samples collected from six patients prior to olaparib treatment and at disease progression, to study mechanisms of secondary resistance to PARP inhibition. In a seventh case, we performed WES in the progression sample and targeted sequencing in the baseline cfDNA sample, due to a low DNA yield.

In both patients with a germline *BRCA2* frameshift mutation, we identified at the time of tumour progression additional somatic BRCA2 mutations in cfDNA, which restored the normal open reading frame (**Figure 5**). One of these patients had a germline BRCA2 p.-1056fs mutation and loss of heterozygosity (LOH) in the pre-trial tumour biopsy. At the time of disease progression, a further somatic deletion of four base-pairs (bp) emerged, resulting in an overall in-frame change of four amino acids (p.K1057_Q1063delinsTEQA). In parallel, three other events were detected in different positions in the same genomic region, all of which also restored the *BRCA2* normal open reading frame, and probably represented the coexistence of several resistant tumour subclones in the cfDNA. This patient had a partial response to olaparib, and progressed after 9 months; a bone marrow biopsy of a relapse focused in the right hemipelvis showed that only one of the three emerging somatic reversions (p.K1057_Q1063delinsTEQA) was detected, suggesting that these other emerging subclones may have originated in different metastases. A second germline *BRCA2* mutation carrier (p.E1514fs*15) developed an additional deletion of 28 bp at progression, reverting *BRCA2* back in frame and also showing a new somatic *ARID1A* mutation (p.Q1145*). Reversion mutations in *BRCA2*, at the time of progression, were also identified in nongermline mutation carriers. In addition, secondary genomic events causing reversion back to the normal reading frame were also detected for one patient with a somatic *PALB2*

mutation. These new mutations, which emerged at the time of progression, might have evolved as a consequence of defective homologous recombination and the utilization of alternative error-prone DNA repair mechanisms. Among the remaining patients with plasma cfDNA evaluated at secondary resistance, we did not detect any other such events, although two of these patients discontinued the drug due to tolerability issues prior to radiologic progression. No emerging mutations or copy-number changes in *PARP1* or *PARP2* were observed in any of these samples.

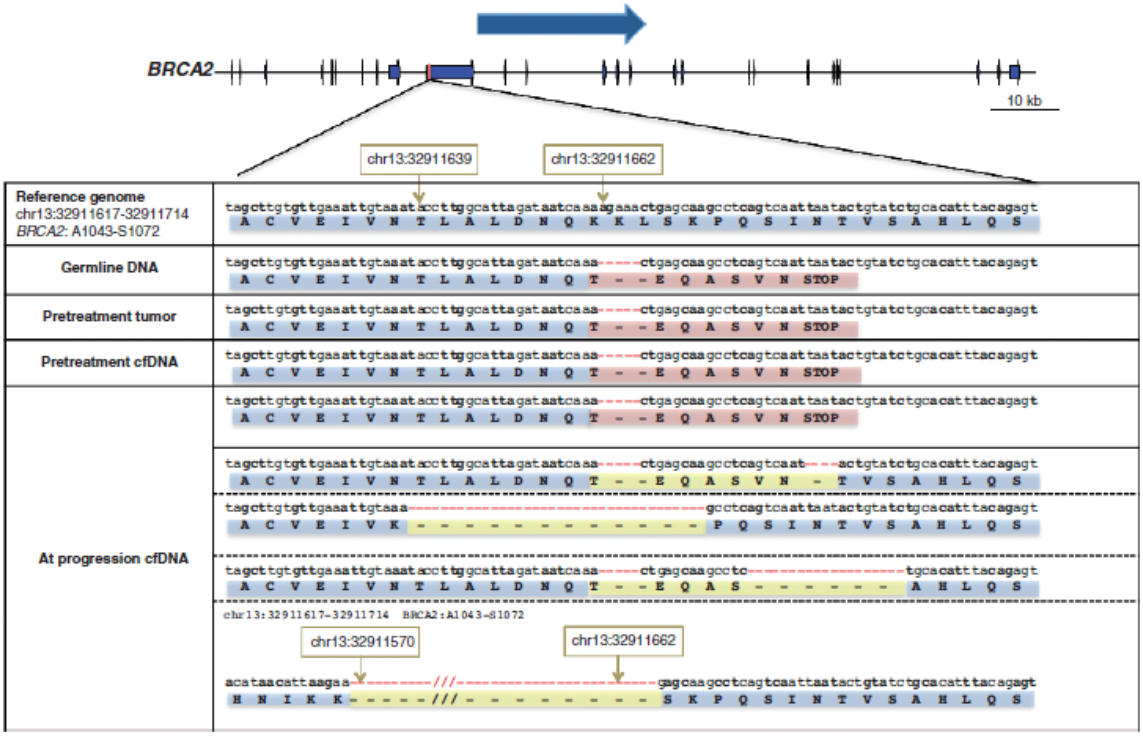

Figure 5 Visual representation of emerging *de novo* mutations at progression that likely resulted in acquired drug resistance in a patient with germline BRCA2 mutations. In this case, at progression, cfDNA WES identified multiple clones with different previously undetected mutations, which all resulted in reversion of the BRCA2 reading frame to normal.

5.3.2 Mismatch Repair Defective mCRPC

Given the clinical need to identify and characterize dMMR tumours in advanced prostate cancers, we analysed 127 mCRPC biopsies from a cohort of 124 men who had castration-

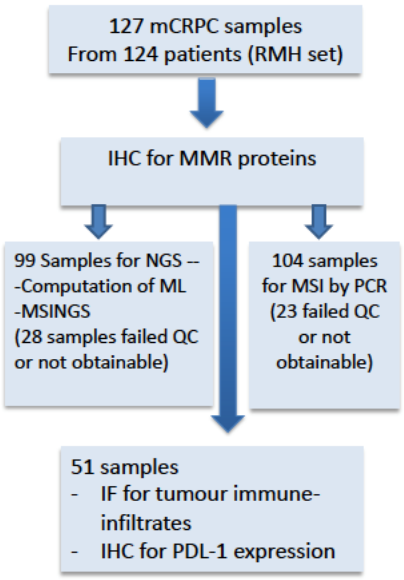

Figure *6* Consort diagram of this study

resistant prostate cancer (CRPC). For 85 patients, we matched HNPC and CRPC samples (Figure 6).

We first analysed orthogonal assays for dMMR; these tests evaluated dMMR by: 1) immunohistochemistry (dMMR_IHC); 2) MSI by PCR (dMMR_MSI; Promega MSI Assay v1.2); 3) targeted next-generation sequencing (NGS) of MMR-pathway gene coding sequences (dMMR_MUT); and 4) MSI by NGS (dMMR_MSINGS). Overall, ten patients had at least one tumour biopsy identified as having dMMR by either IHC and/or MSI (8.1%, 10/124), and were therefore considered biomarker positive, i.e. MMR defective. Patient characteristics, by dMMR status, using these two methods are shown in Table 3.

Table 3 Demographic and clinical characteristics of patients in this study.

Characteristics	MMR proficient (n = 114)	MMR defective (n = 10)	p-value
	n (%)	n (%)	
Gleason score at diagnosis (>7)	69/92 (75%)	7/9 (78%)	0.61a
Stage at diagnosis (≥T3)	58/69 (84%)	4/5 (80%)	0.60a
Nodal involvement at diagnosis	35/59 (59%)	1/2 (50%)	0.66a
Metastatic disease at diagnosis	56/101 (55%)	5/8 (63%)	0.50a
Prostatectomy	16/114 (14%)	1/10 (10%)	0.59a
Radiotherapy	40/114 (35%)	3/10 (30%)	0.52a
	Median (Q1-Q3)	Median (Q1-Q3)	
Age at diagnosis	62.2 (58.4-65.8)	62.9 (55.3-68.6)	0.71b
PSA at diagnosis	75 (17-200)	76 (45-155)	0.68b

PSA = Prostate-specific antigen; a = Fisher's exact test; b = Mann–Whitney test

Using 698 (of 3214) unstable microsatellites present in our previously published genomic panel, consisting of the coding regions of 113 genes (0.6 MB panel), Dr George Seed, a bioinformatician with the Prostate Cancer Targeted Therapy Group ICR, determined microsatellite instability by next-generation sequencing (MSI-NGS) [200]. Of the ten cases defined as dMMR by conventional assays, i.e. IHC negativity in ≥1 MMR proteins and/or ≥2 markers in the Promega MSI Assay v1.2, one case had DNA that failed the quality control (QC) for MSI-NGS. By ranking cases based on their MSI-NGS score, analyses revealed that prostate cancers with dMMR_IHC or dMMR_MSI often, but not always, have higher mutational loads and higher dMMR_MSINGS scores. Comparisons between the different assays are shown in **Figure 7.** There was no easily defined cut-off value for the MSI-NGS data that divided the tumours that were definitely MMR defective from other cancers. However, a cut-off of 0.0244 with this targeted MSI-NGS panel had an area-under-the-curve (AUC) of

0.79, a sensitivity of 60% and a specificity of 98% for predicting MMR cases defined as positive by IHC and/or MSI (Figure 8). For mutational loads based on the targeted panel the AUC was 0.75, with a cut-off point of 6, and was able to detect dMMR with a sensitivity of 78% and a specificity of 72% (Figure 8).

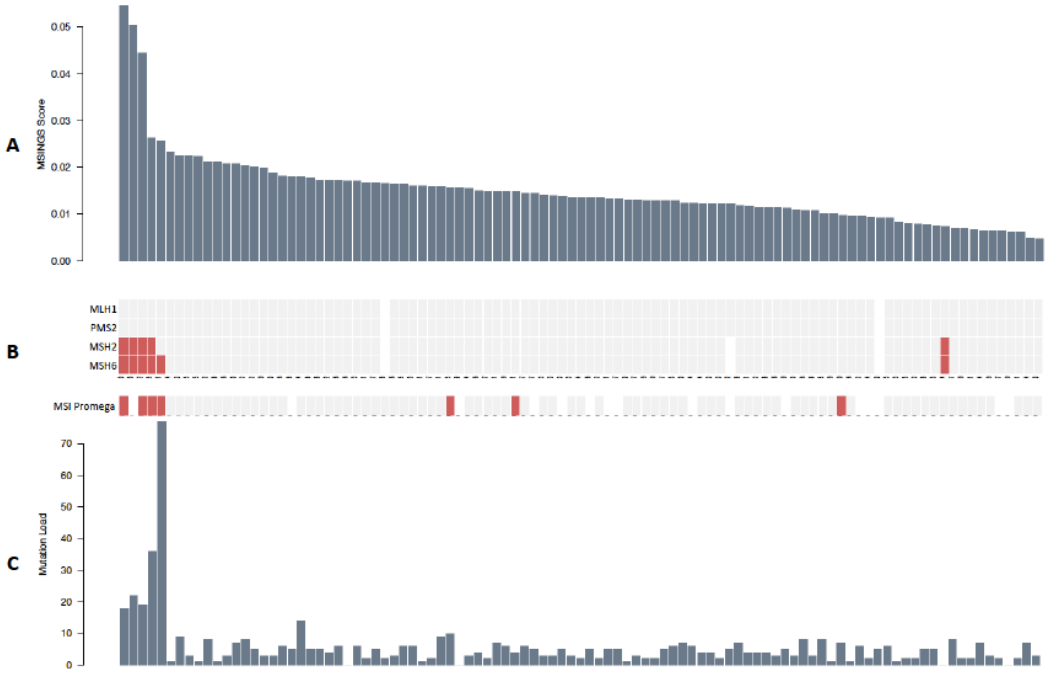

Figure *7* (A) Cases ranked by MSI-NGS (performed by George Seed). (B) Cases with high MSI-NGS scores often, but not always, showed an absence of protein on IHC and are MSI by Promega Assay V2.1 definition. A clear cut-off could not be derived from these data. (C) The highest mutational loads were clustered with higher MSI-NGS scores, but a non-linear relationship was seen between the two variables.

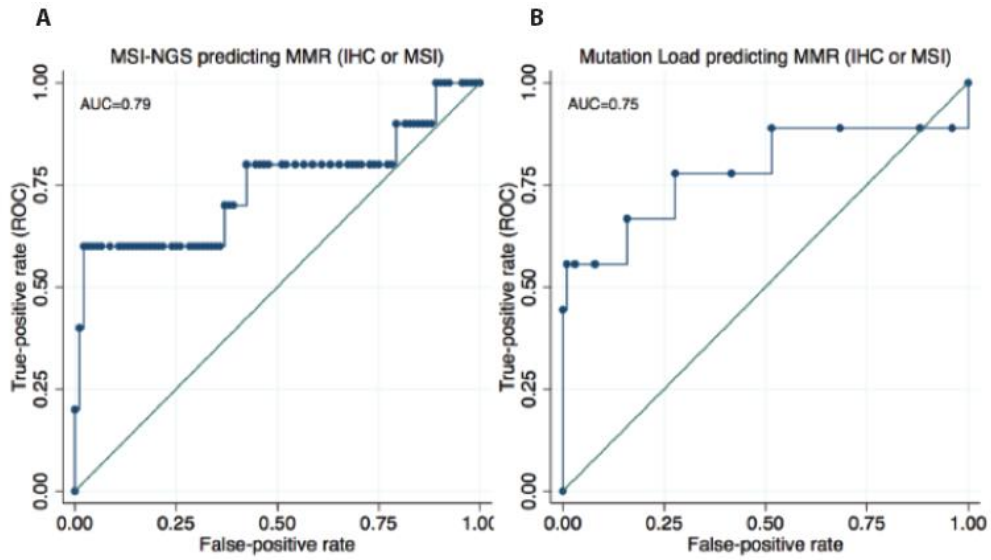

Figure *8* ROC curves were used to determine optimal cut-off points for MSI-NGS and mutational load values to predict dMMR. (A) An MSI-NGS score of 0.024 had an AUC of 0.79 with a sensitivity of 60% and a specificity of 98% to predict dMMR according to the conventional assays definition. (B) A mutational load of six aberrations in the targeted panel had an AUC of 0.75 with a sensitivity of 78% and a specificity of 72% to predict dMMR according to the conventional assays definition.

5.3.3 Impact of Mismatch DNA Repair Defects on Outcomes of Prostate Cancer

The median OS for the dMMR_IHC/dMMR_MSI group was shorter than that in the MMR proficient (pMMR) group, by both univariable and multivariable analyses (3.8 vs 7.0 years from the start of LHRH; aHR: 4.09; 95% CI; 1.52–10.94; p = 0.005), as shown in **Figure 9**.

Patients with pMMR and dMMR disease were balanced in terms of clinical features, and no statistically significant differences between the two groups were observed in terms of radical treatment, Gleason score, presence of metastatic disease at diagnosis, PSA, age, or stage at diagnosis (**Table 4**). Importantly, in this cohort of clinically aggressive tumours, 56% of the patients had metastatic disease at diagnosis.

Table 4 Univariable and multivariable Cox regression analyses.

Variable	OS from diagnosis				OS from LHRHa			
	Univariable HR (95% CI)	p-value	Multivariable HR (95% CI)	p-value	Univariable HR (95% CI)	p-value	Multivariable HR (95% CI)	p-value
MMRd	1.96 (0.94-4.10)	0.08	3.48 (1.36-8.91)	0.009a	2.98 (1.41-6.32)	0.004	4.09 (1.52-10.94)	0.005a
Metastatic disease at diagnosis	2.02 (1.23-3.31)	0.005	1.62 (0.76 – 3.45)	0.21a	1.47 (0.90-2.39)	0.12	1.35 (0.64-2.85)	0.43a
Nodal involvement at diagnosis	1.63 (0.81-3.29)	0.17	1.73 (0.74-4.02)	0.20a	1.44 (0.77-2.67)	0.25	1.75 (0.80-3.84)	0.16a
Stage at diagnosis (≥T3)	1.92 (0.87-4.20)	0.11	1.32 (0.43-4.09)	0.63a	1.41 (0.64-3.11)	0.39	1.05 (0.34-3.30)	0.93a
GS >7	2.53 (1.29-4.95)	0.007	1.55 (0.63-3.85)	0.34a	2.30 (1.17-4.53)	0.02	1.67 (0.65-4.28)	0.28a
Previous treatment (prostatectomy or radiotherapy)	0.46 (0.28-0.75)	0.002	0.63 (0.29-1.34)	0.23a	0.64 (0.39-1.05)	0.08	0.76 (0.36-1.59)	0.47a
PSA at diagnosis (log_{10} ng/mL)	1.34 (0.99-1.82)	0.06	0.87 (0.58-1.32)	0.52a	1.21 (0.90-1.64)	0.21	0.91 (0.62-1.35)	0.64a
Age (10 years, from diagnosis or LHRH)	1.66 (1.15-2.39)	0.007	1.71 (1.12-2.61)	0.01a	1.59 (1.10-2.30)	0.01	1.78 (1.14-2.77)	0.01a

OS = overall survival; HR = hazards ratio; GS = Gleason score; a = univariable and multivariable Cox regression analyses

5.3.4 Intra-patient dMMR Heterogeneity in Primary Disease

Overall, 85 patients had matched HSPC and CRPC samples available for IHC studies. Of these, five patients (5.88%; 5/85) had evidence of IHC-negative foci within their primary disease samples acquired at diagnosis. Of these five, four (80%) had diffusely negative dMMR_IHC in mCRPC biopsies, and one patient relapsed with an MMR IHC-positive tumour. Two of the five HSPC samples with IHC-negative foci demonstrated the co-existence of IHC-positive prostate cancer, i.e. heterogeneous staining (**Figure 10**). In contrast, a single CRPC sample had MMR protein IHC heterogeneity, these biopsies having been acquired from a large pelvic mass arising from a previously irradiated prostate. These data indicate that dMMR can be focal in primary disease, but that having dMMR in primary disease is strongly associated with developing dMMR CRPC.

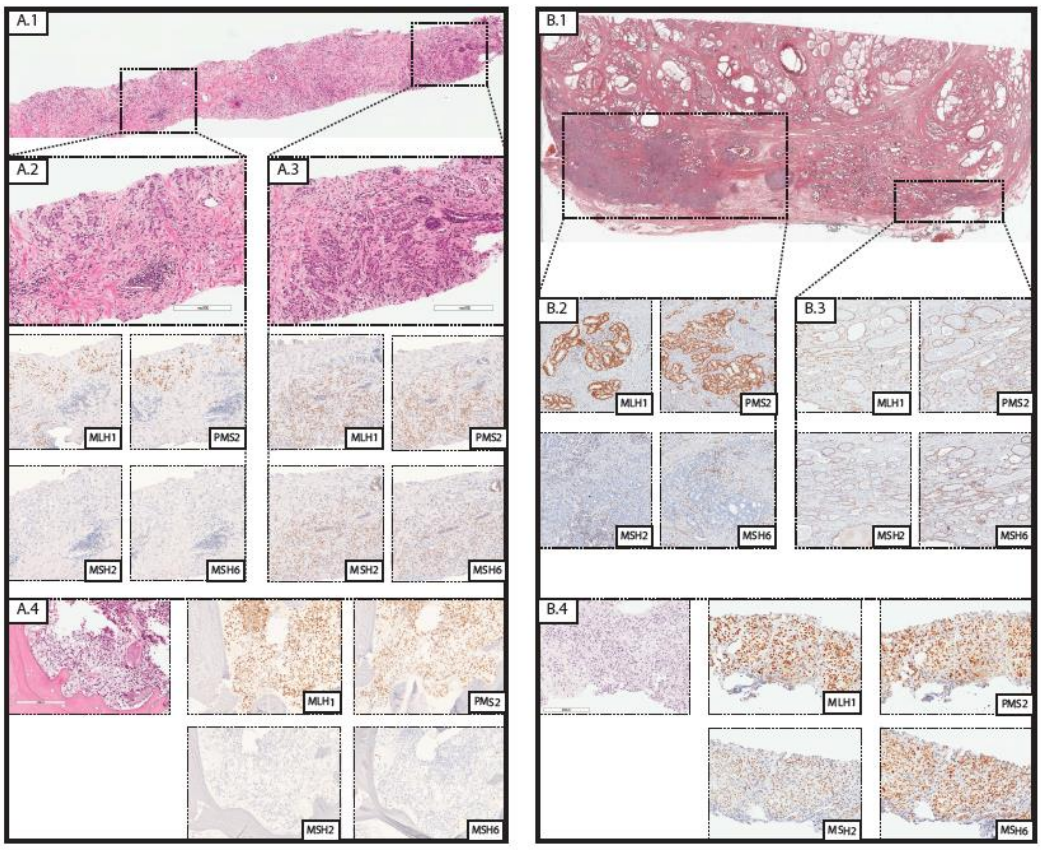

Figure *10* Two of five HSPCs from patients with paired mCRPC samples showed heterogeneous staining in primary disease. One of the patients (A) relapsed with a dMMR mCRPC while the other (B) presented with a mCRPC with

preserved expression of MMR proteins. MMR IHC-negative (A.2, B.2) and MMR-IHC positive areas (A.3, B.3) in HSPCs are highlighted. The IHC statuses of matching mCRPC samples are shown (A.4, B.4).

5.3.5 PD-L1 Expression and Tumour Infiltrating Lymphocytes (TILs) in dMMR CRPC

I next evaluated whether dMMR mCRPC is enriched for PD-L1 (CD274) protein expression, given the key role of this protein in regulating anti-cancer immune responses. PD-L1 immunohistochemistry was performed in 51 mCRPC biopsies using a validated antibody, and a pathologist who was blinded to the MMR status scored membranous staining in tumour cells for PD-L1 in each biopsy (e.g. **Figure 11**).

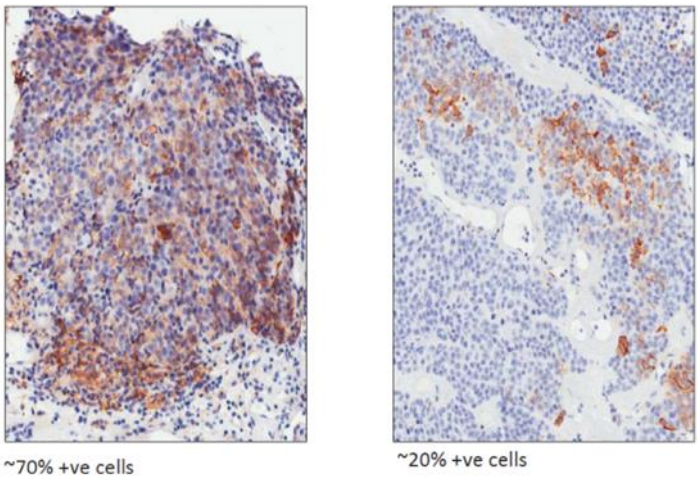

Figure *11* Examples of PD-L1-positive tumours. Partial or complete membranous staining in tumour cells was counted as positive.

Five of ten (50%) dMMR mCRPC samples were scored as PD-L1 positive, while four of 41 (9.8%) pMMR tumours had some positive PD-L1 staining (Figure 12). Although the optimal staining cut-off and optimal assay for determining PD-L1 expression as it pertains to therapeutic responses remains controversial, these data indicate a higher likelihood of PD-L1 positivity in dMMR mCRPC (mixed-effect logistic regression model; OR = 14; 95% CI: 2–84; p = 0.005), providing further evidence for dMMR as a potential predictive biomarker for

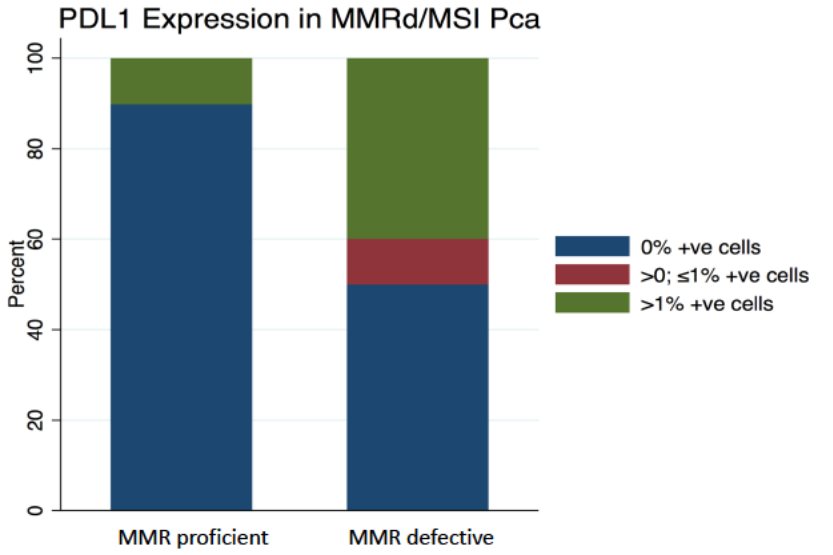

Figure 12 Stacked bar chart depicts proportion of PD-L1 immunohistochemical positivity in samples reviewed by pathologists blinded for dMMR resuls.

immune checkpoint inhibition in lethal prostate cancer.

We next quantified the density of tumour-infiltrating T lymphocytes (D-TILs) in biopsies from this cohort from patients with sufficient tumour tissue to do so. D-TILs were here defined as the number of CD4+ cells(with and without FOXP3) and CD8+ lymphocytes per mm^2 of tumour, as determined through 180 multi-spectral, multicolour, immunofluorescence image

cubes (200× magnification; median of three images per case; n = 51 selected mCRPC biopsies). Tissue sites included lymph node biopsies (n = 35), bone (n = 12), liver (n = 2), soft tissue metastases (n = 1), and one sample from a transurethral resection of the prostate (this last sample was excluded from this analysis as it was not metastatic). T cell infiltration was strikingly heterogeneous, ranging from 0 to 828 lymphocytes/mm^2.

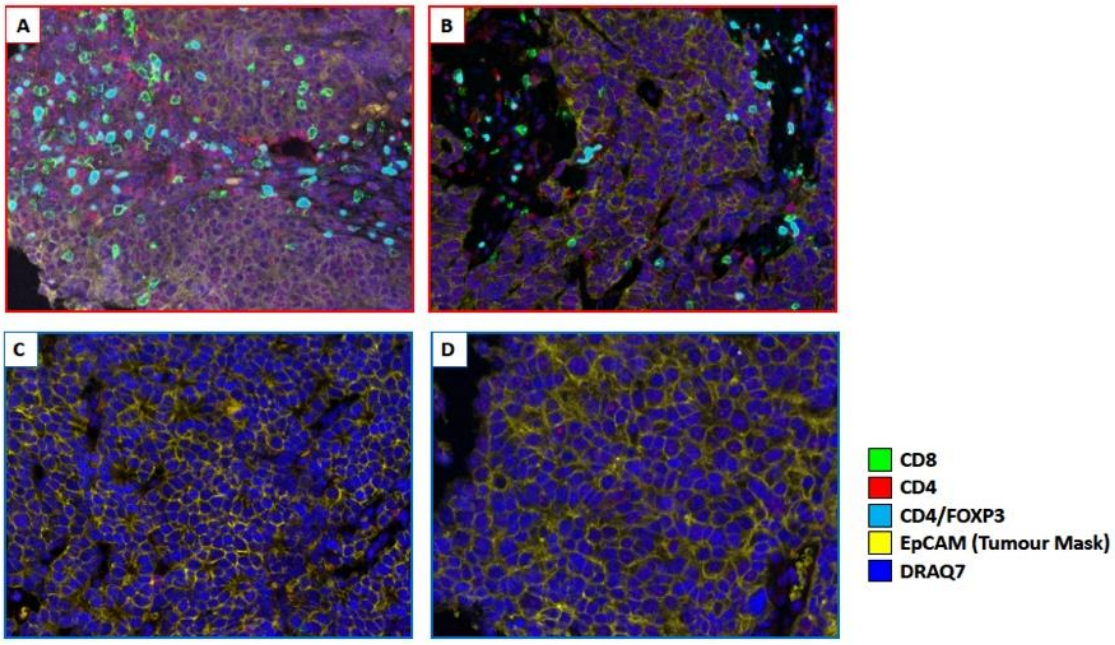

Figure *13* Four examples of mCRPCs in lymph nodes using multicolour immunofluorescence. Only lymphocytes within EpCam-positive areas were counted. (7A, 7B) Two cases were from the upper quartile of D-TILs in the cohort. (7C, 7D) Two cases were from the lower quartile of D-TILs in the cohort.

Ranking tumours by T cell density showed that five of the nine (55.5%) dMMR_IHC/dMMR_MSI cases were allotted to the upper quartile of D-TILs in this cohort and three of these five cases had >10 mutations (>90th centile; 113-gene panel). The remaining four dMMR_IHC/dMMR_MSI cases, however, did not show relatively increased D-TILs in relation to this cohort. These data suggest that some, but not all, mCRPCs with dMMR_IHC/dMMR_MSI have higher D-TILs than tumours without dMMR (**Figure 14**).

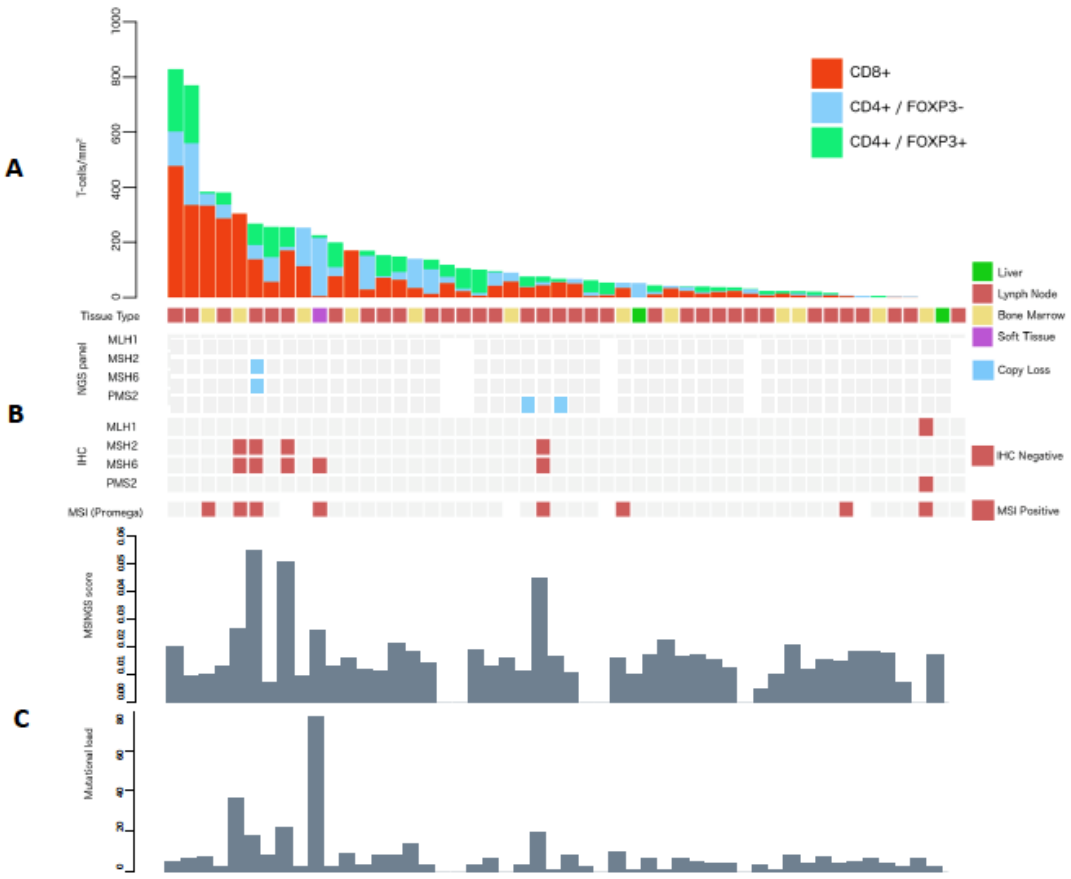

Figure *14* (A) Fifty cases from the study ranked by D-TILs. (B) NGS determination of aberrations involving MMR genes and biomarker status for IHC and Promega v1.2. Five of nine dMMR cases defined by conventional assays were within to the upper quartile of D-TILs. Four dMMR cases did not show increased D-TILs relative to the cohort. (C) MSI-NGS and mutational load for the 50 cases analysed for D-TILs.

Of the remaining pMMR samples in the upper quartile of D-TILs, none had pathogenic DNA repair defects by the targeted NGS panel. Two samples in this group showed impactful mutations in other pathways (PIK3CA E542K; JAK1 E1051*). In this cohort of tumours analysed for D-TILs, PD-L1 expression was associated with increased T-cell infiltration in dMMR mCRPC samples (incidence rate ratio = 11.47; 95% CI: 4.08–32.22; p < 0.001; **Figure 15**).

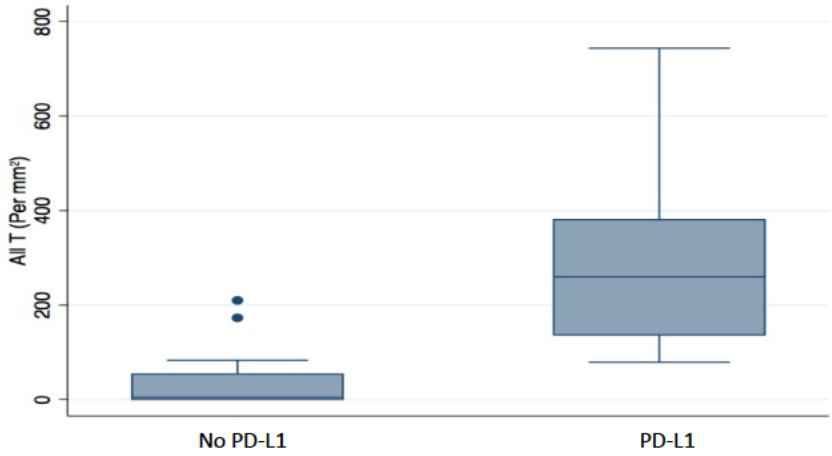

Figure *15* Expression of PD-L1 in relation to D-TILs. Cases with any proportion of PD-L1-positive tumour cells had a higher mean number of D-TILs compared with that of PD-L1-negative cases.

5.4 Discussion

Contrary to what was previously believed, PC is a highly heterogeneous disease. Many PCs harbour germline or somatic DNA repair gene aberrations; of these, *BRCA2* is the most commonly aberrant gene, although other HRD genes can be deleteriously aberrant, including *BRCA1, PALB2, RAD51* and *FANCA* [92]. Preclinical studies have shown that bi-allelic loss of one of these genes can result in sensitisation to PARP inhibition (PARPi), to differing degrees, with the loss of *BRCA2* being the most sensitising [201][92]. Therefore,

with multiple PARP inhibitors available, defining qualified predictive biomarkers for identifying tumours sensitive to these agents is of paramount importance.

In the first section of this chapter, I described the results of the TOPARP-B trial, which has confirmed the antitumour activity of olaparib against metastatic castration-resistant prostate cancer with specific DDR gene aberrations. The number of composite responses observed in the cohort of patients who received 400 mg tablets of olaparib twice daily met the predefined criteria for success**, validating the DDR aberration as being a predictive biomarker of response.**

The antitumour activity observed varied considerably for different DDR gene aberrations, with the greatest antitumour activity seen in the subgroup with BRCA1/2 alterations. Antitumour activity was also observed in other DDR gene aberration subgroups. Responses in tumours with PALB2 mutations were frequent, although the low prevalence of these mutations requires further data to confirm these findings. The antitumour activity for ATM-loss cancers seemed to be less striking than that for BRCA-altered tumours; nevertheless, a subset of patients with ATM-altered mCRCP appears to derive some benefit. Our data suggest that a 400 mg dose is more effective, although the higher percentage of CDK12-loss cancers in the 300 mg cohort might explain the inferior composite response in this cohort.

Recently, other phase II trials have been conducted which have confirmed our data. The TRITON2 study is a phase II study evaluating the efficacy of rucaparib 600 mg twice a day in patients with a deleterious germline or somatic alteration in HRR genes. The latest update on this trial was presented at the 2019 American Society of Clinical Oncology (ASCO) annual

meeting. Among evaluable patients with either germline or somatic deleterious BRCA1/2 alterations, 44.0% (11/25) had a confirmed radiographic response and 51.1% (23/45) had a confirmed PSA response [202]. Based on these data, the US FDA granted rucaparib the designation of Breakthrough Therapy for BRCA1/BRCA2-mutated mCRPC. Niraparib was tested in the phase II GALAHAD study on 39 mCRPC patients with mutations in BRCA1, BRCA2, ATM, FANCA, PALB2, CHEK2, BRIP1, or HDAC2. A plasma-based test was developed to screen patients with mutations in these genes. Preliminary results were reported at the ASCO Genitourinary Cancers Symposium 2019. Among 23 patients with BRCA mutations, there was a 38% (5/13) ORR by RECIST, a 57% (13/23) PSA response, and a 48% (11/23) CTC conversion [203].

In the second section of this chapter, I described the clinical utility of cfDNA analyses as **multipurpose biomarkers for treatment with PARP inhibition** in mCRPC. Critically, our cfDNA analyses detected all somatic HRD-associated mutations identified in tumour biopsies, as well as new mutations emerging at disease progression. These new mutations likely represent tumour subclones induced by therapeutic selective pressure driving drug resistance. **Therefore, cfDNA is a useful biomarker to define response to treatment and to anticipate disease progression when new tumour clones emerge, more comprehensively than single-site biopsies, and to guide early treatment-switch decisions in the presence of ineffective therapies.**

Monitoring this subclonal equilibrium between the original clone and resistant clones merits further evaluation, as PARP inhibitor discontinuation and administration of other treatments

could potentially restore the dominance of the original clone that was sensitive to PARP inhibitors or platinum.

In the third section of this chapter, I studied the prevalence of dMMR in mCRPC and also demonstrated that PC patients with dMMR exhibit worse outcomes overall; furthermore, I showed that these patients also progress quickly through androgen-deprivation therapy for reasons that have yet to be determined. **Therefore, defects in this DNA repair system clearly represent a prognostic factor associated with worse survival in the metastatic setting**, which also confirms the data from Nghiem and colleagues, who demonstrated a substantially shorter OS from diagnosis in patients with dMMR [199].

In our analysis, there was a significant concordance between different assays describing dMMR PCs; generally speaking, these cancers are characterised by a high mutational load and microsatellite instability, confirming other case-control studies [204]. Discrimination between *self* and *non-self* is at the core of the immune system's functionality [205]. Moreover, hypermutating tumours with defective MMR are important candidates for higher immunogenicity; the emergence of neoantigens from mutated genes enables self/non-self discrimination and is indeed necessary for tumour-specific immune responses [206]. The association between tumour infiltration and dMMR seemed to be less clear in our analysis; just over half (5/9) of the dMMR mCRPCs showed a higher mutational burden with a targeted 113 gene NGS panel. Interestingly, cases with the highest mutational loads had relatively higher lymphocytic infiltration. Of the remaining four cases defined as dMMR by IHC or Promega v1.2, mutational load, MSI assessment by NGS, and lymphocytic infiltration were unremarkable relative to the rest of cohort. Perhaps most relevant from the immuno-

oncologic perspective, **PD-L1 IHC expression, an established predictive biomarker for anti-PD1 therapy [207-209], was significantly more common in dMMR tumours**, but was largely restricted to those tumours that showed significant T cell infiltration. These data support PD-L1 expression as an adaptive event in tumours that become a target of inflammation [210-212], rather than constitutive expression underpinned by specific genomic aberrations, as reported in glioblastomas and carcinomas of the lung [213, 214].

Overall, my data indicate that **the presence of defects in MMR/high mutational load/high MSI can be used as predictive biomarkers of response to immune checkpoint inhibitors**, which are currently used in disease such as melanomas, lung cancer and bladder carcinomas.

In summary, in this chapter I explored how genomic studies of tumour tissues or blood samples are able to identify specific aberrations associated to subsets of mCRPC that are likely to benefit from new anticancer treatments such as PARP inhibitors and immune checkpoint inhibitors.

6 Final Conclusions

Prostate cancer (PC) is one of the most common diseases in men. When diagnosed before spreading outside the organ of origin, it is a curable disease; however, nearly a quarter of patients with PC develop metastatic disease (mPC). Most mPCs are responsive to anti-androgenic treatments but eventually progress into a castration-resistant state, known as mCRPC. This is a lethal condition but the clinical course of patients varies greatly, with some individuals responding for years to cytotoxic or endocrine treatments, such as abiraterone and enzalutamide, while others progress within months through all the standard treatments approved in this setting. Therefore, defining biomarkers to improve patient stratification and predict outcomes on treatment is of paramount importance.

The studies I have described in my thesis express the aims of my work: to discover biomarkers that are better able to define mCRPC as a heterogeneous disease, but also to offer putative new biomarkers of response/resistance to both standard treatments and novel therapeutic agents in this setting.

A **summary of the main conclusions** derived from this thesis include:

- PSA changes, as early as 4 weeks from the treatment start, in mCRPC patients treated with hormonal agents, such as abiraterone and enzalutamide, are associated with patients' overall survival and responses to these agents.
- Using IHC assays to determine the presence of splicing variant 7 of the androgen receptor (AR-V7), I confirmed that:

    - The expression of AR-V7 increases with the development of the castration-resistant status.
    - AR-V7 protein expression is a biomarker of poorer prognosis that increases with emerging drug resistance and can potentially be used to predict a lack of response to hormonal agents, such as abiraterone or enzalutamide.
    - AR-V7 positive status in CTC associates with burden of disease and poor survival.
- PTEN loss is an early event in the biological history of PC and is associated with the more aggressive nature of these tumours (a prognostic biomarker).
- Loss of PTEN is a promising predictive biomarker of response to AKT inhibitors.
- Defects in the mechanism of DNA repair known as homologous recombination are able to predict responses to PARP inhibitors.
- Liquid biomarkers, such as cfDNA, are able to predict outcomes in patients treated with PARP inhibitors and responses to these agents at as early as 4 weeks.
- PC with defective MMR machinery comprises a heterogeneous group of diseases enriched for, but not exclusively constituted of, hypermutated, microsatellite unstable, highly inflamed, PD-L1 expressing tumours. Therefore, dMMR status could be used to predict response to immunotherapy agents.

In summary, clinically aggressive PCs are characterised by a variety of molecular aberrations, some of which are associated with differential prognoses and sensitivities to systemic therapeutic agents.

7 Materials and Methods

7.1 Patient populations

All patients (chapters 3, 4, 5; except for some of the TOPARP-B trial) were enrolled on institutional protocols approved by the Royal Marsden NHS Foundation Trust Hospital (London, UK), Ethics Review Committees (Research Ethics Committee (RCE) Reference number: 04/Q0801/60). Clinical data were retrieved from the Royal Marsden Hospital's electronic patient records.

7.1.1 Chapter 3 (PSA study)

7.1.1.1 Study design and data collection

Patients with biochemically or histologically confirmed progressive mCRPC and castrate levels of testosterone treated with AA and/or enzalutamide outside of a clinical trial between 06.01.06 and 31.12.17 in 13 cancer centres worldwide were considered eligible for this analysis. Additional inclusion criteria were the availability of PSA levels assessed at baseline, after 4-weeks and/or 12-weeks of treatment, a physical examination, including Eastern Cooperative Oncology Group performance status (ECOG PS), and routine safety blood tests laboratory studies, including a full blood count (haemoglobin, neutrophil and lymphocyte count), biochemistry comprising alkaline phosphatase (ALP), lactate dehydrogenase (LDH) at baseline and during treatment. Every institution has received ethic board approval for the treatment of patient data.

7.1.2 Chapter 4 (phase I trial with Enzalutamide and Capivasertib)

7.1.2.1 Inclusion Criteria:

1. Written informed consent.

2. Histological diagnosis of adenocarcinoma of the prostate and with tumour tissue accessible for research analyses for this trial (e.g. PTEN testing).

Patients who have no histological diagnosis must be willing to undergo a biopsy to prove prostate adenocarcinoma.

3. Metastatic Castration-Resistant Prostate Cancer (mCRPC).

4. Progressed after 1 or 2 lines of taxane based chemotherapy.

5. Progressed after abiraterone or enzalutamide (pre or post chemotherapy). Patients must have received at least 12 weeks of treatment with either abiraterone or enzalutamide.

6. Age ≥18 years.

7. Eastern Cooperative Oncology Group (ECOG) performance status (PS) 0 – 2.

8. PSA ≥ 10ng/ml.

9. Documented willingness to use an effective means of contraception while participating in the study and for 12 months post last dose of treatment (see section 4.5).

10. Documented ongoing castrate serum testosterone <50 ng/dL (<2.0 nM).

11. Received prior castration by orchiectomy and/or ongoing Luteinizing Hormone-Releasing Hormone (LH-RH) agonist treatment.

12. Progression of disease by PSA utilizing PCWG2 criteria and at least another of the following criteria:

a. Bone scan: disease progression as defined by at last 2 new lesions on bone scan.

b. Soft tissue disease progression defined by modified RECIST 1.1.

c. Clinical progression with worsening pain and the need for palliative radiotherapy for bone metastases.

13. Willing to have a biopsy to obtain tumour tissue for biomarker analyses prior to and after treatment.

7.1.2.2 Exclusion Criteria:

1. Prior treatment with PI3K, AKT, TOR kinase or mTOR inhibitors (see Appendix C).

2. Surgery, chemotherapy, or other anti-cancer therapy within 4 weeks prior to trial entry / randomisation into the study (6 weeks for bicalutamide). Any other therapies for prostate cancer, other than LHRH analogue therapy, such as progesterone, medroxyprogesterone, progestins (megesterol), or 5-alpha reductase inhibitors (e.g., finasteride or dutasteride), must be discontinued at least 2 weeks before the first dose of study drug.

3. Participation in another clinical trial and any concurrent treatment with any investigational drug within 4 weeks prior to trial entry / randomisation.

4. Prior limited field radiotherapy within 2 weeks or wide field radiotherapy within 4 weeks of trial entry / randomisation.

5. History of seizure or any condition that may predispose to seizure including, but not limited to underlying brain injury, stroke, primary brain tumours, brain metastases, or alcoholism.

6. History of loss of consciousness or transient ischemic attack within the previous 12 months of trial entry / randomisation.

7. Known brain or leptomeningeal involvement.

8. Use of potent inhibitors or inducers of CYP3A4, CYP2C9 and CYP2C19 within 2 weeks before trial entry / randomisation (3 weeks for St John's Wort) must be avoided.

9. Clinically significant abnormalities of glucose metabolism as defined by any of the following:

a. Diagnosis of diabetes mellitus type I or II (irrespective of management).

b. Glycosylated haemoglobin (HbA1C) ≥8.0% at screening (64 mmol/mol) (conversion equation for HbA1C [IFCC-HbA1C (mmol/mol) = [DCCT-HbA1C (%) – 2.15] x 10.929).

c. Fasting Plasma Glucose ≥ 8.9mmol/L at screening. Fasting is defined as no caloric intake for at least 8 hours.

10. Inadequate organ and bone marrow function as evidenced by:

a. Haemoglobin <8.5 g/dL

b. Absolute neutrophil count <1.0 x 109/L

c. Platelet count < 75 x 109/L

d. Albumin ≤25 g/dL.

e. AST / SGOT and/or ALT / SGPT ≥ 2.5 x ULN (≥ 5 x ULN if liver metastases present)

f. Total bilirubin ≥ 1.5 x ULN (except for patient with documented Gilbert's disease)

g. Serum Creatinine > 1.5 x ULN

11. Inability or unwillingness to swallow oral medication.

12. Malabsorption syndrome or other condition that would interfere with enteral absorption.

13. Any of the following cardiac criteria;

a. Mean resting corrected QT interval (QTcF) >470msec obtained from 3 consecutive ECGs taken within 5 minutes.

b. Any clinically important abnormalities in rhythm, conduction, or morphology of a resting ECG (e.g., complete left bundle branch block, third degree heart block).

c. Any factors that increase the risk of QTc prolongation or risk of arrhythmic events such as heart failure, hypokalaemia, congenital long QT syndrome, family history of long QT.

d. syndrome or unexplained sudden death under 40 years-of-age, or any concomitant.

e. medication known to prolong the QT interval or with a potential for Torsades de pointes.

f. Experience of any of the following procedures or conditions in the preceding six months: coronary artery bypass graft, angioplasty, vascular stent, myocardial infarction, angina pectoris, congestive heart failure NYHA ≥ Grade2.

g. Uncontrolled hypotension defined as – systolic blood pressure (BP) <90mmHg and/or diastolic BP <50mmHg.

14. Clinically significant history of liver disease consistent with Child-Pugh Class B or C, including viral or other hepatitis, current alcohol abuse, or cirrhosis.

15. Any other finding giving reasonable suspicion of a disease or condition that contraindicates the use of an investigational drug or that may affect the interpretation of the results or renders the patients at high risk from treatment complications.

16. Need for chronic corticosteroid therapy of >10 mg of prednisolone or >0.5mg of dexamethasone per day or an equivalent dose of other anti-inflammatory corticosteroid, for the use of concomitant steroids on this trial please refer to section 12.1. Patients in which corticosteroids cannot be stopped prior to entering the trial are allowed a maximum of 10mg of prednisolone per day or equivalent. In the case of corticosteroids discontinuation, a 2-week

(14 days) washout is required with a mandatory PSA check prior to starting the trial. If the PSA has declined compared to the value obtained prior to stopping corticosteroids, patients

will not be eligible for study. Patients can only enter the study with a confirmed PSA increase.

17. Malignancies other than prostate cancer within 5 years prior to trial entry / randomisation, except for adequately treated basal or squamous cell skin cancer.

18. Unresolved clinically significant toxicity from prior therapy except for alopecia and Grade peripheral neuropathy.

19. Inability to comply with study and follow-up procedures.

20. Patients with predominately small cell or neuroendocrine differentiated prostate cancer are not eligible.

7.1.3 Chapter 5 (ToparpB phase II trial)

See appendix page 1-3 https://doi.org/10.1016/S1470-2045(19)30684-9

7.2 Patient Samples

All samples used in my investigations came from patients who had given written informed consent in line with Good Clinical Practice guidelines and the Declaration of Helsinki.

7.2.1 Chapters 3, 4, 5: Sample collection

Primary hormone-sensitive prostate cancers (HSPC) were obtained from prostate needle biopsies, transurethral resections of the prostate (TURP), and radical prostatectomies. Metastatic castration-resistant prostate cancer (CRPC) tissues were acquired from bone (bone marrow trephines), lymph node, viscera, and soft tissues (needle biopsies). Matched HSPC-CRPC samples coming from the same individual at two different time-points were available for a subset of patients. The samples used for my Whole-Genome Sequencing studies were fresh-frozen material taken exclusively from lymph-nodes, viscera, and soft tissues. All other samples were routinely processed formalin-fixed paraffin embedded (FFPE) tissue blocks. Blocks were sectioned and tumour content estimated from haematoxylin-eosin stained slides. Immunohistochemistry assays were performed on 4µm thick sections adjacent to tumour confirmation H&E sections.

7.3 Immunophenotyping

Conventional 3,3'-diaminobenzidine (DAB) chromogen-based immunohistochemistry and brightfield analyses were used in all investigations described in this dissertation. In chapter 5, multi-colour immunofluorescence, multispectral imaging, and computerised image analysis were also used.

7.3.1 Immunohistochemistry (IHC) – Technical Aspects

Immunohistochemistry assays were performed by members of the Cancer Biomarkers Team using the Launch i6000 autostainer (Biogenex). This team was formed, at the time of data collection for this dissertation, by biomedical scientists Ruth Riisnaes, Mateus Crespo, Susana Miranda, and Ines Figueiredo. IHC assays were performed by the Pathologists Daniel Nava Rodrigues and Bora Gurel. Methods for specific markers are summarised in **Table 1.1**. Only monoclonal antibodies were used in the investigations herein described.

Sections from FFPE blocks were first heated at 60^{o}C for 30 minutes then dewaxed in three 5 minute washes of xylene. Removal of xylene was done by submerging slides twice for 3 minutes in absolute ethanol followed by 1 minute in running tap water and a quick rinse with distilled water.

Table 1.1 Summary of antibodies and immunohistochemistry methods used in this dissertation.

ANTIBODY	CODE	COMPANY	CLONE	DILUTION	Species	VISUALISATION	RETRIEVAL BUFFER	CONTROLS (+ / -)
AR-NTD	#M3562	Agilent-Dako	AR441	1:200	Mouse	DAKO Envision	pH8.1 TRIS/EDTA	VCaP; 22RV1 **/** PC3
AR-V7 (Ab1)	#EPR15656	Abcam-Epitomics	EP343	1:200	Rabbit	Leica Novolink	pH6 Citrate	VCaP; 22RV1 **/** DU145
PTEN	#9559	Cell Signaling Technology	138G6	1:250	Rabbit	Rabbit ABC	pH6 Citrate	22RV1 **/** PC3
MSH2	#M3639	Agilent-Dako	FE11	1:50	Mouse	DAKO Envision	pH8.1 TRIS/EDTA	Appx (germinal center) **/** LNCAP
MSH6	#M3646	Agilent-Dako	EP49	1:500	Rabbit	DAKO Envision	pH8.1 TRIS/EDTA	Appx (germinal center) **/** skeletal muscle
MLH1	#M3640	Agilent-Dako	ES05	1:100	Mouse	DAKO Envision	pH8.1 TRIS/EDTA	Appx (germinal center) **/** HCT116; skeletal muscle
PMS2	#M3647	Agilent-Dako	EP51	1:100	Rabbit	DAKO Envision	pH8.1 TRIS/EDTA	Appx (germinal center) **/** HCT116; skeletal muscle
PD-L1	#13684	Cell Signaling Technology	E1L3N	1:200	Rabbit	DAKO Envision	pH8.1 TRIS/EDTA	Placenta (trophoblast) **/** Ovarian stroma

- Solutions used in the IHC assays are detailed below:
  - **3% Hydrogen Peroxide (per 10mL):** Mix 1 mL hydrogen peroxide and 9 mL distilled water. Store at room temperature, use on the day of preparation.

  - **Tris Buffered Saline (Plus Tween 20) Wash Buffer, pH7.4 (TBST) (per 5L):** Mix the following in 5 litres of distilled water: 40g sodium chloride, 3.025g TRIS, 22 mL hydrochloric acid and 10 mL Tween 20. Adjust pH to 7.4 with 1M HCl or 1M NaOH. Store at room temperature. Use within a week. Re-adjust pH daily.

  - **TRIS/EDTA Buffer Stock (per 50mL)**: Dissolve 1.25g Trizma® base (#T1502; Sigma) and 1.6g trisodium citrate dihydrate in 50 mL distilled water. Add 2.5 g EDTA disodium salt dihydrate and mix. Store at room temperature, expiry date 2 months.

  - **TRIS/EDTA buffer pH 8.1 (Retrieval buffer):** Dilute TRIS/EDTA Buffer Stock 1:10 with distilled water. Adjust pH to 8.1 (+/- 0.1) using 1M HCl or 1M NaOH. Prepare fresh and discard after use.

  - **Citrate Buffer pH6 (Retrieval buffer)** (#HDS05; TCS Biosciences)**:** Dilute antigen retrieval buffer concentrate 1:100 with distilled water. Adjust pH to 6.0 (+/- 0.1) using 1M HCl or 1M NaOH. Prepare fresh and discard after use.

  - **Antibody diluent:** Dako REAL (#2022; Agilent-Dako).

The generic workflow following dewaxing is: **(1)** ***antigen retrieval,*** **(2)** ***peroxidase block,*** **(3)** ***protein (non-specific binding) block,*** **(4)** ***primary antibody incubation,*** **(5)** ***detection system,*** **(6)** ***DAB, and*** **(7)** ***counterstaining.*** Protocols for specific markers are detailed below. To avoid needless repetitions, methods will refer to the section 7.3.1.1 and only differences are otherwise specified.

7.3.1.1 AR-NTD

AR-NTD IHC was performed as previously described [215]. **(1)** Briefly, antigen retrieval was done by heating tissue sections in TRIS/EDTA (pH8.1) buffer using a water bath at 97^{o}C for 30 minutes. Slides were left to cool down at room temperature for 20 minutes then washed in running tap water for 5 minutes, then rinsed with distilled water. Sections were then soaked in a dish containing 300ml of TBST (Tris buffered saline with 0.2% Tween 20) for a minimum of 25 minutes. Excess liquid was carefully blotted to avoid contact with tissue and to avoid tissue drying up followed by marking of the slide with a PAP pen to concentrate reagents over tissue. The auto-stainer performed the next steps according to previously programmed protocols. Briefly, a wash with TBST is included in the beginning of all protocols to avoid sections drying up. **(2)** Endogenous peroxidase was blocked using 250μl of a 3% H_2O_2 solution incubated for 10 minutes at room temperature followed by washes with TBST (5x). **(3)** Nonspecific binding was blocked by incubating 250μl of Dako Protein Block (#X0909; Agilent-Dako) for 10 minutes at room temperature. **(4)** Slides were incubated with 250μl of appropriately diluted (1:200 or 1:5000) mouse monoclonal anti-AR-NTD antibody clone AR441 (#M3562; Agilent-Dako) for one hour. Two different dilutions were used with different purposes: *i)* in chapter 4, where we investigate AR-NTD expression in mCRPCs (which frequently overexpress AR), I used a 1:5000 dilution to increase the dynamic range of signal allowing for the identification of a gradient of intensities; *ii)* in chapter 7, my goal was to segregate between true AR positive and negative (small cell/high grade neuroendocrine carcinomas) tumours, so antibody was concentrated to 1:200 to increase sensitivity. Primary antibody was then washed with TBST (5x). **(5)** 250μl of secondary antibody labelled with polymer/horseradish peroxidase (HRP) from the EnVision kit (#K5007; Agilent-Dako) was applied to each section, incubated for 30 minutes then washed with TBST (5x). **(6)** 250μl of the chromogen 3,30-diaminobenzidine tetrahydrochloride (DAB) (diluted according to manufacturer's specifications) was applied to tissue and incubated for 5 minutes. Following staining, slides were washed with distilled water. Slides were then removed from the auto-stainer for counterstaining. **(7)** Slides were counterstained with Harris' haematoxylin for 3 minutes, then rinsed with running tap water, quickly dipped into 1% acid alcohol (approximately 5 seconds) for differentiation and again washed in running

tap water. Tissue sections were dehydrated in 3 changes of absolute ethanol (3 minutes) and diaphonised in 3 changes of xylene (3 minutes). Slides were then coverslipped using DPX mountant (#44581; Sigma) and analysed using an Olympus BX41 compound light microscope (Olympus). VCaP and 22RV1 were used as positive; PC3 as negative controls.

7.3.1.2 AR-V7 (Clone EP343)

AR-V7 (Clone EP343) IHC was performed as previously described [215]. **(1)** Briefly, antigen retrieval was done by microwaving tissue sections in citrate buffer (#HDS05; TCS Biosciences) (pH6) at full power (900W) for 18 minutes. Slides were left to cool down at room temperature for 20 minutes then washed in running tap water for 5 minutes, then rinsed with distilled water. Sections were then soaked in a dish containing 300ml of TBST (Tris buffered saline with 0.2% Tween 20) for at least 25 minutes. Excess liquid was carefully blotted to avoid contact with tissue and to avoid tissue drying up followed by marking of the slide with a PAP pen to concentrate reagents over tissue. **(2)** Endogenous peroxidase was blocked using the ready-made solution Peroxidase Block (#RE7157; Leica-Novocastra) from the Novolink™ Max Polymer Detection System (#RE7280-K; Leica-Novocastra) incubated for 10 minutes at room temperature followed by washes with TBST (5x). **(3)** Nonspecific binding was blocked by incubating 250μl of using the ready-made solution Protein Block (#RE7158; Leica-Novocastra) from the Novolink™ Max Polymer Detection System (#RE7280-K; Leica-Novocastra) for 5 minutes. **(4)** Slides were incubated with 250μl of appropriately diluted (1:200) rabbit monoclonal anti-AR-V7 antibody clone EP343 (#EPR15656; Abcam-Epitomics) for one hour then washed with TBST (5x). **(5)** 250μl of secondary antibody labelled with polymer/horseradish peroxidase (HRP) of ready-made Novolink™ Polymer (#RE7161; Leica-Novocastra) solution from the Novolink™ Max Polymer Detection System (#RE7280-K; Leica-Novocastra) was applied to each section, incubated for 30 minutes, and then washed with TBST (5x). **(6)** 250μl of the chromogen 3,30-diaminobenzidine tetrahydrochloride (DAB) (diluted according to manufacturer's specifications) from the Novolink™ Max Polymer Detection System (#RE7280-K; Leica-Novocastra) was applied to tissue and incubated for 5 minutes. Following staining, slides were washed with distilled water. Slides were then

removed from the auto-stainer for counterstaining. **(7)** VCaP and 22RV1 were used as positive; DU145 as negative controls.

7.3.1.3 AR-V7 (Clone RM7) and pERK protein expression

IHC for AR-V7 (Clone RM7, GTX33604, GeneTex) and pERK (Clone D13.14.4E, 4370, Cell Signalling Technology) was performed on CRPC patient biopsies as previously described10. All tissue blocks from CRPC biopsies were sectioned and only considered for IHC analyses if adequate tumour material was present (≥ 50 tumour cells by author DNR). For AR-V7 IHC (Clone RM7, GTX33604, GeneTex), following antigen retrieval (Tris/EDTA buffer, pH8.1) in microwave for 18 minutes at 800W, the antibody was diluted (1:500) in Dako REAL diluent (Dako, Agilent Technologies) and tissue was incubated for 1 hour. For pERK IHC (Clone D13.14.4E, 4370, Cell Signalling Technology), following antigen retrieval (Citrate buffer, pH6.0) in microwave for 18 minutes at 800W, the antibody was diluted (1:400) in Dako REAL diluent (Dako, Agilent Technologies) and tissue was incubated for 1 hour. After washes, bound antibody was visualized using the Dako EnVision Detection System (Dako, Agilent Technologies). Sections were counterstained with hematoxylin. Mouse xenografts from 22Rv1 (AR-V7 positive) and PC3 (AR- V7 negative), and cell pellets from VCaP (AR-V7 positive) and DU145 (AR-V7 negative), were used as controls for AR-V7 IHC. Cell pellets from 22Rv1 treated with vehicle (pERK positive) or trametinib (pERK negative) were used as controls for pERK IHC. Rabbit IgGs were used as negative controls. Nuclear AR-V7 expession was determined for each case using a modified H-score method and pERK expression was reported as percentage positive cells.

7.3.1.4 PTEN

PTEN IHC was performed as previously described [117, 216]. Protein block was pursued with 5% goat serum from the VECTASTAIN® Elite ABC kit (#PK-6101; Maravai Lifesciences - Vector Laboratories) for 20 minutes. Slides were incubated with appropriately diluted (1:250) rabbit monoclonal anti-PTEN antibody clone 138G6 (#9559; Cell Signaling Technology)

followed by washes with TBST (5x). This was followed by 30-minute incubation with biotinylated secondary antibody, followed by the avidin/biotinylated enzyme complex (ABC) mixture (#PK-6101; VECTASTAIN® Elite ABC kit). 22RV1 were used as positive and PC3 were used as negative controls. Endothelial and stromal cells used as internal positive controls for PTEN in patient samples.

Cases were dichotomised as either PTEN IHC positive or negative. For equivocal cases, an arbitrary cut-off of H-Score ≤ 10 was used to define PTEN IHC negativity. A fraction of primary tumours showed intratumoural heterogeneity for PTEN IHC, with coexistence of PTEN IHC positive and negative foci, a phenomenon that has been previously described [217]. For the purpose of clinical analyses (Chapter 4), presence of any amount of PTEN IHC negative disease in primary tumours classified these cases as PTEN negative disease. When discordances between PTEN status was observed between HSPC and CRPC, cases were classified according to CRPC PTEN status for clinical analyses.

7.3.1.5 MSH2

Antigen retrieval was pursued by heating slides in in TRIS/EDTA (pH8.1) buffer using a pressure cooker (program: 125^{o}C for 2 minutes then 90^{o}C for 1 minute). Slides were left to cool at room temperature for 20 minutes. Slides were incubated with 250μl of appropriately diluted (1:50) mouse monoclonal anti-MSH2 antibody clone FE11 (#M3639; Agilent-Dako) for one hour then washed with TBST (5x). Germinal centres in the appendix were used as positive and LNCAP were used as negative controls.

7.3.1.6 MSH6

Slides were incubated with 250μl of appropriately diluted (1:500) rabbit monoclonal anti-MSH6 antibody clone EP49 (#M3646; Agilent-Dako) for one hour then washed with TBST (5x). Germinal centres in the appendix were used as positive and skeletal muscle fibers were used as negative controls.

7.3.1.7 MLH1

Slides were incubated with 250μl of appropriately diluted (1:100) mouse monoclonal anti-MLH1 antibody clone ES05 (#M3640; Agilent-Dako) for one hour then washed with TBST (5x). Germinal centres in the appendix were used as positive and skeletal muscle fibres and HCT-116 were used as negative controls.

7.3.1.8 PSM2

Slides were incubated with 250μl of appropriately diluted (1:100) rabbit monoclonal anti-PMS2 antibody clone EP51 (#M3640; Agilent-Dako) for one hour then washed with TBST (5x). Germinal centres in the appendix were used as positive and skeletal muscle fibres and HCT-116 were used as negative controls.

7.3.1.9 PD-L1

Slides were incubated with 250μl of appropriately diluted (1:100) rabbit monoclonal anti-PD-L1 antibody clone E1L3N (#13684; Cell Signaling Technology) for one hour then washed with TBST (5x). Trophoblastic cells (placenta) were used as positive and ovarian stroma were used as negative controls.

7.3.2 Immunohistochemistry (IHC) – Assay Analyses

All IHC analyses were performed by Dr Daniel Nava Rodrigues or Bora Gurel unless otherwise specified. All IHC analyses were performed blinded to clinical or pathological data (i.e. previously assigned Gleason Scores).

- The H-Score system described by Detre [218]:
    - The H-Score system is described as the formula: *(% of negative)x0 + (% of weak positivity)x1 + (% of moderate positivity)x2 + (% of strong positivity)x3*,

yielding a result between 0 and 300. Both nuclear and cytoplasmic compartments were evaluated for AR-NTD, AR-V7, and PTEN.

- Mismatch Repair proteins (MSH2, MSH6, MLH1, and PMS2) were dichotomously analysed as either positive or negative according to the College of American Pathologists criteria for biomarker reporting in colorectal carcinomas. In brief, nuclear positive tumours, regardless of intensity, were called positive, and cases with absent nuclear staining with good internal controls were called negative.
- PD-L1 was scored by another pathologist (L.S.T.M.) blinded to the hypothesis and any data regarding the sample's molecular status. Partial or complete membranous staining was scored as a % of positive cells/all viable tumour cells.

7.3.3 Multicolour Immunofluorescence

Multiplex sequential IF staining assays were performed by Mateus Crespo. Antigen retrieval was performed using CC1 buffer (#950-224, Ventana Medical Systems) at 98°C for 36 minutes in a water bath. Endogenous peroxidase was inactivated in 3% H_2O_2 for 10 minutes. Tissue sections were incubated for 60 minutes at room temperature with antibodies against CD4 (#104R-16, clone SP35, 1:100, Cell Marque) and CD8 (#M7103, clone C8/144B, 1:200, Dako, Agilent Technologies). A second layer of antibodies using AlexaFluor 555-conjugated IgG (H+L) goat anti-rabbit (#A21429, Invitrogen) and AlexaFluor 488-conjugated IgG (H+L) goat anti-mouse (#A-11029, Invitrogen) were used to detect CD4 and CD8, respectively. Tissue sections were treated with an avidin/biotin blocking kit according to the manufacturer's protocol (#ab64212, Abcam), and rabbit/mouse normal serum at 5% for 30 minutes. Next, tissue sections were incubated for 60 minutes with antibodies against Foxp3 conjugated to biotin (#13-4777-82, clone 236A/E7, 1:100, eBioscience) and EpCAM conjugated to AlexaFluor 647 (#5447S, clone VU1D9, 1:200, Cell Signaling Technology). Tissue sections were incubated with streptavidin peroxidase (HRP) (#K5001, Dako, Agilent Technologies) for 15 minutes followed by TSA Coumarin detection system (#NEL703001KT, PerkinElmer) for 10 minutes. Nuclei were counterstained with DRAQ 7 (#DR71000, Biostatus) and tissue sections were mounted with ProLong Gold antifade reagent (#P36930,

Molecular Probes). After staining, slides were scanned using a multi-spectral camera provided by the Vectra® (PerkinElmer) system [219]. Whenever possible, more than one non-overlapping micrograph at 20x magnification was collected.

7.3.3.1 Multi-Spectral Image Acquisition and Analyses

Multi-spectral imaging offers the advantage of increased precision by allowing for the separation of signal from noise (i.e. auto-fluorescence). Separation is possible by acquiring images formed by light emitted from different fluorophores at multiple wavelength bands and computationally unmixing these. Multi-spectral image acquisition, linear unmixing of multi-spectral images, and tissue analyses algorithms were pursued by Mateus Crespo the pathologists using the Vectra® system (Perkin Elmer) and the inForm® Cell Analysis® software version 2.1.1. Tissue segmentation was pursued using EpCam positivity as a tumour mask to separate neoplastic cells from adjacent stroma and cell segmentation was pursued using DRAQ7 as nuclear marker. Phenotype determination was based on staining for EpCam, CD4, FOXP3 and CD8. Cells in tumour areas selected by the algorithm were separated into bins as follows: CD4+/FOXP3- cells, CD4+/FOXP3+ cells, CD8+ cells, and EpCam+ tumour cells. For each image, the tumour area (in mm^2) and the number of CD4+/FOXP3-, CD4+/FOXP3+, and CD8+ cells were determined to calculate the lymphocytic density of tumour infiltrating lymphocytes (LD-TIL) determined as: (∑ T lymphocytes from all images)/(∑ of areas from all images).

7.4 AdnaTest mRNA extraction, CTC enumeration, and AdnaTest CTC call

Isolation and enrichment of CTCs from mCRPC patient peripheral blood (PB) draws were carried out using the AdnaTest Prostate Cancer Select (Qiagen, Hilden, Germany), and mRNA purification was performed using the AdnaTest Prostate Cancer Detect (Qiagen) as per the manufacturer's instructions.

CTC calls for each sample are presented as CTC call positive (actin positive, and prostate-specific membrane antigen [PSMA] and/or PSA and/or epidermal growth factor

receptor[EGFR] positive; CTC+), CTC call negative (actin positive and all other markers negative; CTC), or failed cDNA conversion (actin negative; failed).

CellSearch CTC enumeration

CTC counts were determined from mCRPC patient PB draws using the CellSearch CTC kit (Menarini; Silicon Biosystems, Pennsylvania, USA) according to the Food and Drug Administration-cleared manufacturer's method.

mRNA quantification of AR-FL and AR-V7

CTC+ samples were used for the measurement and quantification of AR-FL and AR-V7 transcripts. Quantitative real-time polymerase chain reaction (PCR) was carried out with primers for AR-FL (forward: 50-CAGCCTATTGCGAGAGAGCTG-30, reverse: 50-GAAAGGATCTTGGGCACTTGC-30) and AR-V7 (forward: 50-CCATCTTGTCGTCTTCGGAAATGTTA-30, reverse: 50-TTTGAATGAGGCAAGTCAGCCTTTCT-30) along with IQ SYBR Green supermix (Bio-rad, California, USA) and run on a Rotor-Gene Q MDx 2Plex HRM (Qiagen). Ct values were converted to absolute copy numbers using a standard curve using a gBlock gene fragment (Integrated DNA Technologies, Iowa, USA) containing the primer targets and internal amplified sequences for AR-FL and AR-V7. AR-V7 status is presented as continuous (copies/ml) and binary (present ≥1 copy/ml and absent <1 copy/ml) outcomes; AR-FL status is presented as binary (present ≥1 copy/ml and absent <1 copy/ml) outcomes. Blinded control samples were run at the Institute of Cancer Research (ICR) and Johns Hopkins University (JHU) to confirm optimisation of the AdnaTest platform within both laboratories.

7.5 Massive-parallel sequencing (Chapters 4 and 5)

7.5.1 DNA Extraction

- DNA extraction from paraffin was pursued using the using the QIAamp DNA FFPE Tissue kit (Qiagen) and quantified by Quant-iT Picogreen double-stranded DNA (dsDNA) Assay Kits (#P7589; Invitrogen-ThermoFisher Scientific). The Illumina FFPE QC kit (#WG-321-1001, Illumina) was used for DNA quality control tests. Samples with ≤40% tumour content on histological analysis were surgically microdissected

under a stereoscope using nuclear fast red stained slides to ensure at least 80% tumour purity.

- Sections from fresh-frozen samples were taken and stained with H&E to ensure tumour content of >40% prior to DNA extraction. DNA extraction from fresh-frozen samples was pursued using the QIAmp® DNA Mini Kit (#51304; Qiagen) and quantified by Quant-iT Picogreen double-stranded DNA (dsDNA) Assay Kits (#P7589; Invitrogen-ThermoFisher).
- DNA extraction from buccal swabs was pursued using Isolhelix DNA Isolation kit DDK50 (Isohelix) and QIAmp® DNA Mini Kit (#51304; Qiagen).

7.5.2 Targeted Sequencing

Targeted sequencing results are reported in chapters 4 and 5. Library preparation and sequencing assay were performed by Dr. Joaquin Mateo and members of the Cancer Biomarkers DNA sequencing team which included, at the time of data accrual for this thesis, Jane Goodall and Claudia Bertan. DNA input varied as a function of QC testing: 40ng, if QC<Δ2 and 80ng if QC>Δ2 but <Δ4. Samples with QC>Δ4 were not sequenced.

- Library preparation was pursued using a customised gene panel (Generad DNASeq Mix-n-Match v2; Qiagen), designed by Dr. Suzanne Carreira, covering the exonic regions of 113 genes was used for targeted sequencing. The genes present in this panel are summarised below.

AKT1	BARD1	CHEK2	ERCC6	FANCM	MAP4K3	MYD88	PIK3CG	SMARCA4	WTI
AKT2	BLM	CTNNB1	EZH2	FGFR2	MDM2	NBN	PIK3R1	SMARCB1	XPA
ALK	BRAD	DDB2	FAM46C	FGFR3	MET	NFI	PMS2	SPOP	XPC
APC	BRCA1	EGFR	FANCA	HNF1A	MLH1	NF2	PRKDC	SRC	XRCC3
AR	BRCA2	EPCAM	FANCB	HRAS	MLH3	NFKBIA	PTEN	STK11	ZRSR2
ARID1A	BUB1B	ERBB2	FANCC	JAK1	MRE11A	NOTCH1	RAD50	TNFAIP3	
ARID2	CDH1	ERBB3	FANCD2	JAK2	MSH2	NOTCH2	RAD51B	TNFRSF14	
ATM	CDK12	ERBB4	FANCE	KRAS	MSH3	NRAS	RAD51C	TP53	
ATR	CDK4	ERCC2	FANCF	MAP2K1	MSH6	NTRK1	RAD51D	TSC1	
ATRX	CDKN1B	ERCC3	FANCG	MAP2K2	MTOR	PALB2	RB1	TSC2	
AXIN1	CDKN2A	ERCC4	FANCI	MAP2K4	MUTYH	PDGFRA	RECQL4	VHLL	
AXIN2	CHEK1	ERCC5	FANCL	MAP3K1	MYC	PIK3CA	RET	WRN	

- Sequencing was performed using the Illumina MiSeq® platform (Illumina).

7.5.2.1 Targeted Sequencing Analyses

- Alignment was pursued with BWA tools.
- Variant calling was performed using the Genome Analysis Toolkit (GATK) variant annotator in the Qiagen GeneRead Targeted Exon Enrichment Panel Data Analysis website (http://ngsdataanalysis.sabiosciences.com/NGS2/).
- Variants were manually curated.
- Copy number aberrations were assessed using CNVkit v0.3.5 (http://github.com/etal/cnvkit). Performed by George Seed.

7.5.3 Whole Genome Sequencing (Chapter 5)

Downstream analyses and interpretation of sequencing reads were performed by Suzanne Carreira, Wei Yuan and George Seed.

Tissue sections (7 µm) were hematoxylin and eosin (H&E) stained and assessed to be at least 50% tumor. DNA was isolated from five 40 µm tissue sections using the QIAamp Fast DNA Tissue Kit (QIAGEN), with tissue disruption performed by ceramic beads (MP BioMedicals). DNA was quantified by Qubit fluorimeter and verified by a BioAnalyzer DNA 12000 (Agilent). DNA libraries were prepared using 500 ng of DNA as input to the Hyper Kit (Kapa) and barcoded using TruSeq (Illumina), with three cycles of PCR. Whole-exome capture of gene coding regions and a small shoulder region of intron–exon boundaries was performed using SeqCap EZ Exome V3 (64.1 Mb; Nimblegen). Library fragment size was verified by BioAnalyzer High Sensitivity DNA Assay (Agilent). Libraries were sequenced on an Illumina HiSeq 4000 instrument. Patient 1's germline, pre-olaparib, and resistant biopsies were sequenced to a mean depth of 33x, 88x, and 95x, respectively.

7.5.4 cfDNA Sequencing (Chapter 5)

Whole blood was collected in EDTA, centrifuged at 1,600 rcf, and chilled at 4°C within 2 hours of collection. Plasma and buffy coat were stored at −80°C. Germline DNA was

extracted from buffy coat using the DNeasy Blood and Tissue Kit (QIAGEN; manufacturer's instructions) and quantified with a NanoDrop spectrophotometer (Thermo Scientific). Circulating cfDNA was extracted from 6 mL of plasma using the Circulating Nucleic Acids Kit (QIAGEN; manufacturer's instructions) and quantified with a Qubit 2.0 Fluorometer and a Qubit dsDNA HS Assay Kit (Life Technologies). DNA (10 to 100 ng) was used for targeted DNA capture; gDNA was sheared to 180 nt fragments by ultrasonication (Covaris); cfDNA samples do not require shearing. A-tailing, end repair, Illumina-compatible adapter ligation, and between 12 to 17 cycles of PCR amplification were performed. Products were quantified by NanoDrop. Samples were hybridized to a custom NimbleGen SeqCap panel targeting the exonic regions of 73 genes for a minimum of 16 hours at 47°C following the SeqCap EZ system protocols.

Libraries were purified with AMPure beads (Agencourt) and quantitated by Qubit. Sequencing was performed on an Illumina MiSeq (V3 600 cycle kit). Patient 1's pre-olaparib and resistant cfDNA samples were sequenced to a mean depth of 220x. Patient 2's cfDNA samples were sequenced to a mean depth of 400x (germline) and 1,400x (pre-olaparib and resistant).

7.5.5 Sequencing and Bioinformatics (Chapter 5)

7.5.5.1 Mutation load and calls

For panel testing data, the mutation load was extracted from targeted next generation sequencing panel data after filtering out of spurious and germline changes using methods previously described (Garofalo et al, Genome medicine, 2016).

7.5.5.2 mSINGS

mSINGS software (Salipante, Clin Chem, 2014) was used to score samples for an MSI-like phenotype by assessing targeted next generation DNA-sequencing data; due to batch-related exome sequencing variability we were unable to utilize mSINGS on these data. In brief, the algorithm functions by: a) identifying possible DNA repeat regions; b) examining the frequencies of these alleles bearing varying repeat lengths; c) comparing

these values to a baseline reference from MMR intact specimens. Our targeted panel contained 3223 possible loci. Tumor and normal samples were used produce an enriched reference set of 601 loci that could be utilised to predict MSI-status computationally.

7.6 Statistical Analyses

All statistical tests used were two sided and a p value <0.05 being considered significant. The most commonly used tests included:

- **T-Test and Mann-Whitney** – used to compare differences between two datasets.
- **Pearson & Spearman correlation** – used to evaluate whether a linear correlation exists between two numerical variables
- **Kaplan-Meier estimator** – used to estimate the proportion of patients alive at a given time-point.
- **Log-rank test** – used to compare the time-to-event times of two or more patient groups.
- **Cox proportional hazards models** – used to show the hazard ratio (HR; relative risk of an event) for a population with a set of variables compared to an individual (or population) without the same set of predictors. This model takes into account multiple covariates in determining risk of an event (e.g. progression or death).

Statistic tests were run using Stata Version 15.1.

7.6.1.1 Endpoint definition

- OS was defined as the time between treatment initiation and either the date of death, or of last follow-up for surviving patients.
- Progression free survival (PFS) was defined as the time from initiation of a treatment to the time of progression defined as radiological and/or biochemical progression or death.
- In patients with measurable disease on CT scan, radiographic response was also assessed according to the Response Evaluation Criteria in Solid Tumors 1.1 (RECIST).

- PSA decline endpoints (chapter 3) evaluated were consistent with published consensus guidelines [PCWG3]. The percentage change in PSA from baseline at 4- and 12-weeks was categorised as either a decline (≥30% decrease), progression (≥25% increase) or no change. A PSA reading not meeting either criteria of response or progression was considered as 'no-change'.

8 Bibliography

1. Fitzmaurice, C., et al., *Global, Regional, and National Cancer Incidence, Mortality, Years of Life Lost, Years Lived With Disability, and Disability-Adjusted Life-Years for 29 Cancer Groups, 1990 to 2017: A Systematic Analysis for the Global Burden of Disease Study.* JAMA Oncol, 2019.
2. Torre, L.A., et al., *Global cancer statistics, 2012.* CA Cancer J Clin, 2015. **65**(2): p. 87-108.
3. Torre, L.A., et al., *Global Cancer Incidence and Mortality Rates and Trends--An Update.* Cancer Epidemiol Biomarkers Prev, 2016. **25**(1): p. 16-27.
4. Center, M.M., et al., *International variation in prostate cancer incidence and mortality rates.* Eur Urol, 2012. **61**(6): p. 1079-92.
5. Kumar, S., et al., *Prostate cancer health disparities: An immuno-biological perspective.* Cancer Lett, 2018. **414**: p. 153-165.
6. Khani, F., et al., *Evidence for molecular differences in prostate cancer between African American and Caucasian men.* Clin Cancer Res, 2014. **20**(18): p. 4925-34.
7. Kolonel, L.N., *Nutrition and prostate cancer.* Cancer Causes Control, 1996. **7**(1): p. 83-44.
8. Hayes, R.B., et al., *Dietary factors and risks for prostate cancer among blacks and whites in the United States.* Cancer Epidemiol Biomarkers Prev, 1999. **8**(1): p. 25-34.
9. Baade, P.D., D.R. Youlden, and L.J. Krnjacki, *International epidemiology of prostate cancer: geographical distribution and secular trends.* Mol Nutr Food Res, 2009. **53**(2): p. 171-84.
10. Whittemore, A.S., et al., *Prostate cancer in relation to diet, physical activity, and body size in blacks, whites, and Asians in the United States and Canada.* J Natl Cancer Inst, 1995. **87**(9): p. 652-61.
11. Kimura, T., *East meets West: ethnic differences in prostate cancer epidemiology between East Asians and Caucasians.* Chin J Cancer, 2012. **31**(9): p. 421-9.
12. Hamilton, W., et al., *Clinical features of prostate cancer before diagnosis: a population-based, case-control study.* Br J Gen Pract, 2006. **56**(531): p. 756-62.
13. Jacobs, S.C., *Spread of prostatic cancer to bone.* Urology, 1983. **21**(4): p. 337-44.
14. Han, M., et al., *Association of hemospermia with prostate cancer.* J Urol, 2004. **172**(6 Pt 1): p. 2189-92.
15. Jahn, J.L., E.L. Giovannucci, and M.J. Stampfer, *The high prevalence of undiagnosed prostate cancer at autopsy: implications for epidemiology and treatment of prostate cancer in the Prostate-specific Antigen-era.* Int J Cancer, 2015. **137**(12): p. 2795-802.
16. Eggener, S.E., et al., *Gleason 6 Prostate Cancer: Translating Biology into Population Health.* J Urol, 2015. **194**(3): p. 626-34.
17. Carter, H.B., et al., *Gleason score 6 adenocarcinoma: should it be labeled as cancer?* J Clin Oncol, 2012. **30**(35): p. 4294-6.

18. Wilt, T.J., et al., *Follow-up of Prostatectomy versus Observation for Early Prostate Cancer.* N Engl J Med, 2017. **377**(2): p. 132-142.
19. Neal, D.E. and J.L. Donovan, *Prostate cancer: to screen or not to screen?* Lancet Oncol, 2000. **1**(1): p. 17-24.
20. Etzioni, R., et al., *Asymptomatic incidence and duration of prostate cancer.* Am J Epidemiol, 1998. **148**(8): p. 775-85.
21. Sandhu, G.S. and G.L. Andriole, *Overdiagnosis of prostate cancer.* J Natl Cancer Inst Monogr, 2012. **2012**(45): p. 146-51.
22. Schroder, F.H., et al., *Screening and prostate-cancer mortality in a randomized European study.* N Engl J Med, 2009. **360**(13): p. 1320-8.
23. Schroder, F.H., et al., *Prostate-cancer mortality at 11 years of follow-up.* N Engl J Med, 2012. **366**(11): p. 981-90.
24. Schroder, F.H., et al., *Screening and prostate cancer mortality: results of the European Randomised Study of Screening for Prostate Cancer (ERSPC) at 13 years of follow-up.* Lancet, 2014. **384**(9959): p. 2027-35.
25. Cooperberg, M.R., J.M. Broering, and P.R. Carroll, *Risk assessment for prostate cancer metastasis and mortality at the time of diagnosis.* J Natl Cancer Inst, 2009. **101**(12): p. 878-87.
26. Kattan, M.W., et al., *A preoperative nomogram for disease recurrence following radical prostatectomy for prostate cancer.* J Natl Cancer Inst, 1998. **90**(10): p. 766-71.
27. Stephenson, A.J., et al., *Preoperative nomogram predicting the 10-year probability of prostate cancer recurrence after radical prostatectomy.* J Natl Cancer Inst, 2006. **98**(10): p. 715-7.
28. Mahal, B.A., et al., *Clinical and Genomic Characterization of Low-Prostate-specific Antigen, High-grade Prostate Cancer.* Eur Urol, 2018. **74**(2): p. 146-154.
29. Gasinska, A., et al., *Prognostic Significance of Serum PSA Level and Telomerase, VEGF and GLUT-1 Protein Expression for the Biochemical Recurrence in Prostate Cancer Patients after Radical Prostatectomy.* Pathol Oncol Res, 2019.
30. Mohler, J.L., et al., *Prostate Cancer, Version 2.2019, NCCN Clinical Practice Guidelines in Oncology.* J Natl Compr Canc Netw, 2019. **17**(5): p. 479-505.
31. Sanda, M.G., et al., *Clinically Localized Prostate Cancer: AUA/ASTRO/SUO Guideline. Part I: Risk Stratification, Shared Decision Making, and Care Options.* J Urol, 2018. **199**(3): p. 683-690.
32. Loblaw, A., et al., *Follow-up Care for Survivors of Prostate Cancer - Clinical Management: a Program in Evidence-Based Care Systematic Review and Clinical Practice Guideline.* Clin Oncol (R Coll Radiol), 2017. **29**(11): p. 711-717.
33. Amling, C.L., et al., *Defining prostate specific antigen progression after radical prostatectomy: what is the most appropriate cut point?* J Urol, 2001. **165**(4): p. 1146-51.
34. Roach, M., 3rd, et al., *Defining biochemical failure following radiotherapy with or without hormonal therapy in men with clinically localized prostate cancer: recommendations of the RTOG-ASTRO Phoenix Consensus Conference.* Int J Radiat Oncol Biol Phys, 2006. **65**(4): p. 965-74.
35. Pound, C.R., et al., *Natural history of progression after PSA elevation following radical prostatectomy.* Jama, 1999. **281**(17): p. 1591-7.

36. Van den Broeck, T., et al., *Prognostic Value of Biochemical Recurrence Following Treatment with Curative Intent for Prostate Cancer: A Systematic Review.* Eur Urol, 2019. **75**(6): p. 967-987.
37. Frydenberg, M. and H.H. Woo, *Early Androgen Deprivation Therapy Improves Survival, But How Do We Determine in Whom?* Eur Urol, 2018. **73**(4): p. 519-520.
38. Brand, D. and C. Parker, *Management of Men with Prostate-specific Antigen Failure After Prostate Radiotherapy: The Case Against Early Androgen Deprivation.* Eur Urol, 2018. **73**(4): p. 521-523.
39. Studer, U.E., et al., *Immediate or deferred androgen deprivation for patients with prostate cancer not suitable for local treatment with curative intent: European Organisation for Research and Treatment of Cancer (EORTC) Trial 30891.* J Clin Oncol, 2006. **24**(12): p. 1868-76.
40. Hussain, M., et al., *Enzalutamide in Men with Nonmetastatic, Castration-Resistant Prostate Cancer.* N Engl J Med, 2018. **378**(26): p. 2465-2474.
41. Smith, M.R., et al., *Apalutamide Treatment and Metastasis-free Survival in Prostate Cancer.* N Engl J Med, 2018. **378**(15): p. 1408-1418.
42. Fizazi, K., et al., *Darolutamide in Nonmetastatic, Castration-Resistant Prostate Cancer.* N Engl J Med, 2019. **380**(13): p. 1235-1246.
43. Huggins, C.H., C., *The effect of castration, of estrogen and of androgen injection on serum phosphatases in metastatic carcinoma of the prostate.* 1941. **1**: p. 293-297.
44. Huggins, C., *Effect of Orchiectomy and Irradiation on Cancer of the Prostate.* Ann Surg, 1942. **115**(6): p. 1192-200.
45. Huggins, C., *Endocrine Control of Prostatic Cancer.* Science, 1943. **97**(2529): p. 541-4.
46. Attard, G., et al., *Prostate cancer.* Lancet, 2016. **387**(10013): p. 70-82.
47. Berry, W., et al., *Phase II trial of single-agent weekly docetaxel in hormone-refractory, symptomatic, metastatic carcinoma of the prostate.* Semin Oncol, 2001. **28**(4 Suppl 15): p. 8-15.
48. Tannock, I.F., et al., *Docetaxel plus prednisone or mitoxantrone plus prednisone for advanced prostate cancer.* N Engl J Med, 2004. **351**(15): p. 1502-12.
49. Petrylak, D.P., et al., *Docetaxel and estramustine compared with mitoxantrone and prednisone for advanced refractory prostate cancer.* N Engl J Med, 2004. **351**(15): p. 1513-20.
50. Zhu, M.L., et al., *Tubulin-targeting chemotherapy impairs androgen receptor activity in prostate cancer.* Cancer Res, 2010. **70**(20): p. 7992-8002.
51. de Bono, J.S., et al., *Abiraterone and increased survival in metastatic prostate cancer.* N Engl J Med, 2011. **364**(21): p. 1995-2005.
52. Ryan, C.J., et al., *Abiraterone in metastatic prostate cancer without previous chemotherapy.* N Engl J Med, 2013. **368**(2): p. 138-48.
53. Beer, T.M., et al., *Enzalutamide in metastatic prostate cancer before chemotherapy.* N Engl J Med, 2014. **371**(5): p. 424-33.
54. Scher, H.I., et al., *Increased survival with enzalutamide in prostate cancer after chemotherapy.* N Engl J Med, 2012. **367**(13): p. 1187-97.
55. Watson, P.A., V.K. Arora, and C.L. Sawyers, *Emerging mechanisms of resistance to androgen receptor inhibitors in prostate cancer.* Nat Rev Cancer, 2015. **15**(12): p. 701-11.
56. Smith, M.R., et al., *Apalutamide Treatment and Metastasis-free Survival in Prostate Cancer.* N Engl J Med, 2018. **378**(15): p. 1408-1418.

57. de Bono, J.S., et al., *Prednisone plus cabazitaxel or mitoxantrone for metastatic castration-resistant prostate cancer progressing after docetaxel treatment: a randomised open-label trial.* Lancet, 2010. **376**(9747): p. 1147-54.
58. Henriksen, G., et al., *Significant antitumor effect from bone-seeking, alpha-particle-emitting (223)Ra demonstrated in an experimental skeletal metastases model.* Cancer Res, 2002. **62**(11): p. 3120-5.
59. Parker, C., et al., *Alpha emitter radium-223 and survival in metastatic prostate cancer.* N Engl J Med, 2013. **369**(3): p. 213-23.
60. Kantoff, P.W., et al., *Sipuleucel-T immunotherapy for castration-resistant prostate cancer.* N Engl J Med, 2010. **363**(5): p. 411-22.
61. Gravis, G., et al., *Androgen-deprivation therapy alone or with docetaxel in non-castrate metastatic prostate cancer (GETUG-AFU 15): a randomised, open-label, phase 3 trial.* Lancet Oncol, 2013. **14**(2): p. 149-58.
62. Sweeney, C.J., et al., *Chemohormonal Therapy in Metastatic Hormone-Sensitive Prostate Cancer.* N Engl J Med, 2015. **373**(8): p. 737-46.
63. James, N.D., et al., *Addition of docetaxel, zoledronic acid, or both to first-line long-term hormone therapy in prostate cancer (STAMPEDE): survival results from an adaptive, multiarm, multistage, platform randomised controlled trial.* Lancet, 2016. **387**(10024): p. 1163-77.
64. James, N.D., et al., *Abiraterone for Prostate Cancer Not Previously Treated with Hormone Therapy.* N Engl J Med, 2017. **377**(4): p. 338-351.
65. Fizazi, K., et al., *Abiraterone acetate plus prednisone in patients with newly diagnosed high-risk metastatic castration-sensitive prostate cancer (LATITUDE): final overall survival analysis of a randomised, double-blind, phase 3 trial.* Lancet Oncol, 2019. **20**(5): p. 686-700.
66. Armstrong, A.J., et al., *ARCHES: A Randomized, Phase III Study of Androgen Deprivation Therapy With Enzalutamide or Placebo in Men With Metastatic Hormone-Sensitive Prostate Cancer.* J Clin Oncol, 2019. **37**(32): p. 2974-2986.
67. Davis, I.D., et al., *Enzalutamide with Standard First-Line Therapy in Metastatic Prostate Cancer.* N Engl J Med, 2019. **381**(2): p. 121-131.
68. Chi, K.N., et al., *Apalutamide for Metastatic, Castration-Sensitive Prostate Cancer.* N Engl J Med, 2019. **381**(1): p. 13-24.
69. Cancer Genome Atlas Research Network. Electronic address, s.c.m.o. and N. Cancer Genome Atlas Research, *The Molecular Taxonomy of Primary Prostate Cancer.* Cell, 2015. **163**(4): p. 1011-25.
70. Tomlins, S.A., et al., *Recurrent fusion of TMPRSS2 and ETS transcription factor genes in prostate cancer.* Science, 2005. **310**(5748): p. 644-8.
71. Tomlins, S.A., et al., *Distinct classes of chromosomal rearrangements create oncogenic ETS gene fusions in prostate cancer.* Nature, 2007. **448**(7153): p. 595-9.
72. Grasso, C.S., et al., *Integrative molecular profiling of routine clinical prostate cancer specimens.* Ann Oncol, 2015.
73. Gasi Tandefelt, D., et al., *ETS fusion genes in prostate cancer.* Endocr Relat Cancer, 2014. **21**(3): p. R143-52.
74. Carver, B.S., et al., *Aberrant ERG expression cooperates with loss of PTEN to promote cancer progression in the prostate.* Nat Genet, 2009. **41**(5): p. 619-24.
75. King, J.C., et al., *Cooperativity of TMPRSS2-ERG with PI3-kinase pathway activation in prostate oncogenesis.* Nat Genet, 2009. **41**(5): p. 524-6.

76. Baca, S.C., et al., *Punctuated evolution of prostate cancer genomes.* Cell, 2013. **153**(3): p. 666-77.
77. Fearon, E.R. and B. Vogelstein, *A genetic model for colorectal tumorigenesis.* Cell, 1990. **61**(5): p. 759-67.
78. Vukovic, B., et al., *Correlating breakage-fusion-bridge events with the overall chromosomal instability and in vitro karyotype evolution in prostate cancer.* Cytogenet Genome Res, 2007. **116**(1-2): p. 1-11.
79. Bates, S., et al., *p14ARF links the tumour suppressors RB and p53.* Nature, 1998. **395**(6698): p. 124-5.
80. Mateo, J., et al., *Genomics of lethal prostate cancer at diagnosis and castration-resistance.* The Journal of Clinical Investigation, 2019.
81. Li, C., et al., *Tumor-suppressor role for the SPOP ubiquitin ligase in signal-dependent proteolysis of the oncogenic co-activator SRC-3/AIB1.* Oncogene, 2011. **30**(42): p. 4350-64.
82. Zhang, L., et al., *Tumor suppressor SPOP ubiquitinates and degrades EglN2 to compromise growth of prostate cancer cells.* Cancer Lett, 2017. **390**: p. 11-20.
83. Yang, Y.A. and J. Yu, *Current perspectives on FOXA1 regulation of androgen receptor signaling and prostate cancer.* Genes Dis, 2015. **2**(2): p. 144-151.
84. Shenoy, T.R., et al., *CHD1 loss sensitizes prostate cancer to DNA damaging therapy by promoting error-prone double-strand break repair.* Ann Oncol, 2017. **28**(7): p. 1495-1507.
85. Goodrich, D.W., et al., *The retinoblastoma gene product regulates progression through the G1 phase of the cell cycle.* Cell, 1991. **67**(2): p. 293-302.
86. Beltran, H., et al., *Divergent clonal evolution of castration-resistant neuroendocrine prostate cancer.* Nat Med, 2016. **22**(3): p. 298-305.
87. Aparicio, A.M., et al., *Combined Tumor Suppressor Defects Characterize Clinically Defined Aggressive Variant Prostate Cancers.* Clin Cancer Res, 2016. **22**(6): p. 1520-30.
88. Ku, S.Y., et al., *Rb1 and Trp53 cooperate to suppress prostate cancer lineage plasticity, metastasis, and antiandrogen resistance.* Science, 2017. **355**(6320): p. 78-83.
89. Mu, P., et al., *SOX2 promotes lineage plasticity and antiandrogen resistance in TP53- and RB1-deficient prostate cancer.* Science, 2017. **355**(6320): p. 84-88.
90. Robinson, D., et al., *Integrative clinical genomics of advanced prostate cancer.* Cell, 2015. **161**(5): p. 1215-28.
91. Cancer Genome Atlas Research, N., *The Molecular Taxonomy of Primary Prostate Cancer.* Cell, 2015. **163**(4): p. 1011-25.
92. Armenia, J., et al., *The long tail of oncogenic drivers in prostate cancer.* Nat Genet, 2018.
93. Woodcock, J., *A Framework for Biomarker and Surrogate Endpoint Use in Drug Development*. 2004.
94. Sarker, D. and P. Workman, *Pharmacodynamic biomarkers for molecular cancer therapeutics.* Adv Cancer Res, 2007. **96**: p. 213-68.
95. Adjei, A.A., *What is the right dose? The elusive optimal biologic dose in phase I clinical trials.* J Clin Oncol, 2006. **24**(25): p. 4054-5.
96. Huang, R.S. and M.J. Ratain, *Pharmacogenetics and pharmacogenomics of anticancer agents.* CA Cancer J Clin, 2009. **59**(1): p. 42-55.

97. Ruberg, S.J. and L. Shen, *Personalized Medicine: Four Perspectives of Tailored Medicine.* Statistics in Biopharmaceutical Research, 2015. **7**(3): p. 214-229.
98. de Bono, J.S. and A. Ashworth, *Translating cancer research into targeted therapeutics.* Nature, 2010. **467**(7315): p. 543-9.
99. Dar, J.A., et al., *N-terminal domain of the androgen receptor contains a region that can promote cytoplasmic localization.* J Steroid Biochem Mol Biol, 2014. **139**: p. 16-24.
100. Visakorpi, T., et al., *In vivo amplification of the androgen receptor gene and progression of human prostate cancer.* Nat Genet, 1995. **9**(4): p. 401-6.
101. Romanel, A., et al., *Plasma AR and abiraterone-resistant prostate cancer.* Sci Transl Med, 2015. **7**(312): p. 312re10.
102. Azad, A.A., et al., *Androgen Receptor Gene Aberrations in Circulating Cell-Free DNA: Biomarkers of Therapeutic Resistance in Castration-Resistant Prostate Cancer.* Clin Cancer Res, 2015. **21**(10): p. 2315-24.
103. Dehm, S.M., et al., *Splicing of a novel androgen receptor exon generates a constitutively active androgen receptor that mediates prostate cancer therapy resistance.* Cancer Res, 2008. **68**(13): p. 5469-77.
104. Hu, R., et al., *Distinct transcriptional programs mediated by the ligand-dependent full-length androgen receptor and its splice variants in castration-resistant prostate cancer.* Cancer Res, 2012. **72**(14): p. 3457-62.
105. Mostaghel, E.A., et al., *Resistance to CYP17A1 inhibition with abiraterone in castration-resistant prostate cancer: induction of steroidogenesis and androgen receptor splice variants.* Clin Cancer Res, 2011. **17**(18): p. 5913-25.
106. Li, Y., et al., *Androgen receptor splice variants mediate enzalutamide resistance in castration-resistant prostate cancer cell lines.* Cancer Res, 2013. **73**(2): p. 483-9.
107. Antonarakis, E.S., et al., *AR-V7 and resistance to enzalutamide and abiraterone in prostate cancer.* N Engl J Med, 2014. **371**(11): p. 1028-38.
108. Scher, H.I., et al., *Association of AR-V7 on Circulating Tumor Cells as a Treatment-Specific Biomarker With Outcomes and Survival in Castration-Resistant Prostate Cancer.* JAMA Oncol, 2016.
109. Heller, G., et al., *Circulating Tumor Cell Number as a Response Measure of Prolonged Survival for Metastatic Castration-Resistant Prostate Cancer: A Comparison With Prostate-Specific Antigen Across Five Randomized Phase III Clinical Trials.* J Clin Oncol, 2018. **36**(6): p. 572-580.
110. Sarker, D., et al., *Targeting the PI3K/AKT pathway for the treatment of prostate cancer.* Clin Cancer Res, 2009. **15**(15): p. 4799-805.
111. Taylor, B.S., et al., *Integrative genomic profiling of human prostate cancer.* Cancer Cell, 2010. **18**(1): p. 11-22.
112. Munkley, J., et al., *The PI3K regulatory subunit gene PIK3R1 is under direct control of androgens and repressed in prostate cancer cells.* Oncoscience, 2015. **2**(9): p. 755-64.
113. Carver, B.S., et al., *Reciprocal feedback regulation of PI3K and androgen receptor signaling in PTEN-deficient prostate cancer.* Cancer Cell, 2011. **19**(5): p. 575-86.
114. Grasso, C.S., et al., *The mutational landscape of lethal castration-resistant prostate cancer.* Nature, 2012. **487**(7406): p. 239-43.
115. Robinson, D.R., et al., *Integrative clinical genomics of metastatic cancer.* Nature, 2017. **548**(7667): p. 297-303.

116. Jamaspishvili, T., et al., *Clinical implications of PTEN loss in prostate cancer.* Nat Rev Urol, 2018. **15**(4): p. 222-234.
117. Reid, A.H., et al., *Novel, gross chromosomal alterations involving PTEN cooperate with allelic loss in prostate cancer.* Mod Pathol, 2012. **25**(6): p. 902-10.
118. Fraser, M., et al., *Genomic hallmarks of localized, non-indolent prostate cancer.* Nature, 2017. **541**(7637): p. 359-364.
119. Shah, R.B., et al., *Heterogeneity of PTEN and ERG expression in prostate cancer on core needle biopsies: implications for cancer risk stratification and biomarker sampling.* Hum Pathol, 2015. **46**(5): p. 698-706.
120. Lotan, T.L., et al., *PTEN loss is associated with upgrading of prostate cancer from biopsy to radical prostatectomy.* Mod Pathol, 2015. **28**(1): p. 128-37.
121. Pritchard, C.C., et al., *Inherited DNA-Repair Gene Mutations in Men with Metastatic Prostate Cancer.* N Engl J Med, 2016. **375**(5): p. 443-53.
122. Struewing, J.P., et al., *The risk of cancer associated with specific mutations of BRCA1 and BRCA2 among Ashkenazi Jews.* N Engl J Med, 1997. **336**(20): p. 1401-8.
123. Gallagher, D.J., et al., *Germline BRCA mutations denote a clinicopathologic subset of prostate cancer.* Clin Cancer Res, 2010. **16**(7): p. 2115-21.
124. Mateo, J., et al., *Clinical Outcome of Prostate Cancer Patients with Germline DNA Repair Mutations: Retrospective Analysis from an International Study.* Eur Urol, 2018. **73**(5): p. 687-693.
125. Antonarakis, E.S., et al., *Germline DNA-repair Gene Mutations and Outcomes in Men with Metastatic Castration-resistant Prostate Cancer Receiving First-line Abiraterone and Enzalutamide.* Eur Urol, 2018.
126. Robson, M., et al., *Olaparib for Metastatic Breast Cancer in Patients with a Germline BRCA Mutation.* N Engl J Med, 2017. **377**(6): p. 523-533.
127. Pujade-Lauraine, E., et al., *Olaparib tablets as maintenance therapy in patients with platinum-sensitive, relapsed ovarian cancer and a BRCA1/2 mutation (SOLO2/ENGOT-Ov21): a double-blind, randomised, placebo-controlled, phase 3 trial.* Lancet Oncol, 2017. **18**(9): p. 1274-1284.
128. Mateo, J., et al., *DNA-Repair Defects and Olaparib in Metastatic Prostate Cancer.* N Engl J Med, 2015. **373**(18): p. 1697-708.
129. Pritchard, C.C., et al., *Complex MSH2 and MSH6 mutations in hypermutated microsatellite unstable advanced prostate cancer.* Nat Commun, 2014. **5**: p. 4988.
130. Ryan, S., M.A. Jenkins, and A.K. Win, *Risk of prostate cancer in Lynch syndrome: a systematic review and meta-analysis.* Cancer Epidemiol Biomarkers Prev, 2014. **23**(3): p. 437-49.
131. Guedes, L., et al., *MSH2 Loss in Primary Prostate Cancer.* Clin Cancer Res, 2017.
132. Le, D.T., et al., *PD-1 Blockade in Tumors with Mismatch-Repair Deficiency.* N Engl J Med, 2015. **372**(26): p. 2509-20.
133. Graff, J.N., et al., *Early evidence of anti-PD-1 activity in enzalutamide-resistant prostate cancer.* Oncotarget, 2016. **7**(33): p. 52810-52817.
134. Callewaert, L., N. Van Tilborgh, and F. Claessens, *Interplay between two hormone-independent activation domains in the androgen receptor.* Cancer Res, 2006. **66**(1): p. 543-53.
135. Neuschmid-Kaspar, F., et al., *CAG-repeat expansion in androgen receptor in Kennedy's disease is not a loss of function mutation.* Mol Cell Endocrinol, 1996. **117**(2): p. 149-56.

136. Heinlein, C.A. and C. Chang, *Androgen receptor in prostate cancer.* Endocr Rev, 2004. **25**(2): p. 276-308.
137. Williams, S.A., et al., *Does PSA play a role as a promoting agent during the initiation and/or progression of prostate cancer?* Prostate, 2007. **67**(3): p. 312-29.
138. Nash, A.F. and I. Melezinek, *The role of prostate specific antigen measurement in the detection and management of prostate cancer.* Endocr Relat Cancer, 2000. **7**(1): p. 37-51.
139. Ryan, C.J., et al., *Persistent prostate-specific antigen expression after neoadjuvant androgen depletion: an early predictor of relapse or incomplete androgen suppression.* Urology, 2006. **68**(4): p. 834-9.
140. Scher, H.I., et al., *Trial Design and Objectives for Castration-Resistant Prostate Cancer: Updated Recommendations From the Prostate Cancer Clinical Trials Working Group 3.* J Clin Oncol, 2016. **34**(12): p. 1402-18.
141. Sridhara, R., et al., *Evaluation of prostate-specific antigen as a surrogate marker for response of hormone-refractory prostate cancer to suramin therapy.* J Clin Oncol, 1995. **13**(12): p. 2944-53.
142. Hussain, M., et al., *Prostate-specific antigen progression predicts overall survival in patients with metastatic prostate cancer: data from Southwest Oncology Group Trials 9346 (Intergroup Study 0162) and 9916.* J Clin Oncol, 2009. **27**(15): p. 2450-6.
143. Petrylak, D.P., et al., *Evaluation of prostate-specific antigen declines for surrogacy in patients treated on SWOG 99-16.* J Natl Cancer Inst, 2006. **98**(8): p. 516-21.
144. Halabi, S., et al., *Prostate-specific antigen changes as surrogate for overall survival in men with metastatic castration-resistant prostate cancer treated with second-line chemotherapy.* J Clin Oncol, 2013. **31**(31): p. 3944-50.
145. Xu, X.S., et al., *Correlation between Prostate-Specific Antigen Kinetics and Overall Survival in Abiraterone Acetate-Treated Castration-Resistant Prostate Cancer Patients.* Clin Cancer Res, 2015. **21**(14): p. 3170-7.
146. Berthold, D.R., et al., *Treatment of hormone-refractory prostate cancer with docetaxel or mitoxantrone: relationships between prostate-specific antigen, pain, and quality of life response and survival in the TAX-327 study.* Clin Cancer Res, 2008. **14**(9): p. 2763-7.
147. Angelergues, A., et al., *Prostate-specific antigen flare induced by cabazitaxel-based chemotherapy in patients with metastatic castration-resistant prostate cancer.* Eur J Cancer, 2014. **50**(9): p. 1602-9.
148. Burgio, S.L., et al., *PSA flare with abiraterone in patients with metastatic castration-resistant prostate cancer.* Clin Genitourin Cancer, 2015. **13**(1): p. 39-43.
149. Alberts, B., *Molecular biology of the cell*. Sixth edition. ed. 2015, New York, NY: Garland Science, Taylor and Francis Group. 1 volume (various pagings).
150. Wang, E.T., et al., *Alternative isoform regulation in human tissue transcriptomes.* Nature, 2008. **456**(7221): p. 470-6.
151. Roy, B., L.M. Haupt, and L.R. Griffiths, *Review: Alternative Splicing (AS) of Genes As An Approach for Generating Protein Complexity.* Curr Genomics, 2013. **14**(3): p. 182-94.
152. Stamm, S., *Signals and their transduction pathways regulating alternative splicing: a new dimension of the human genome.* Hum Mol Genet, 2002. **11**(20): p. 2409-16.
153. Venables, J.P., *Aberrant and alternative splicing in cancer.* Cancer Res, 2004. **64**(21): p. 7647-54.

154. Tepper, C.G., et al., *Characterization of a novel androgen receptor mutation in a relapsed CWR22 prostate cancer xenograft and cell line.* Cancer Res, 2002. **62**(22): p. 6606-14.
155. Lu, J., T. Van der Steen, and D.J. Tindall, *Are androgen receptor variants a substitute for the full-length receptor?* Nat Rev Urol, 2015. **12**(3): p. 137-44.
156. Cao, B., et al., *Androgen receptor splice variants activating the full-length receptor in mediating resistance to androgen-directed therapy.* Oncotarget, 2014. **5**(6): p. 1646-56.
157. Hu, R., et al., *Ligand-independent androgen receptor variants derived from splicing of cryptic exons signify hormone-refractory prostate cancer.* Cancer Res, 2009. **69**(1): p. 16-22.
158. Freedland, S.J., et al., *The prostatic specific antigen era is alive and well: prostatic specific antigen and biochemical progression following radical prostatectomy.* J Urol, 2005. **174**(4 Pt 1): p. 1276-81; discussion 1281; author reply 1281.
159. Catalona, W.J., et al., *Selection of optimal prostate specific antigen cutoffs for early detection of prostate cancer: receiver operating characteristic curves.* J Urol, 1994. **152**(6 Pt 1): p. 2037-42.
160. Royce, T.J., et al., *Surrogate End Points for All-Cause Mortality in Men With Localized Unfavorable-Risk Prostate Cancer Treated With Radiation Therapy vs Radiation Therapy Plus Androgen Deprivation Therapy: A Secondary Analysis of a Randomized Clinical Trial.* JAMA Oncol, 2017. **3**(5): p. 652-658.
161. Lorente, D., et al., *Interrogating Metastatic Prostate Cancer Treatment Switch Decisions: A Multi-institutional Survey.* Eur Urol Focus, 2018. **4**(2): p. 235-244.
162. Liu, L.L., et al., *Mechanisms of the androgen receptor splicing in prostate cancer cells.* Oncogene, 2014. **33**(24): p. 3140-50.
163. Nakazawa, M., E.S. Antonarakis, and J. Luo, *Androgen receptor splice variants in the era of enzalutamide and abiraterone.* Horm Cancer, 2014. **5**(5): p. 265-73.
164. Datta, S.R., A. Brunet, and M.E. Greenberg, *Cellular survival: a play in three Akts.* Genes Dev, 1999. **13**(22): p. 2905-27.
165. Nitulescu, G.M., et al., *Akt inhibitors in cancer treatment: The long journey from drug discovery to clinical use (Review).* Int J Oncol, 2016. **48**(3): p. 869-85.
166. Jia, S., T.M. Roberts, and J.J. Zhao, *Should individual PI3 kinase isoforms be targeted in cancer?* Curr Opin Cell Biol, 2009. **21**(2): p. 199-208.
167. Fruman, D.A. and G. Bismuth, *Fine tuning the immune response with PI3K.* Immunol Rev, 2009. **228**(1): p. 253-72.
168. Ersahin, T., N. Tuncbag, and R. Cetin-Atalay, *The PI3K/AKT/mTOR interactive pathway.* Mol Biosyst, 2015. **11**(7): p. 1946-54.
169. Tamura, M., et al., *Inhibition of cell migration, spreading, and focal adhesions by tumor suppressor PTEN.* Science, 1998. **280**(5369): p. 1614-7.
170. Weng, L.P., J.L. Brown, and C. Eng, *PTEN coordinates G(1) arrest by down-regulating cyclin D1 via its protein phosphatase activity and up-regulating p27 via its lipid phosphatase activity in a breast cancer model.* Hum Mol Genet, 2001. **10**(6): p. 599-604.
171. Shen, W.H., et al., *Essential role for nuclear PTEN in maintaining chromosomal integrity.* Cell, 2007. **128**(1): p. 157-70.
172. Bassi, C., et al., *Nuclear PTEN controls DNA repair and sensitivity to genotoxic stress.* Science, 2013. **341**(6144): p. 395-9.

173. Correia, N.C., et al., *The multiple layers of non-genetic regulation of PTEN tumour suppressor activity.* Eur J Cancer, 2014. **50**(1): p. 216-25.
174. Baselga, J., et al., *Everolimus in postmenopausal hormone-receptor-positive advanced breast cancer.* N Engl J Med, 2012. **366**(6): p. 520-9.
175. Peng, W., et al., *Loss of PTEN Promotes Resistance to T Cell-Mediated Immunotherapy.* Cancer Discov, 2016. **6**(2): p. 202-16.
176. Sangale, Z., et al., *A robust immunohistochemical assay for detecting PTEN expression in human tumors.* Appl Immunohistochem Mol Morphol, 2011. **19**(2): p. 173-83.
177. Lotan, T.L., et al., *PTEN protein loss by immunostaining: analytic validation and prognostic indicator for a high risk surgical cohort of prostate cancer patients.* Clin Cancer Res, 2011. **17**(20): p. 6563-73.
178. Chen, Y., et al., *ETS factors reprogram the androgen receptor cistrome and prime prostate tumorigenesis in response to PTEN loss.* Nat Med, 2013. **19**(8): p. 1023-9.
179. Nan, B., et al., *The PTEN tumor suppressor is a negative modulator of androgen receptor transcriptional activity.* J Mol Endocrinol, 2003. **31**(1): p. 169-83.
180. Mulholland, D.J., et al., *Cell autonomous role of PTEN in regulating castration-resistant prostate cancer growth.* Cancer Cell, 2011. **19**(6): p. 792-804.
181. Hodgson, M.C., et al., *Decreased expression and androgen regulation of the tumor suppressor gene INPP4B in prostate cancer.* Cancer Res, 2011. **71**(2): p. 572-82.
182. Antonarakis, E.S., et al., *An immunohistochemical signature comprising PTEN, MYC, and Ki67 predicts progression in prostate cancer patients receiving adjuvant docetaxel after prostatectomy.* Cancer, 2012. **118**(24): p. 6063-71.
183. McKay, M.M. and D.K. Morrison, *Integrating signals from RTKs to ERK/MAPK.* Oncogene, 2007. **26**(22): p. 3113-21.
184. Rozengurt, E., *Mitogenic signaling pathways induced by G protein-coupled receptors.* J Cell Physiol, 2007. **213**(3): p. 589-602.
185. Zimmermann, S. and K. Moelling, *Phosphorylation and regulation of Raf by Akt (protein kinase B).* Science, 1999. **286**(5445): p. 1741-4.
186. Guan, K.L., et al., *Negative regulation of the serine/threonine kinase B-Raf by Akt.* J Biol Chem, 2000. **275**(35): p. 27354-9.
187. Cheung, M., et al., *Akt3 and mutant V600E B-Raf cooperate to promote early melanoma development.* Cancer Res, 2008. **68**(9): p. 3429-39.
188. de Bono, J.S., et al., *Randomized Phase II Study Evaluating Akt Blockade with Ipatasertib, in Combination with Abiraterone, in Patients with Metastatic Prostate Cancer with and without PTEN Loss.* Clin Cancer Res, 2019. **25**(3): p. 928-936.
189. Hanahan, D. and R.A. Weinberg, *Hallmarks of cancer: the next generation.* Cell, 2011. **144**(5): p. 646-74.
190. Tubbs, A. and A. Nussenzweig, *Endogenous DNA Damage as a Source of Genomic Instability in Cancer.* Cell, 2017. **168**(4): p. 644-656.
191. Parkes, E.E., et al., *Activation of STING-Dependent Innate Immune Signaling By S-Phase-Specific DNA Damage in Breast Cancer.* J Natl Cancer Inst, 2017. **109**(1).
192. Ferguson, L.R., et al., *Genomic instability in human cancer: Molecular insights and opportunities for therapeutic attack and prevention through diet and nutrition.* Semin Cancer Biol, 2015. **35 Suppl**: p. S5-s24.
193. Lord, C.J. and A. Ashworth, *PARP inhibitors: Synthetic lethality in the clinic.* Science, 2017. **355**(6330): p. 1152-1158.

194. Fong, P.C., et al., *Inhibition of poly(ADP-ribose) polymerase in tumors from BRCA mutation carriers.* N Engl J Med, 2009. **361**(2): p. 123-34.
195. Nilbert, M., et al., *Microsatellite instability is rare in rectal carcinomas and signifies hereditary cancer.* Eur J Cancer, 1999. **35**(6): p. 942-5.
196. Davar, D., Y. Lin, and J.M. Kirkwood, *Unfolding the mutational landscape of human melanoma.* J Invest Dermatol, 2015. **135**(3): p. 659-62.
197. Alexandrov, L.B., et al., *Signatures of mutational processes in human cancer.* Nature, 2013. **500**(7463): p. 415-21.
198. Van Allen, E.M., et al., *Genomic correlates of response to CTLA-4 blockade in metastatic melanoma.* Science, 2015. **350**(6257): p. 207-11.
199. Nghiem, B., et al., *Mismatch repair enzyme expression in primary and castrate resistant prostate cancer.* Asian J Urol, 2016. **3**(4): p. 223-228.
200. Salipante, S.J., et al., *Microsatellite instability detection by next generation sequencing.* Clin Chem, 2014. **60**(9): p. 1192-9.
201. Murai, J., et al., *Trapping of PARP1 and PARP2 by Clinical PARP Inhibitors.* Cancer Research, 2012. **72**(21): p. 5588-5599.
202. Abida, W., et al., *Genomic characteristics of deleterious BRCA1 and BRCA2 alterations and associations with baseline clinical factors in patients with metastatic castration-resistant prostate cancer (mCRPC) enrolled in TRITON2.* Journal of Clinical Oncology, 2019. **37**(15_suppl): p. 5031-5031.
203. Smith, M.R., et al., *Phase II study of niraparib in patients with metastatic castration-resistant prostate cancer (mCRPC) and biallelic DNA-repair gene defects (DRD): Preliminary results of GALAHAD.* Journal of Clinical Oncology, 2019. **37**(7_suppl): p. 202-202.
204. Abida, W., et al., *Analysis of the Prevalence of Microsatellite Instability in Prostate Cancer and Response to Immune Checkpoint Blockade.* JAMA Oncol, 2019. **5**(4): p. 471-478.
205. Gonzalez, S., et al., *Conceptual aspects of self and nonself discrimination.* Self Nonself, 2011. **2**(1): p. 19-25.
206. Schumacher, T.N. and R.D. Schreiber, *Neoantigens in cancer immunotherapy.* Science, 2015. **348**(6230): p. 69-74.
207. Diggs, L.P. and E.C. Hsueh, *Utility of PD-L1 immunohistochemistry assays for predicting PD-1/PD-L1 inhibitor response.* Biomark Res, 2017. **5**: p. 12.
208. Brunnstrom, H., et al., *PD-L1 immunohistochemistry in clinical diagnostics of lung cancer: inter-pathologist variability is higher than assay variability.* Mod Pathol, 2017. **30**(10): p. 1411-1421.
209. George, D.J., et al., *Immune Biomarkers Predictive for Disease-Free Survival with Adjuvant Sunitinib in High-Risk Locoregional Renal Cell Carcinoma: From Randomized Phase III S-TRAC Study.* Clin Cancer Res, 2018. **24**(7): p. 1554-1561.
210. Sznol, M. and L. Chen, *Antagonist antibodies to PD-1 and B7-H1 (PD-L1) in the treatment of advanced human cancer.* Clin Cancer Res, 2013. **19**(5): p. 1021-34.
211. Kondo, A., et al., *Interferon-gamma and tumor necrosis factor-alpha induce an immunoinhibitory molecule, B7-H1, via nuclear factor-kappaB activation in blasts in myelodysplastic syndromes.* Blood, 2010. **116**(7): p. 1124-31.
212. Taube, J.M., et al., *Colocalization of inflammatory response with B7-h1 expression in human melanocytic lesions supports an adaptive resistance mechanism of immune escape.* Sci Transl Med, 2012. **4**(127): p. 127ra37.

213. Parsa, A.T., et al., *Loss of tumor suppressor PTEN function increases B7-H1 expression and immunoresistance in glioma.* Nat Med, 2007. **13**(1): p. 84-8.
214. Marzec, M., et al., *Oncogenic kinase NPM/ALK induces through STAT3 expression of immunosuppressive protein CD274 (PD-L1, B7-H1).* Proc Natl Acad Sci U S A, 2008. **105**(52): p. 20852-7.
215. Welti, J., et al., *Analytical Validation and Clinical Qualification of a New Immunohistochemical Assay for Androgen Receptor Splice Variant-7 Protein Expression in Metastatic Castration-resistant Prostate Cancer.* Eur Urol, 2016.
216. Sandhu, S.K., et al., *Poly (ADP-ribose) polymerase (PARP) inhibitors for the treatment of advanced germline BRCA2 mutant prostate cancer.* Ann Oncol, 2013. **24**(5): p. 1416-8.
217. Gumuskaya, B., et al., *Assessing the order of critical alterations in prostate cancer development and progression by IHC: further evidence that PTEN loss occurs subsequent to ERG gene fusion.* Prostate Cancer Prostatic Dis, 2013. **16**(2): p. 209-15.
218. Detre, S., G. Saclani Jotti, and M. Dowsett, *A "quickscore" method for immunohistochemical semiquantitation: validation for oestrogen receptor in breast carcinomas.* J Clin Pathol, 1995. **48**(9): p. 876-8.
219. Levenson, R.M., A. Fornari, and M. Loda, *Multispectral imaging and pathology: seeing and doing more.* Expert Opin Med Diagn, 2008. **2**(9): p. 1067-81.